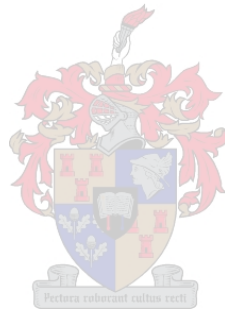


Spatial Reproductive Separation in a Handed Flower: Variation Across Space and Time



Celeste de Kock

Thesis presented in the partial fulfilment
of the requirements for the degree of
Master of Science
at Stellenbosch University

Supervisor: Prof. Bruce Anderson

Co-supervisor: Dr. Corneile Minnaar

December 2021

DECLARATION

By submitting this thesis/dissertation electronically, I declare that the entirety of the work contained therein is my own, original work, that I am the sole author thereof (save to the extent explicitly otherwise stated), that reproduction and publication thereof by Stellenbosch University will not infringe any third-party rights and that I have not previously in its entirety or in part submitted it for obtaining any qualification.

December 2021

Copyright © 2021 Stellenbosch University

All rights reserved

DEDICATION

“I do not think that anything in my scientific life has given me so much satisfaction as making out the meaning of the structure of these plants.” ~ Charles Darwin on heterostyly.

When posed with a complex biological question that seems to generate more questions than answers, I am reminded of a quote by the Greek philosopher Protagoras, who, at around 425 BC was asked if he believed in the Greek gods. He replied, “the question is complex and life is short.”

“An understanding of the natural world is a source of not only great curiosity, but great fulfilment” ~ Sir David Attenborough

“[Boundless curiosity.] That’s what being alive is about. I mean, it’s the fun of it all, making sense of it, understanding it. There’s a great pleasure in knowing why trees shed their leaves in winter. Everybody knows they do, but why? If you lose that, then you’ve lost pleasure.” ~ Sir David Attenborough

“Absence of evidence is not evidence of absence.” ~ Carl Sagan

To all those who have explored and investigated the natural world in the pursuit of knowledge.

ACKNOWLEDGEMENTS

First and foremost, I would like to express my immense thanks to Prof. Bruce Anderson, my main supervisor. Bruce, thank you for your seemingly unlimited patience and your belief in what your students are capable of. Your insatiable curiosity and infectious enthusiasm has shown me just how wondrous and fun evolutionary biology can be. If there is one piece of wisdom that I will take away from your supervision style, it is your ability to motivate and encourage your students through the use of constructive criticism and reinforcement. You are never demeaning and you always treat your students with respect. Your positive comments and unwavering support throughout motivated me to create a thesis that I can be proud of.

To Corneile Minnaar, thank you for highlighting the interesting nature of *Wachendorfia paniculata*. The precision with which you approach all your projects is inspiring. I have especially learned much from you regarding statistical analysis, and how one needs to perform statistics that are appropriate for the complexity of the data.

Thank you to Kayleigh Murray, my primary field assistant, for your dedication to my project. My second chapter would have been an impossible endeavour without your help. Not only did you act as a sounding board to my ideas and doubts regarding the methodology; you also kept me sane during our time in the field. You completely committed yourself to my project, and that is an incredibly rare quality. I didn't expect that I would gain such a good friend and have such a good time spending ten hours in the field each day.

To Nanike Esterhuizen: thank you for providing unwavering support throughout my entire masters. Your sound advice, reassuring conversations and pep-talks were essential to me managing my stress. Thank you for being such a wonderful and thoughtful friend.

I also want to thank Cape Nature, Karien Buys, Liohan Giliomee, Peter Goemans, Richelle Brink, Handré Basson, Hein Tinderholm, Leanda Coetzee, Dave Pepler, Taariq Fakier, Michael and John Duckitt, Porcupine Hills and Genevieve Theron for

allowing me onto their property, alerting me of safe field sites, providing accommodation or assistance regarding my field work. And thank you to Chris Broeckhoven for taking the time to proofread my thesis; it is greatly appreciated.

Finally I want to give thanks to my parents, who have supported me emotionally and financially for my entire masters. Thank you for always believing in me and having patience with me even if I feel it wasn't always warranted.

ABSTRACT

In many angiosperms, pollinator-driven selection has led to adaptive radiation, specialisation and phenotypic variation over space and time. Most specialised floral adaptations function by improving the efficiency of cross-pollination, while also limiting or delaying the chances of self-pollination. This study focuses on the variation of the distances between reproductive parts in *Wachendorfia paniculata*, an enantiostylous geophyte that occurs predominantly in the Western Cape, South Africa. *Wachendorfia paniculata* displays geographic variation in reproductive separation between populations, as well as temporal variation facilitated by floral movement over time within populations. In Chapter 2, I investigated whether geographic variation in the separation between reproductive parts corresponded with shifts in pollinator environments between populations, and whether floral movement has any functional significance during pollination. I expected that upper anther-stigma distance would decrease in populations where large pollinators were scarce or absent, whilst lower anther distances were expected to remain relatively similar. Within each population, I recorded reproductive separation distances, pollinator visitation rates, abundances and wingspans, which varied significantly between study sites. Surprisingly, large pollinators appeared unimportant in the present pollinator landscape. Even though the mean weighted wingspan of pollinators in a population did not predict the degree of reproductive separation, honeybee visitation rate was negatively correlated with the distance between the lower anthers, suggesting that frequent visits by small pollinators might select for narrower distances. I also found that floral movement contributed to the observed variation by reducing the distance between reproductive parts throughout the day. These findings prompted me to investigate whether floral movement could be beneficial in populations that are dominated by small pollinators in Chapter 3. Here, I explored the functional significance of floral movement by recording floral narrowing for the duration of anthesis in a single population. I hypothesised that floral narrowing acts as a mechanism of reproductive assurance by increasing the likelihood of pollinators making contact with the stigma

and/or anthers later in the day. I measured the lateral and vertical reproductive separation distances hourly and presented virgin donor and recipient inflorescences to honey bees to record how pollen deposition and receipt rates changed with floral narrowing. Floral movement was substantial and highly variable, especially for anther-stigma narrowing. The likelihood of stigmatic pollen receipt did not change with time or floral narrowing, and was dependent on the density of pollen on bee wings. I propose that floral movement might act as a reproductive assurance strategy when large pollinators are absent or when pollinator visitation rates are low. I argue that stigmatic movement is the result of a trade-off between receiving high quality pollen and getting pollinated: stigmas are positioned to receive high quality pollen in the morning, but they shift to positions that maximize the chances of pollen receipt later in the day. While lower anther movement was not as noticeable as stigmatic movement, lower anthers were more likely to deposit pollen on pollinators at smaller separation distances. I conclude that the variation in reproductive separation at spatial and temporal scales is likely to be influenced by multiple biotic and abiotic factors, but that pollinator availability could still play an important part in shaping the floral morphology of *W. paniculata*.

Key words:

Geographic variation; Floral movement; Herkogamy; Enantiostyly; Pollinator adaptation

OPSOMMING

Vir baie angiosperme het bestuiwingsgedrewe seleksie gelei tot diversifikasie, spesialisasie en fenotipiese variasie oor ruimte en tyd. Die meeste gespesialiseerde blomaanpassings funksioneer om die doeltreffendheid van kruisbestuiwing te verbeter, terwyl dit ook die kans op selfbestuiwing beperk of vertraag. Hierdie studie fokus op die variasie van die voortplantingsstruktuur-skeidingsafstand in *Wachendorfia paniculata*, 'n geofiet met links- en regshandige blomme wat hoofsaaklik in die Wes-Kaap, Suid-Afrika voorkom. *Wachendorfia paniculata* vertoon geografiese variasie in voortplantingsstruktuur-skeidingsafstand tussen populasies, sowel as intrapopulasie variasie oor tyd wat deur blombeweging bewerkstellig word. In hoofstuk twee het ek bepaal of geografiese variasie in voortplantingsstruktuur-skeidingsafstand ooreenstem met verskuiwings in die samestelling van bestuiwer gemeenskappe tussen bevolkings, en of blombeweging enige funksionele betekenis inhou vir bestuiwing. Ek het verwag dat die afstand tussen die boonste helmknop en die stempel sou afneem in populasies waar groot bestuiwers skaars of afwesig is, terwyl die afstand tussen die twee onderste helmknoppe relatief dieselfde sou bly. Vir elke populasie het ek die skeidingsafstande, bestuiwer besoeke en hul vlerkspanne aangeteken, wat aansienlik gewissel het tussen die populasies. Dit blyk dat groot bestuiwers nie belangrike bestuiwers in die huidige bestuiwingslandskap is nie. Alhoewel die gemiddelde geweegde vlerkspan van bestuiwers in 'n bevolking nie voortplantingsstruktuur-skeidingsafstand voorspel het nie, het die afstand tussen die onderste twee helmknoppe afgeneem met 'n toename in heuningby bestuiwing. Dit suggereer dat gereelde besoeke deur klein bestuiwers die evolusie van kleiner skeidingsafstande kan bewerkstellig. Ek wou ook vasstel of blombeweging moontlik bydra tot die variasie in voortplantingsstruktuur-skeidingsafstand. In hoofstuk 3 het ek hierdie ondersoek. Hier het ek die funksionele belang van blombeweging ondersoek deur die vernouing van blomstrukture te meet oor die verloop van die dag. Ek het voorspel dat die vernouing van afstande tussen voortplantingsstrukture dien as 'n meganisme van voortplantingsversekering deur die kans dat bestuiwers meer gereeld in aanrak-

ing sou kom met die voortplantingstrukture te vergroot oor tyd. Ek het die laterale en vertikale voortplantingsstruktuur-skeidingsafstand elke uur gemeet en het ook aangeteken hoe stuifmeel neerslag en stuifmeel ontvangs verander het met blombeweging. Dit het ek bepaal deur skenker- en ontvanger-bloeiwyses aan heuningbye te bied. Blombeweging was opvallend en baie wisselvallig, veral rakende die vernouing tussen die stempel en die boonste helmknop. Die koers waarteen die stempel stuifmeel ontvang het, het onveranderd gebly ten spyte van blombeweging. Die koers van stuifmeel ontvangs was ook afhanklik van die digtheid van stuifmeel op bye se vlerke. Ek stel voor dat blombeweging as 'n voortplantingsversekeringsstrategie kan dien. Ek voer aan dat die beweging van die styl 'n balans handhaaf tussen die ontvangs van hoë gehalte stuifmeel en suksesvolle bestuiwing. Die aanvanklike posisie van die stempel laat die blom toe om stuifmeel van hoë gehalte in die oggend te ontvang, maar die beweging van die styl vergroot die stempel se kanse om stuifmeel later in die dag te verkry, selfs al is dit moontlik van laer kwaliteit. Terwyl die beweging van die onderste helmknoppe nie so opvallend was soos die beweging van die styl nie, was onderste helmknoppe meer geneig om stuifmeel op kleiner skeidingsafstande op bestuiwers te plaas. Ek kom tot die gevolgtrekking dat die variasie in die mate van voortplantingsstruktuur-skeidingsafstande op ruimtelike en temporale skale waarskynlik beïnvloed word deur verskeie biotiese en abiotiese faktore, maar dat die beskikbaarheid van bestuiwers steeds 'n belangrike rol mag speel in die vorming van die blommorfologie van *W. paniculata*.

Sleutelwoorde:

Geografiese variasie; Blombeweging; Herkogamie; Links- en regshandigheid; Bestuiver seleksie

TABLE OF CONTENTS

DECLARATION	ii
DEDICATION	iii
ACKNOWLEDGEMENTS	iv
ABSTRACT	vi
OPSOMMING	viii
LIST OF FIGURES	xii
LIST OF TABLES	xix
1 GENERAL INTRODUCTION	1
2 GEOGRAPHIC AND TEMPORAL VARIATION IN THE SPATIAL REPRODUCTIVE SEPARATION OF A HANDED FLOWER: A MOVING TARGET	11
Abstract	11
Introduction	12
Materials and Methods	18
Results	23
Discussion	30
APPENDIX A	36
I. Supplementary Figures & Tables	36
II. Spectral Reflectance	42
3 STAYING ON TARGET? THE FUNCTIONAL SIGNIFICANCE OF FLORAL MOVEMENT IN A HANDED FLOWER	43
Abstract	43

Introduction	44
Materials and Methods	50
Results	57
Discussion	64
APPENDIX B	71
I. Supplementary Figures & Tables	71
II. Reproductive Viability	76
III. Stigma Saturation Rate	79
IV. Pollinator Visitation Rates & Abundances	80
4 GENERAL CONCLUSIONS	82
APPENDIX C	87
I. Honey Bee Efficiency	87
REFERENCES	89

LIST OF FIGURES

1.1	Diagrams of left-handed flowers that show four main variations of enantiostyly – A) feeding anthers (blue) centrally located; pollinating anther (orange) situated opposite the stigma, B) multiple anthers on one side; stigma and some anthers grouped together on the opposite side, C) complete separation of male and female parts on opposite sides, D) anthers grouped centrally; only the stigma deflects.	2
1.2	Diagrams depicting the composition of left- and right-handed flowers in monomorphic (left) and dimorphic (right) enantiostylous plants. . .	3
1.3	An example of a <i>Wachendorfia paniculata</i> inflorescence from the Overberg, Western Cape, South Africa (left). These flowers often occur in mass-flowering populations after fire, like the one seen here at Houwhoek Pass, Western Cape (right).	5
1.4	Examples of left-handed (left) and right-handed (right) <i>W. paniculata</i> morphs, showing how the style is deflected left or right. Photographs: Bruce Anderson.	6
2.1	The structural anatomy of a left-handed <i>Wachendorfia paniculata</i> flower. For this study, three floral measurements were taken, namely the distance between the lower anthers (LA), the distance between the upper anther and the stigma (UAS) and flower size (FS).	14
2.2	A map of the 16 <i>Wachendorfia paniculata</i> populations that were sampled throughout the Western Cape, South Africa (map insert). Pie charts depict the proportion of main functional pollinator types present for sites where pollinator data were collected. Site names with asterisks only have a single day of pollinator observations. Site names and coordinates are listed in full in appendix table A.1. Pollinator community compositions are displayed in detail in appendix figure A.1 and appendix tables A.2 & A.3.	18

2.3	Photographs of the maximum and minimum absolute floral distances recorded for UAS and LA demonstrate the variation seen in flower size and the degree of reproductive separation for <i>W. paniculata</i> between populations. Bold white crosses indicate the position of the stigma, while diamonds represent the position of the relevant anthers. The scale bar is shown in millimeters. For UAS, WAY had a maximum of 27.55 mm while HP had a minimum of 10.84 mm. For LA, SL had a maximum of 21.83 mm, while SW had a minimum of 7.93 mm.	19
2.4	Means \pm SE of standardised floral distances for 16 <i>W. paniculata</i> populations for UAS (top) and LA (bottom) floral measurements. Sites that have letters in common are not significantly different from each other. See Table A.1 for site abbreviations.	24
2.5	The effect of time of day (hours after sunrise) on the standardised floral distance for UAS (top) and LA (bottom) measurements of 16 <i>W. paniculata</i> populations. Sites indicated with an asterisk and dashed lines were measured over less than 2.5 hours, while those measured over a period of more than 2.5 hours have solid lines. Linear trends for the pooled data are indicated in bold black lines. R^2 and p -values reflect results for the pooled data	25
2.6	Honey bees (<i>Apis mellifera capensis</i> , left) were the most common pollinators of <i>W. paniculata</i> , while carpenter bees (<i>Xylocopa caffra</i> , right) were the largest pollinators. Note the typical <i>W. paniculata</i> pollen deposition visible on the wings of the honey bee. Photographs: Bruce Anderson.	26

- 2.7 Mean absolute floral distance \pm SE (UAS – filled circles and LA – unfilled circles) for fifteen *W. paniculata* populations plotted against the mean \pm SE functional pollinator visitation rate recorded for each site. The top two figures have the overall visitation rate per site as the predictor variable, which includes all functional pollinator types, whilst the two bottom figures have honey bee visitation rate as the predictor variable, which excludes all other visitors. Linear and exponential decay curves were fitted, but since exponential decay only improved the R^2 marginally (by 1%), it was decided to use linear trends to simplify the statistical analyses. 29
- A.1 The ratio of functionally significant pollinators of *W. paniculata* observed during random walks in 15 populations. Pollinator species names are arranged in ascending order of overall pollinator abundance. 37
- A.2 Mean \pm SE absolute UAS (filled circles) and LA (unfilled circles) distances plotted against the grand mean functional pollinator wingspan \pm SE. The Stellenbosch Mountain population had a disproportionately large SE (± 33.52), which has been truncated for display purposes. 37
- A.3 Aggregate plots of mean \pm SE spectral reflectance measurements done for flowers from WAY (red; $n = 9$) and DBF (blue; $n = 8$). Points of interest (black circles) included the nectar guide (top right), the distal tip (bottom left) and the middle (top left) of the tepal. 42

3.1	A) Floral measurements performed on flowers to determine whether movement over time is significant (UAS, LA and LAS). Anther colours correspond to the colours of quantum-dot solutions used to label lower opposite anther (green), stigma-side anther (yellow) and upper anther (red) pollen grains of left-handed donors. B) Schematic of how the inflorescence presentation pole was designed, and how left-handed donor (D) and right-handed recipient (R) inflorescences were arranged during the quantum dot tracking experiment.	52
3.2	Means \pm SE of the standardised floral measurements (as a proportion of the initial measurement of each flower) over time. Days on which measurements were taken are displayed in different colours. Flower insets illustrate the respective measurements that were taken.	57
3.3	Conditional density plot (filled areas) showing how the mean absolute UAS distance (mm) is associated with the conditional probability of pollen receipt by the stigma (conditional probability of success). Open circles show the raw distribution of data points when pollen grains were received (1) or not (0).	59
3.4	Conditional density plots (filled areas) showing how the density of pollen grains on different parts of bee wings (indicated by colour-fills on wing diagram insets) is associated with the conditional probability of pollen receipt by the stigma (conditional probability of success). Open circles show the raw distribution of data points when pollen grains were received (1) or not (0).	59

3.5	Conditional density plots (filled areas) showing how the mean floral distance (UAS or LA) is associated with the conditional probability that bee wings received yellow- or red-labelled pollen (conditional probability of success). Open circles show the raw distribution of data points when labelled pollen grains were present on a bee (1) or not (0). Wing heat map insets display a rough distribution of all the labelled grains received, with darker colours representing grains received when floral distances were narrower (i.e. later in the day). For further reference see appendix fig. B.4.	62
3.6	Mean (\pm SE) density of pollen grains (number of grains per mm ²) on the central forewing (orange), the hind wing (green) and the wing tip (blue) over time. The y-axis is displayed on a logarithmic scale. The photographic insets show the density of pollen grains on bee wings at 10:30 (4 – 5 hours after sunrise) and 15:30 (9 – 10 hours after sunrise). Scale bars represent 5 mm.	63
B.1	An example of how floral structures narrow over the course of the day for a single <i>W. paniculata</i> flower in the field. The green lines show the starting positions of the upper anther (red oval) and the stigma (white cross), whereas red lines show the end positions. For LAS, the yellow oval represents the position of the lower stigma-side anther, while the white cross represents the position of the stigma, which visibly move toward each other between 9:00 and 17:00. The scale bar for UAS is denoted in mm.	71
B.2	Time-lapse footage of two cut flowers (left: front view; right: distal view) that were picked the previous day and allowed to open naturally. The tepals were taped to a piece of cardboard to prevent the corolla from moving. Note the wide-angled position of the stigma upon opening.	72

B.3	A honey bee visiting a <i>W. paniculata</i> flower. A white cross shows the point of stigma contact upon departure (bottom), while arrows show where lower anthers made contact during landing (top). Bright yellow pollen is clearly visible on the stigma in the top frame (inset). Photos: Kayleigh Murray	73
B.4	Diagrams depicting the approximate distribution and numbers of quantum dot-labelled grains deposited by lower (yellow) and upper (red) anthers onto bee wings. Darker shades correspond with smaller mean floral distances and later times of the day. The top diagram displays the raw distribution of all pollen grains, coloured according to the time of day at which they were received. Wing cell colour reflects the average floral distance or hour after sunrise at which a grain was deposited. This was used to generate the heat maps in the bottom diagram by approximating the concentration of colour in the top figure.	74
B.5	The proportion of total fruit that developed after being hand-pollinated at different times of the day (A) and the mean seed set per fruit that developed after being hand-pollinated at different times (B). 3.5 – 5.5 hours after sunrise was during the morning, whilst the other two intervals occurred in the afternoon. Intervals that share the same letter are not significantly different from each other ($p > 0.05$).	76
B.6	Stigma saturation over time. The mean percentage of harvested stigmas that had at least one pollen grain (blue) and three pollen grains (purple) over time.	79
B.7	Z-standardised honeybee visitation rates over time, which corrects data so that the mean for each day equals zero, which controls for variation in data between days. Different symbols show the variation of visitation rates between different days, while the dashed line represents the visitation rate averaged over all days.	81

C.1 Grand mean (\pm SE) seed set of inflorescences that were left open or caged to exclude large pollinators. Bars that share letters are not significantly different from each other. 87

LIST OF TABLES

2.1	A list of pollinator species that were found to visit <i>W. paniculata</i> across 15 populations. Means \pm SE and (number) of insects measured to obtain wingspans used to calculate the grand weighted wingspan in each population. The number of sites at which a species was present represents how widespread a species was. The mean number of times (\pm SD) that a species was likely to be encountered during a 15-minute random walk is shown as a measure of abundance of each species across all sites.	27
A.1	A list of 16 <i>Wachendorfia paniculata</i> populations that were sampled during this study, including site abbreviations, names, elevations and GPS coordinates.	36
A.2	A complete list of insect visitors (ordered alphabetically) to <i>W. paniculata</i> flowers during plot observations. The total number of visitors recorded at a particular site during plot observations are shown for functionally significant pollinators. Black dots indicate that a visitor was present at that site, but not deemed functionally significant. Site names with asterisks only had a single day of observations.	38
A.3	A complete list of insect visitors (ordered alphabetically) to <i>W. paniculata</i> flowers during random walks. The total number of visitors recorded at a particular site during random walks are shown for functionally significant pollinators. Black dots indicate that a visitor was present at that site, but not deemed functionally significant. Site names with asterisks only had a single day of observations.	40
3.1	Model output of floral narrowing over time describing the fixed effects, their coefficient estimates, standard errors, z - and p -values, as well as the pseudo- R^2 values for each model. Significant p -values are printed in bold text.	58

- 3.2 Output for the hurdle model performed to determine whether stigma pollen receipt changed with floral narrowing (absolute UAS distance measured in mm) and if it is influenced by overall wing pollen density (number of grains per mm²). Fixed effects, coefficient estimates, standard errors and *z*- and *p*-values are displayed for the conditional truncated Poisson model, as well as the zero-inflated model. For the zero-inflated model, the results describe the probability of having an extra zero in the dataset. Significant effects are printed in bold text. 60
- 3.3 Output for the hurdle models performed to determine whether the contribution and deposition of pollen from quantum dot-labelled anthers onto bee wings changed with floral narrowing (mean floral distance in mm). Anther types and their associated fixed effects, coefficient estimates, standard errors and *z*- and *p*-values are displayed for the conditional truncated Poisson models, as well as the zero-inflated models. Fixed effects include the mean floral distance (averaged over hour and measured in mm), the overall wing pollen density (# grains per mm²) and the total number of recipient and donor flowers visited by each bee. For the zero-inflated model, the results describe the probability of having an extra zero in the dataset. Significant effects are printed in bold text. 61
- B.1 Output for the hurdle models performed to determine whether stigma pollen receipt changes with floral narrowing and if it is influenced by wing pollen density (number of grains per mm²) from different wing sections. Fixed effects, coefficient estimates, standard errors and *z*- and *p*-values are displayed for the conditional truncated Poisson models, as well as the zero-inflated models. For the zero-inflated model, the results describe the probability of having an extra zero in the dataset. Significant effects are printed in bold text. 75

CHAPTER 1

GENERAL INTRODUCTION

The remarkable and varied ways in which angiosperms have diversified and specialised to optimise cross-pollination have been the subjects of intense study since Darwin's time (Darwin, 1877). Herkogamy (the spatial separation of male and female reproductive parts within a flower) is one of many strategies that angiosperms employ to minimise the risk of autogamy (selfing within the same flower) and improve chances of effective cross-pollination (Webb and Lloyd, 1986).

However, the simple spatial separation of sexual organs does not remove the risk of geitonogamy (selfing within the same plant), as pollinators often visit multiple flowers within an inflorescence before departing. Furthermore, a mismatch in pollen deposition and stigma contact sites on pollinator bodies might impede, rather than aid, efficient outcrossing (Barrett, 2002; Armbruster *et al.*, 2014; Ye *et al.*, 2019). Reciprocally-herkogamous devices, such as stylar polymorphisms, circumvent these challenges by increasing pollination precision while suppressing the likelihood of selfing (Barrett *et al.*, 2000).

Barrett *et al.* (2000) defined four dominant kinds of stylar polymorphisms, namely distyly, tristyly, stigma-height dimorphism and enantiostyly. Pauw (2005) more recently described a fifth kind, namely inversostyly. The first three polymorphisms are characterised by differences in the height of the style within a flower. Distyly produces two floral morphs, where a flower either has a tall style and short stamens, or tall stamens and a short style. Similarly, long, short and medium morphs are found in tristylous plants, with corresponding varying heights of their reproductive structures. As the name suggests, stigma-height dimorphism displays differences in the height of the style, but not in the stamens. These mechanisms have been suggested to improve pollination precision, promote outcrossing and reduce the interference between stigmas and anthers during pollination. For example, in distyly, inter-morph pollen movement dominates intra-morph and self-pollen movement (Barrett

et al., 2000; Brys *et al.*, 2008; Zhou *et al.*, 2015), meaning that pollen is rarely ‘lost’ to flowers within the same plant or the same morph (especially if the two morphs are incompatible). In this way, distyly increases the precision of pollen movement between high-quality mates.

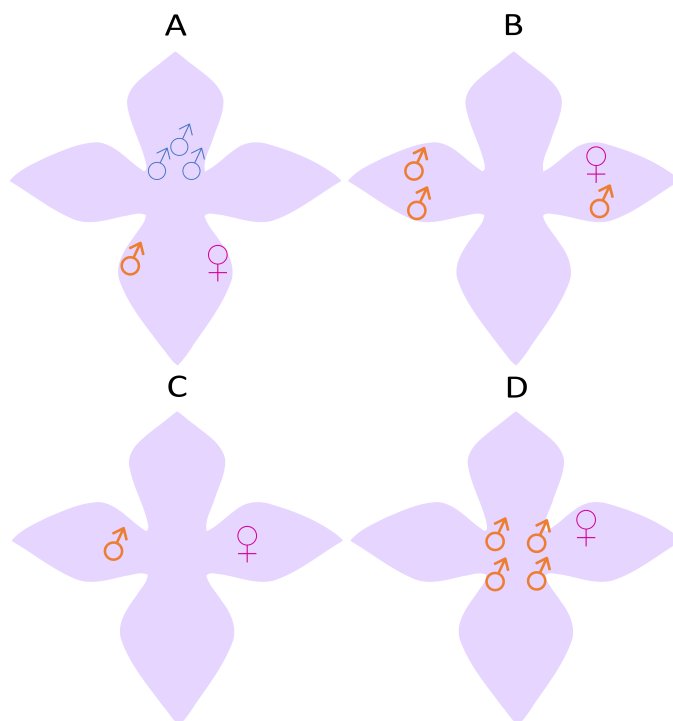


Figure 1.1: Diagrams of left-handed flowers that show four main variations of enantiostyly – A) feeding anthers (blue) centrally located; pollinating anther (orange) situated opposite the stigma, B) multiple anthers on one side; stigma and some anthers grouped together on the opposite side, C) complete separation of male and female parts on opposite sides, D) anthers grouped centrally; only the stigma deflects.

The two remaining stylar polymorphisms (inversostyly and enantiostyly) involve floral morphs that differ with regards to the direction in which the style is deflected in a flower (up or down in inversostyly; left or right in enantiostyly). Enantiostyly (also known as handedness), occurs in less than 3% of angiosperm species (Vallejo-Marín *et al.*, 2010). Many variations of enantiostylous anther-stigma configuration (fig. 1.1) have been recorded in 11 plant families (Vallejo-Marín *et al.*, 2010). The simplest form involves no anther dimorphism, with only the style facing left or right (i.e. non-reciprocal handedness in e.g. *Monochoria australasica*; Jesson and Barrett, 2003). At the other extreme, all the anthers are grouped on one side of the flower,

with the stigma situated on the opposite side (e.g. *Qualea* spp.; Morais *et al.*, 2020). Furthermore, the two mirror-morphs can either occur on the same (i.e. monomorphic enantiostyly in e.g. *Dilatris* spp.) or on separate (i.e. dimorphic enantiostyly in e.g. *Heteranthera multiflora*) plants within a population (fig. 1.2). Many enantiostylous species present two types of functionally distinct anthers (heteranthery), namely ‘feeding’ anthers and ‘pollinating’ anthers (Jesson *et al.*, 2003b). Feeding anthers are commonly vividly-coloured and situated centrally within a flower, thus matching poorly with the position of the stigma which is deflected to one side. Pollinating anthers match the position of the stigma on the opposite side, and are typically cryptically-coloured.

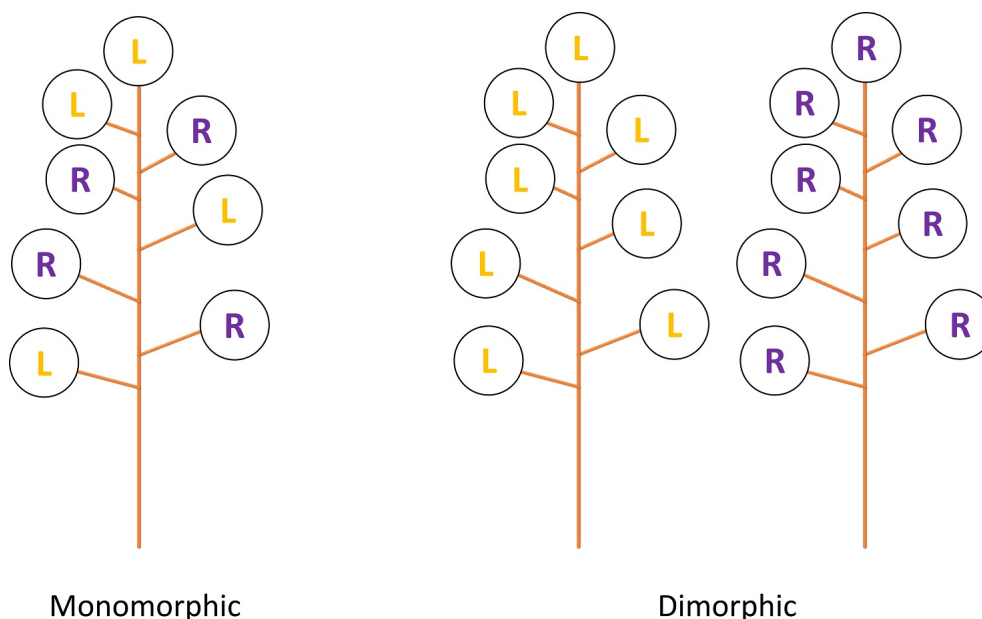


Figure 1.2: Diagrams depicting the composition of left- and right-handed flowers in monomorphic (left) and dimorphic (right) enantiostylous plants.

Like the other styler polymorphisms, enantiostyly promotes pollen movement between, rather than within morphs, since pollen is removed and received on the opposite sides of pollinators; thereby resulting in more efficient cross-pollination and a reduction in geitonogamy and autogamy (Minnaar, 2018; Ornduff and Dulberger, 1978; Barrett *et al.*, 2000; Jesson and Barrett, 2005). Dimorphic enantiostylous species are the best at achieving this, but even monomorphic enantiostyly has been shown to increase outcrossing when compared to non-enantiostylous forms (Jesson

and Barrett, 2005; Morais *et al.*, 2020).

Complete anther-stigma separation (male and female functions on opposite sides) has only been recorded in monomorphic species (e.g. Morais *et al.*, 2020). At first, the combination of dimorphic enantiostyly and complete anther-stigma separation would seem ideal, as it completely eliminates the risk of selfing within flowers and inflorescences, and ensures that pollen transfer occurs exclusively between morphs. However, it also carries a risk – if morph ratios are skewed in a population, such as during colonisation events, flowers will be highly mate-limited (Minnaar, 2018). The presence of non-reciprocally located anthers (such as viable ‘feeding’ anthers and anthers on the same side as the stigma) could mitigate this problem by contributing towards selfing, geitonogamy and/ or intra-morph mating; increasing the chances of pollen receipt when pollinators are scarce or when morph ratios are skewed (Jesson and Barrett, 2005; Minnaar, 2018). Indeed, Jesson and Barrett (2005) found that feeding anther pollen in *Solanum rostratum* contributed significantly to geitonogamous mating.

The family Haemodoraceae contains three South African enantiostylous genera – *Dilatris*, which is monomorphic, as well as *Barberetta* and *Wachendorfia*, which are both typically dimorphic (Helme and Linder, 1992; Ornduff and Dulberger, 1978; but see Jesson and Barrett, 2002; fig. 1.3). Dense stands of *Wachendorfia thyrsiflora* are often seen in wetland areas and have high incidences of clonality and large display sizes (Helme and Linder, 1992; Jesson and Barrett, 2002). *Wachendorfia brachyandra*, the rarest species, has small population sizes and small display sizes, which contribute to low pollinator visitation rates, but have been known to employ delayed selfing to offset this (Helme and Linder, 1992; Jesson and Barrett, 2002). *Wachendorfia multiflora* (syn. *W. parviflora*) flowers almost exclusively in August and September, and resembles *W. paniculata* in many ways except for being shorter in height and having narrow tepals and green bracts (Helme and Linder, 1992).

Wachendorfia paniculata Burm. (fig. 1.3 & fig. 1.4) has the most widespread

distribution of the four *Wachendorfia* species, occurring from Nieuwoudtville to Port Elizabeth in the Western and Eastern Cape provinces, South Africa (Helme and Linder, 1992). Mass-flowering populations (fig. 1.3) are commonly found in sandy soils within recently burnt or disturbed areas and typically flower for one to three months between August and December (Helme and Linder, 1992).



Figure 1.3: An example of a *Wachendorfia paniculata* inflorescence from the Overberg, Western Cape, South Africa (left). These flowers often occur in mass-flowering populations after fire, like the one seen here at Houwhoek Pass, Western Cape (right).

The high variability of floral and vegetative traits in *W. paniculata* across its range has led to taxonomic confusion in the past (Ornduff and Dulberger, 1978; Helme and Linder, 1992). Helme and Linder (1992) classified *W. paniculata* into three distinct ‘forms’ which have been known to co-occur in the same population. Forms 2 and 3 deviated from the ‘typical’ Form 1 by being abnormally tall (with thin, long leaves) and short (with thin, hairy leaves), respectively. Form 1 is particularly variable, with continuous variation being recorded for almost all vegetative and floral traits. Flower size and the distances between reproductive parts are examples of variable

traits which, from limited preliminary observations (Corneile Minnaar, pers. obs.), seem to be population-specific, and might be associated with differences in pollinator community composition between populations. In this study I focused on populations where Form 1 dominated, as it is the most widespread and variable form which made it ideal for this study.



Figure 1.4: Examples of left-handed (left) and right-handed (right) *W. paniculata* morphs, showing how the style is deflected left or right. Photographs: Bruce Anderson.

The floral anatomy of *W. paniculata* is highly unusual – two stamens are situated on one side opposite the stigma, and another stamen is situated on the same side as the style (fig. 1.4). The wide lateral separation distance between anthers means that pollen is placed predominantly on the beating wings of visiting pollinators (Minnaar and Anderson, 2021), which is an uncommon location for pollen placement (see Holmqvist *et al.*, 2005; Cruden and Hermann-Parker, 2016; Daniels *et al.*, 2020). Unlike most enantiostylous species (*sensu* Jesson and Barrett, 2002), *Wachendorfia* flowers have nectar, not pollen, as the main pollinator reward, and the flowers are not heterantherous, but have three identical anthers which vary only in their positions. Moreover, there is evidence that the separation distance between reproductive structures narrow over the course of a flower’s life, which is only a single day (Jesson and Barrett, 2002). This unusual suite of floral traits raises questions regarding the

functional significance of the floral configuration in *W. paniculata* during pollination. Due to the large separation distances between the anthers and stigma, it was previously thought that only large-bodied pollinators such as carpenter bees (*Xylocopa* spp.) or large flies (family Tabanidae) would succeed in pollinating *Wachendorfia* flowers (Goldberg, 1996; Ornduff and Dulberger, 1978; Helme and Linder, 1992). Surprisingly, Minnaar and Anderson (2021) found that wing pollen placement allows the lower anthers to utilise both small and large pollinator types (see appendix fig. B.3), whereas the upper anthers placed most of their pollen on the wings of larger pollinators. Using a novel pollen-labelling technique (namely quantum dot nanoparticles), Minnaar and Anderson (2021) found that the upper anthers contributed most toward inter-morph pollen transfer, with the lower anthers contributing a mixture of inter- and intra-morph pollen. They also found that carpenter bees (*Xylocopa caffra*) appear to be the only pollinators large enough to move pollen from the upper anthers and deposit it onto the stigma, as honey bee (*Apis mellifera capensis*) wings carried very little upper anther pollen. Consequently, Minnaar (pers. obs.) proposed that upper anthers might be adapted to larger pollinators, and that the degree of separation between floral structures might vary with regard to the pollinator community composition across its geographic range.

Even though spatial variability in phenotypic traits can be caused by neutral or random processes (Rafiński, 1979; Herrera *et al.*, 2006), geographic patterns that consistently emerge alongside ecological gradients often result from variation in divergent selective pressures (Stebbins, 1970; Galen, 1999; Johnson, 2010). In particular, geographic variation in floral morphology often corresponds to shifts in the availability of functional pollinator types across a landscape (Anderson *et al.*, 2010; Grant, 1949; Johnson, 2010; Stebbins, 1970; Theron *et al.*, 2019; but see Ellis and Johnson, 2009). Changes in pollinator quality, quantity, morphology or community composition can shape floral morphology, leading to adaptive radiation which creates floral ecotypes of the same species (Stebbins, 1970; Anderson *et al.*, 2014;

Boberg *et al.*, 2014; Opedal *et al.*, 2017). For instance, Anderson *et al.* (2014) found that floral tube length variation in *Tritoniopsis revoluta* corresponded to the average tongue lengths of local long-tongued fly assemblages. These ecotypes can then later diverge into separate species if the causal selective pressure persists for long enough and if reproductive isolation is in place between the different ecotypes (Stebbins, 1970; Johnson, 2010). Ecotype formation is especially prevalent in the Greater Cape Floristic Region (CFR), where ever-changing ecological and environmental gradients have led to the continuing adaptive radiation and diversification of the local flora and fauna (Johnson, 2010). Shifts in the utilisation of pollinators, habitat or other ecological resources have been put forward as major contributors of species diversification in the CFR, giving rise to extremely high levels of biodiversity (Johnson, 2010).

Apart from displaying substantial levels of phenotypic variation across its range, *W. paniculata* also exhibits variation in anther-anther and anther-stigma separation at the local scale through floral movement (Jesson and Barrett, 2002). Temporal variation in anther-stigma separation that is achieved through the lengthening (Liu *et al.*, 2020) or curving (Ruan *et al.*, 2009b) of reproductive structures can be interpreted as a reproductive assurance strategy if the degree of herkogamy decreases over time and if anthers and stigmas end up touching. Delayed autonomous selfing is a commonly cited consequence of this ‘movement herkogamy’ (Ruan *et al.*, 2009b; Ren and Tang, 2012; Liu *et al.*, 2020).

Lloyd (1992) maintained that delayed autonomous selfing is the most beneficial form of reproductive assurance, since it has fewer disadvantages associated with it than other selfing strategies. This is because delayed selfing postpones self-pollination until the opportunity for cross-pollination has passed, thus maximising outcrossing, while ensuring pollen receipt. This is particularly useful at times when pollinators are scarce (Ruan *et al.*, 2009a) and/or when there is small time window in which to achieve pollination (Liu *et al.*, 2020). For this reason, reproductive assurance might

be particularly important for flowers that only last for a single day, such as *W. paniculata*. Even though Jesson and Barrett (2002) indicated that floral movement in *W. paniculata* does not result in delayed autonomous selfing, it might still have a reproductive assurance function. It is possible that floral narrowing increases the frequency of contact between the reproductive structures and pollinators, thus maximising the chances of pollen receipt. This could be useful during periods of inclement weather when pollinators might be scarce (Jesson and Barrett, 2002).

Evidently, *W. paniculata* is a unique and highly complex species that exhibits both spatial and temporal variation in the degree of spatial reproductive separation. Few studies have investigated variation in reproductive separation distances with relation to pollinator shifts, and even fewer have done so for enantiostylous species. For instance, Lázaro *et al.* (2020) found that long-tongued pollinators were more frequent in *Lonicera implexa* populations where the anthers were exerted far past the stigma (reverse herkogamy), while short-tongued pollinators associated more with flowers where the anthers were situated behind the stigma (approach herkogamy). Moreover, floral movement has rarely been recorded in enantiostylous species which means that studies that investigate its functional significance are almost unheard of (but see Jesson and Barrett, 2002).

For the sake of brevity and clarity, the use of the term ‘herkogamy’ in this manuscript will strictly refer to anther-stigma spatial separation only. The term ‘reproductive separation’ will refer to the spatial separation distance between any of the sexual organs, including anther-anther separation. ‘Floral narrowing’ is defined as the active movement of the reproductive structures towards each other to decrease the reproductive separation distances over time.

In this study, I examined the variation in the degree of reproductive separation in *W. paniculata* at the spatial scale as well as the temporal scale, and whether this variation is functionally significant with regards to pollination within and between populations. This was divided into two parts:

1. I described the extent of geographic variation in the degree of reproductive separation for *W. paniculata*, and assessed pollinator community compositions in 15 *W. paniculata* populations. I hypothesised that the variation in the distances between reproductive structures in *W. paniculata* associate with corresponding shifts in pollinator community composition across its geographic range. Upper anther-stigma distance was expected to decrease in populations where large pollinators (e.g. carpenter bees) were scarce or absent, whilst lower anther distances were expected to remain relatively the same, regardless of flower size. Within each population, floral measurements were taken and pollinator visitation rates and abundances were assessed through observations that were conducted over two non-consecutive days. I also investigated whether floral movement could have been a possible contributing factor in past observations of geographic variation in reproductive separation. The resulting findings prompted me to examine floral movement in more detail in the second part of the study.
2. I examined the temporal variation in the degree of reproductive separation by recording floral movement for the duration of anthesis in a single population. I established the extent and variation of floral narrowing in *W. paniculata* and whether it held any functional significance for pollination performed by honey bees. I hypothesised that the narrowing of the distances between reproductive structures acts as a mechanism of reproductive assurance either by promoting pollinator-mediated selfing (via geitonogamy or autogamy) or by increasing the likelihood of wings making contact with the stigma and/or anthers later in the day when larger pollinators are absent or when visitation rates are low. I measured the lateral and vertical separation distances hourly and presented virgin donor and recipient inflorescences to honey bees to record how pollen deposition and receipt rates changed with floral narrowing.

CHAPTER 2

GEOGRAPHIC AND TEMPORAL VARIATION IN THE SPATIAL REPRODUCTIVE SEPARATION OF A HANDED FLOWER: A MOVING TARGET

ABSTRACT

Geographic variation in floral morphology has often been associated with co-variation in the availability of regionally-specific functional pollinator types, giving rise to plant ecotypes that are finely adapted to the morphology of local pollinators. *Wachendorfia paniculata* is a geographically variable handed flower with preliminary observations suggesting that differences in pollinator wingspans between populations might be driving differences in the spatial separation between floral reproductive structures across the Western Cape, South Africa. I investigated the extent of this geographic variation and whether it was related to the local pollinator types in 15 *W. paniculata* populations. Additionally, floral movement throughout the day was investigated as a possible source of variation in 16 populations. The distances between the upper anther and the stigma and between the two lower anthers varied significantly between populations. Contrary to expectation, large pollinators appeared unimportant in the extant pollinator landscape. Even though the mean weighted wingspan of pollinators in a population did not predict the degree of reproductive separation, increasing pollinator visitation rates were associated with a narrowing of the distance between the lower anthers. This trend, which was driven by honey bees, suggests that frequent visits by small pollinators might result in a narrower distance between lower anthers. Floral narrowing over time explained a significant proportion of the variation in the degree of reproductive separation when locality was included in the statistical model. I conclude that the variation in the degree of reproductive separation cannot be explained by one variable alone, but rather that various biotic and abiotic selective pressures are likely at play.

INTRODUCTION

The mechanisms through which angiosperms diverge into separate lineages have been one of the central questions within the field of evolutionary biology (Van Der Niet *et al.*, 2014). Although geographic patterns in the phenotypic traits of plants can be caused by neutral processes such as founder effects (Rafiński, 1979) or genetic drift (Herrera *et al.*, 2006), frequent geographic associations between plant morphology and ecological gradients suggest that trait divergence is more often the product of divergent selection (Stebbins, 1970; Galen, 1999; Johnson, 2010).

Divergence in plant phenotypes has often been linked to geographic variation of either biotic and/ or abiotic factors (Herrera *et al.*, 2006; Lambrecht and Dawson, 2007; Pérez-Barrales *et al.*, 2009; Zhao and Wang, 2015; Weber *et al.*, 2020) which are thought to generate divergent selective pressures on plants across their ranges. For example, variation in floral morphology has commonly been associated with varying selective pressures imposed by pollinators (Anderson *et al.*, 2010; Grant, 1949; Johnson, 2010; Stebbins, 1970; Theron *et al.*, 2019; but see Ellis and Johnson, 2009). Differences in pollinator community (Boberg *et al.*, 2014; Opedal, 2019), pollinator preferences (Gómez *et al.*, 2008), morphology (Anderson *et al.*, 2010; Newman *et al.*, 2015), pollinator quality or quantity (Stebbins, 1970) can all affect floral trait variation. Consequently, exposure to different pollinator environments can lead to fine-scale adaptation of a flower to local pollinator types (Johnson, 2006; Peter and Johnson, 2014; Newman *et al.*, 2015). This form of adaptive radiation gives rise to distinct floral ecotypes of the same plant species, which might subsequently evolve into separate species (Grant, 1949; Stebbins, 1970; Anderson *et al.*, 2014; Van Der Niet *et al.*, 2014; Newman *et al.*, 2015). For example, Anderson *et al.* (2010) showed that long- and short-tubed *Gladiolus longicollis* populations matched the bimodal distribution of proboscis lengths of hawkmoth visitors, and that an overlap in pollinator types resulted in flowers with intermediate tube lengths.

The Cape Floristic Region (CFR) is a biodiversity hotspot in South Africa that

contains a species-rich array of unique angiosperms adapted to highly variable biotic and abiotic environments across a small geographic range (Johnson, 2010). Ecotype formation and speciation in response to divergent pollinator pressures has occurred multiple times in the CFR (Johnson, 2010; Anderson *et al.*, 2014; Theron *et al.*, 2019). For example, Newman *et al.* (2015) found that variation in the length of floral reproductive parts in *Nerine humilis* co-varied with the mean pollinator length across its geographic range.

In hermaphroditic flowers, the degree of herkogamy (the spatial separation of stigmas and anthers in a flower) may also be under pollinator selection. Increasing the distance between stigmas and anthers promotes outcrossing and limits pollinator-mediated selfing (Barrett *et al.*, 2000; Takebayashi *et al.*, 2006). The narrowing of this distance has been associated with low pollinator visitation rates and a resulting shift towards autonomous selfing (Ruan *et al.*, 2009a; De Waal *et al.*, 2012). While most studies investigating variation in the degree of reproductive separation have focused on its role in selfing strategies or the maintenance of heterostyly (Kálmán *et al.*, 2007), few have looked at the associations between pollinators, geographic variation and the distances between floral reproductive structures. For instance, Lázaro *et al.* (2020) suggested that variation in herkogamy in *Lonicera implexa* was associated with differences in the visitation rates and assemblages of long- and short-tongued pollinators in different populations.

Wachendorfia paniculata (family Haemodoraceae) is a common geophyte that can be found in the sandy soils of the fynbos throughout the CFR (Ornduff and Dulberger, 1978). Mass-flowering populations can usually be found in young vegetation types after recent fires (Helme and Linder, 1992). Inflorescences bear multiple flowers daily and each flower lasts a single day. All species within the genus display enantiostyly or handedness which is a form of reciprocal herkogamy (Helme and Linder, 1992). Here, the styles of *Wachendorfia* plants can either be deflected to the left or the right. Two of the three anthers are always deflected in the opposite direction to the style

(see fig. 2.1) and one anther is deflected in the same direction (Helme and Linder, 1992; Barrett *et al.*, 2000; Jesson and Barrett, 2002; Jesson *et al.*, 2003a). Left- and right-handed morphs place and receive most of their pollen from alternate sides of their pollinators. Consequently, most pollen movement occurs between different morphs rather than within morphs, leading to disassortative outcrossing (Ornduff and Dulberger, 1978; Barrett *et al.*, 2000). Inter-morph mating reduces selfing and the loss of pollen to flowers in the same plant (Barrett *et al.*, 2000).

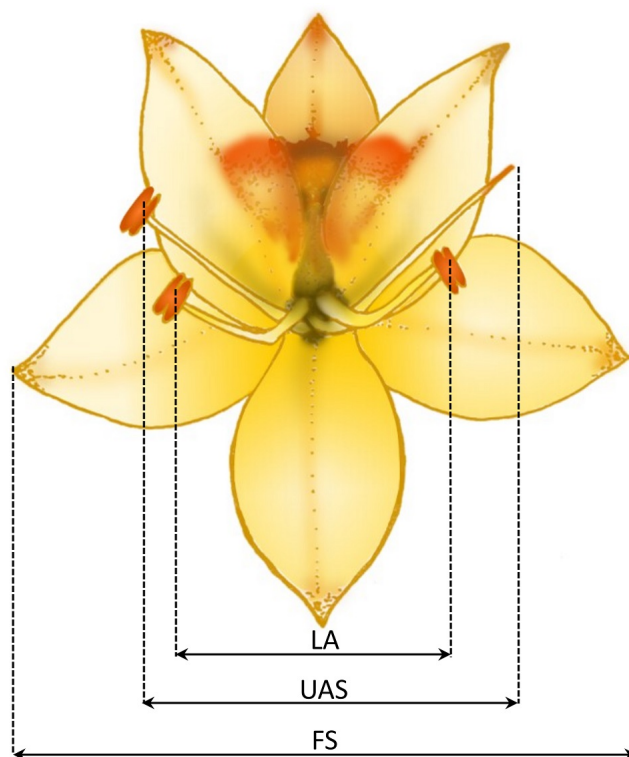


Figure 2.1: The structural anatomy of a left-handed *Wachendorfia paniculata* flower. For this study, three floral measurements were taken, namely the distance between the lower anthers (LA), the distance between the upper anther and the stigma (UAS) and flower size (FS).

Wachendorfia paniculata is the most widespread and variable species within the genus. Vegetative (e.g. plant size and leaf morphology) and floral traits (e.g. inflorescence size, perianth width and colour) of *W. paniculata* are highly variable across its range, which has led to taxonomic confusion in the past (Helme and Linder, 1992). Here, I study geographic variation in the degree of reproductive separation (which includes anther-stigma and anther-anther distances). Reproductive separa-

tion varies considerably across *W. paniculata* populations (Ornduff and Dulberger, 1978; Helme and Linder, 1992). While preliminary observations (Corneile Minnaar per. obs.) suggested that the degree of reproductive separation may be an adaptive response to different pollinator environments, Jesson and Barrett (2002) also demonstrated that the distances between reproductive structures decrease during the day. Greater separation distances may be associated with pollination by pollinators with large wingspans (such as carpenter bees – *Xylocopa* spp.) while narrower separation may be associated with visits by pollinators with short wings (such as honey bees – *A. mellifera*). Minnaar and Anderson (2021) further indicated that the upper anther might be intended for pollination by large pollinators, as it only made consistent contact with carpenter bee (*Xylocopa caffra*) wings which were found to export most of the pollen from the upper anthers. Honey bees (*Apis mellifera capensis*) mostly exported pollen from the lower anthers, as their narrow wingspans meant that they rarely made contact with the upper anthers. The unique arrangement of reproductive parts in *W. paniculata* may serve as a type of bet-hedging strategy, where the upper anther exports most of the high-quality inter-morph pollen when large pollinators are present, but lower anthers export at least some inter- and intra-morph pollen via small pollinators when large pollinators are absent (Minnaar, 2018).

Very few studies have investigated the mechanical fit between enantiostylous flowers and their pollinators (e.g. Solís-Montero and Vallejo-Marín, 2017; Morais *et al.*, 2020; Minnaar and Anderson, 2021), presumably since many are buzz-pollinated and are assumed to not require highly precise pollen placement mechanisms for effective pollination. However, in *Solanum rostratum*, a buzz-pollinated enantiostylous flower, it has been shown that the fit between pollinator size and the reproductive parts of flowers influenced the amount of pollen that was deposited on a pollinator, thereby indicating that size matching between floral and pollinator anatomy could be important for at least some enantiostylous species (Solís-Montero and Vallejo-Marín, 2017).

Although comprehensive surveys of the floral visitors of *W. paniculata* have not yet been conducted, Jesson and Barrett (2002) observed visitation by honey bees, anthophorid bees and tabanid flies, whereas Minnaar and Anderson (2021) and Scott Elliot (1891) observed carpenter bees and honey bees visiting flowers, with honey bees being the most common visitors. Goldberg (1996) found that a tabanid fly had the highest *W. paniculata* pollen loads out of four visitor types, including an unspecified bee species, at the Waylands Flower Reserve in Darling, which I revisited in this study. Ornduff and Dulberger (1978) and Helme and Linder (1992) speculated that the wide lateral separation distance between the reproductive structures suggests that large pollinators such as *Xylocopa caffra* or large tabanid flies are likely the intended pollinators, since smaller pollinators were never observed to make contact with the reproductive structures. However, Minnaar (2018) demonstrated that flying pollinators, including honey bees, receive pollen when they approach the flower by beating their wings against the anthers. Consequently, large bodies are not required for pollen receipt to occur.

In this study, I aim to describe the extent of geographic variation in the degree of reproductive separation for *W. paniculata*, focusing on the lateral separation distance between reproductive structures, and to assess pollinator community compositions in *W. paniculata* populations. I hypothesise that the variation in the distances between anthers and stigmas in *W. paniculata* can be explained by corresponding shifts in pollinator community composition across its geographic range. Upper anther-stigma distance is expected to decrease in populations where large pollinators (e.g. carpenter bees) are scarce or absent, whilst lower anther distances are expected to remain relatively constant, regardless of flower size.

Alternatively, one might also expect that smaller distances between the reproductive parts are ideally suited to generalist pollination (Herrera, 1996; Galen, 1999; Muchhala *et al.*, 2010). Most flower species are visited by a range of visitors that vary in pollination efficiency. Instead of adapting to a specific pollinator, floral

anatomy might adapt to a subset of more efficient pollinators or might not show any adaptation (Herrera, 1996). Generalisation of floral anatomy can also result from great temporal fluctuations in the composition of pollinator communities between years (Herrera, 1996). In *W. paniculata* populations with a low overall pollinator visitation rate, efficiency of cross-pollination might be increased by allowing all reproductive structures to contact pollinators' wings, regardless of their size. Conversely, larger distances could indicate pollinator selectivity: in populations with high visitation rates by large pollinators, the plant can afford to be selective towards larger pollinators, thereby excluding the subset of smaller pollinators and increasing the probability of receiving inter-morph pollen.

Finally, it is possible that the movement of reproductive structures throughout the course of a day could account for some of the geographic variation in reproductive separation that has been observed in the past. Therefore, I wanted to test whether the narrowing of floral structures throughout the day could account for significant variation in the degree of reproductive separation across its geographic range.

MATERIALS AND METHODS

Study sites

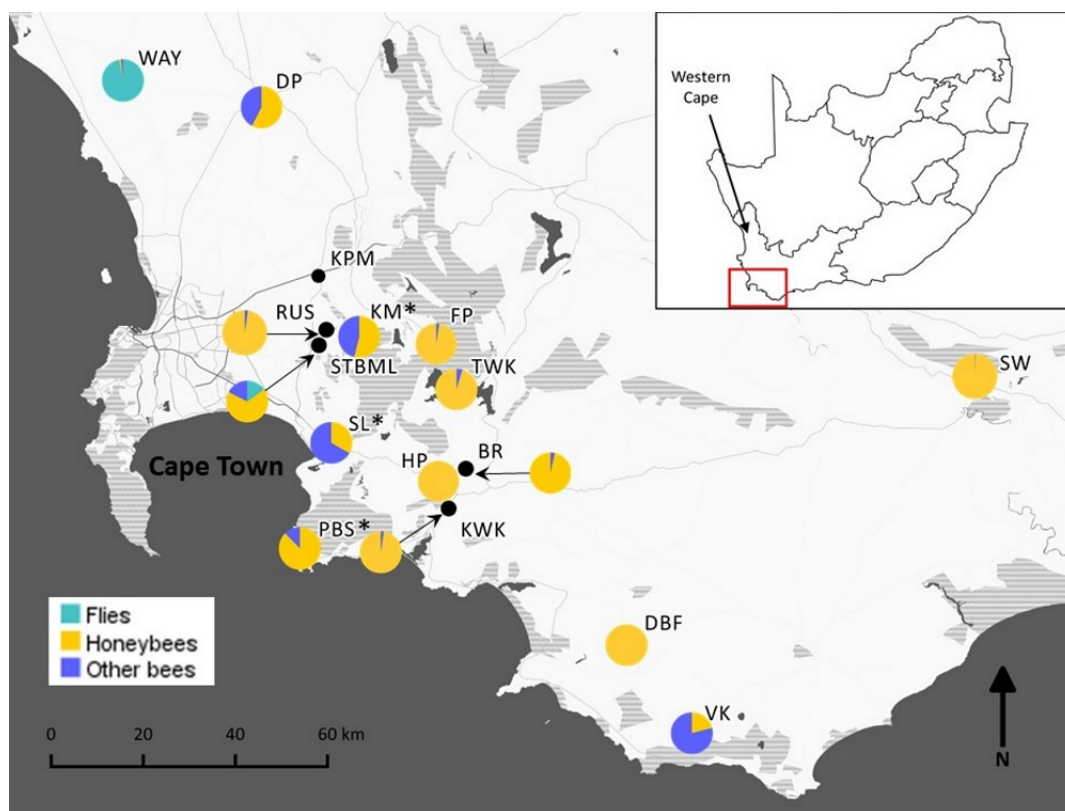


Figure 2.2: A map of the 16 *Wachendorfia paniculata* populations that were sampled throughout the Western Cape, South Africa (map insert). Pie charts depict the proportion of main functional pollinator types present for sites where pollinator data were collected. Site names with asterisks only have a single day of pollinator observations. Site names and coordinates are listed in full in appendix table A.1. Pollinator community compositions are displayed in detail in appendix figure A.1 and appendix tables A.2 & A.3.

A total of 16 *Wachendorfia paniculata* populations (fig. 2.2; Appendix table A.1) were sampled across the Western Cape, South Africa, in the austral springtime of 2018 and 2019. Fifteen of these populations were sampled for pollinator abundances and visitation rates to *W. paniculata* flowers. Study sites covered a wide variety of elevations (25 – 671 m above sea level), peak flowering times (August – November), veld ages (<1 and >10 years after fire) and pollinator environments (appendix table A.2).

Floral measurements



Figure 2.3: Photographs of the maximum and minimum absolute floral distances recorded for UAS and LA demonstrate the variation seen in flower size and the degree of reproductive separation for *W. paniculata* between populations. Bold white crosses indicate the position of the stigma, while diamonds represent the position of the relevant anthers. The scale bar is shown in millimeters. For UAS, WAY had a maximum of 27.55 mm while HP had a minimum of 10.84 mm. For LA, SL had a maximum of 21.83 mm, while SW had a minimum of 7.93 mm.

Within each of the 16 populations, 30 plants were randomly selected and a single mature flower from the centre of each inflorescence was photographed in a set position with a Sony RX 100 VI camera. Since *W. paniculata* corms are known to produce clonal plants (Ornduff and Dulberger, 1978; Jesson and Barrett, 2002), care was taken to select plants that were at least 5 m apart. A metal ruler secured to the camera at a fixed distance ensured that measurements were to scale with minimal depth distortion. Upper anther-stigma distance (UAS, fig. 2.1) and lower anther distance (LA, fig. 2.1) were recorded for each flower, as well as the time at which each measurement was taken. For each floral measurement, two points of interest were aligned parallel to the ruler before a photograph was taken (fig. 2.3). Precise measurements were obtained at a later stage with the use of ImageJ (version 1.52n; Abramoff et al., 2004). Flower size (FS, fig. 2.1) was measured in the field to the

closest millimetre by carefully straightening the two lateral tepals against a ruler.

Flower size was positively associated with the degree of reproductive separation (Pearson's product moment UAS: $r = 0.34$, $n = 479$, $p < 0.001$; LA: $r = 0.30$, $n = 479$, $p < 0.001$), suggesting that separation distance might scale allometrically with flower size. Consequently, distance measurements were standardised for flower size to determine how much these distances deviated from the expected scaling relationships associated with flower size. This was done by dividing individual distance measurements by individual flower size measurements, giving a standardised measurement (as a proportion) relative to flower size. Unstandardised (absolute) measurements were used in analyses associated with pollinator wingspan and visitation rates because any selection imposed by pollinators on the reproductive separation distances is expected to result from the fit between a pollinator's morphology and the absolute distances between floral reproductive structures.

To determine whether the degree of reproductive separation differs between *W. paniculata* sites, ANOVAs were performed with floral size-standardised distance (LA or UAS) as the response variable. Tukey HSD post-hoc tests were done to view individual pairwise comparisons between sites. A Mantel test for spatial autocorrelation determined whether the standardised floral measurements for populations in close proximity to each other are more similar than those that are geographically far apart.

The combined effects of time of day and site on the degree of reproductive separation were examined in multiple regressions with site and hours after sunrise as predictor variables and standardised distance (UAS or LA) as the response variable.

All statistical analyses were performed using R version 3.6.0 (R Core Team, 2020) and the packages lme4 (Bates *et al.*, 2015), nlme (Pinheiro *et al.*, 2021) and ade4 (Thioulouse *et al.*, 2018).

Effects of pollinator visitation and wingspan on geographic floral variation

Pollinator community composition and visitation rates for each population were assessed by observing two small plots of flowers (5 – 9 m² with a density of 0.6 – 17.5 plants per m²) over two non-consecutive days during the flowering peak of each population. Observations commenced when the flowers opened and concluded when pollinator activity decreased markedly during the late afternoon, with an average of eight observations per day. Plot observations of 15 minutes each were done hourly to determine the visitation rates per flower per hour. In addition, I recorded the number of visitors seen on *W. paniculata* flowers during 15-minute long random walks throughout the population. These population surveys provided pollinator abundances and allowed for the detection of uncommon and skittish pollinators. For example, *Xylocopa* species were reluctant to approach a plot with a seated observer nearby, and were thus more likely to be recorded during a walk. Because large insects are easier to detect and identify at a distance, it would be easy to bias counts towards larger pollinators. However, the flight patterns of different pollinators were easily distinguished from a distance, and thus smaller pollinators were confidently detected and identified during walks.

Functional pollinators were defined as non-destructive insects that were observed to consistently alight on a flower in the same orientation and whose wingspan or body width was large enough to make contact with the anthers and stigma. These included most bee species (excluding bees with a wingspan smaller than 10 mm – e.g. bees from the genera *Allodapula* and *Ceratina*) as well as flies from the Bombyliidae and Tabanidae families. I observed that most of these pollinators either made contact with the floral reproductive parts, or had visible pollen on their wings. Butterflies, beetles and smaller insects were not considered functionally significant, as they were inconsistent in their landing orientation, and rarely made contact with the anthers or stigma.

Since visitation rate data were heteroscedastic, the relationship between pollinator

visitation rate and reproductive separation was analysed using a generalised least squares regression (GLS), with the overall mean visitation rate per population as the predictor variable and mean absolute floral distance (UAS or LA) as the response variable. A similar GLS was performed for *A. mellifera* visitation rate only, since honey bees were by far the most abundant and consistent pollinators throughout the landscape and could possibly be the main driving factor behind any patterns observed regarding visitation rate.

To determine whether size differences of pollinators in a population might be driving geographic floral variation, wingspans for 15 functional pollinators (12 species) were measured to the nearest half-millimetre (table 2.1). Forewing lengths and inter-tegula widths were measured individually and summed to produce the total wingspan.

Since the distribution of wingspans were not multimodal, and could not be grouped into distinct size classes, it was decided to calculate a weighted grand mean for each population using the method described by Newman *et al.* (2015) – I calculated a weighted wingspan for each functional pollinator type according to its abundance during random walks within a particular population. The mean wingspan of a pollinator type (table 2.1) was multiplied by its proportion of the total number of pollinators at each site. All weighted wingspans at each site were then summed to obtain a grand weighted mean for that population. Standard errors for the weighted means were calculated using the method described by Cochran (1977). Data from random walks were used to weight the means as uncommon pollinator abundances were better assessed during walks than during plot observations.

To determine whether pollinator wingspan could explain geographical differences in reproductive separation distances, the mean floral distance (UAS or LA) was plotted as a function of the grand mean weighted wingspan of each population. The relationship between these two variables was analysed using a Spearman's rank correlation.

RESULTS

Geographic variation in reproductive separation

The mean (\pm SD) absolute distances measured between the upper anther and the stigma (UAS) and the two lower anthers (LA) across 16 populations were 17.81 ± 2.87 mm and 12.76 ± 2.38 mm, respectively.

The degree of reproductive separation differed significantly between sites (UAS: $F_{15, 463} = 18.45$, $p < 0.001$; LA: $F_{15, 463} = 28.97$, $p < 0.001$; fig. 2.4). The Klapmuts site (KPM) had the largest mean standardised UAS distance (\pm SE) at 0.45 ± 0.01 mm, while the Vlooiakraal (VK) site had the smallest at 0.33 ± 0.01 mm (fig. 2.4). Sir Lowry's Pass (SL) had the largest mean standardised LA distance (\pm SE) at 0.35 ± 0.01 mm, and Swellendam (SW) had the smallest at 0.22 ± 0.01 mm (fig. 2.4).

The degree of reproductive separation was not spatially autocorrelated, since the two matrices – spatial distance and standardised floral measurement – were unrelated (Mantel test – LA: $r = -0.080$, $p = 0.619$; UAS: $r = -0.097$, $p = 0.692$).

The effect of time on reproductive separation

The combined effects of time of day and site explained 44% of the variance seen within standardised UAS ($F_{16, 462} = 22.83$, $p < 0.001$) and 50% of the variance in LA ($F_{16, 462} = 29.20$, $p < 0.001$). While the effect of time appears weak because standardised distance only decreased by 0.017 (UAS) and 0.007 (LA) per hour (fig. 2.5), the effects appear much more impressive when converted to absolute values: if multiplied by the mean (\pm SE) flower size of 48.11 ± 0.21 mm, it amounts to a 0.81 ± 0.004 mm and 0.33 ± 0.002 mm decrease in absolute UAS and LA per hour, respectively, which is in accordance with measurements obtained for chapter 3.

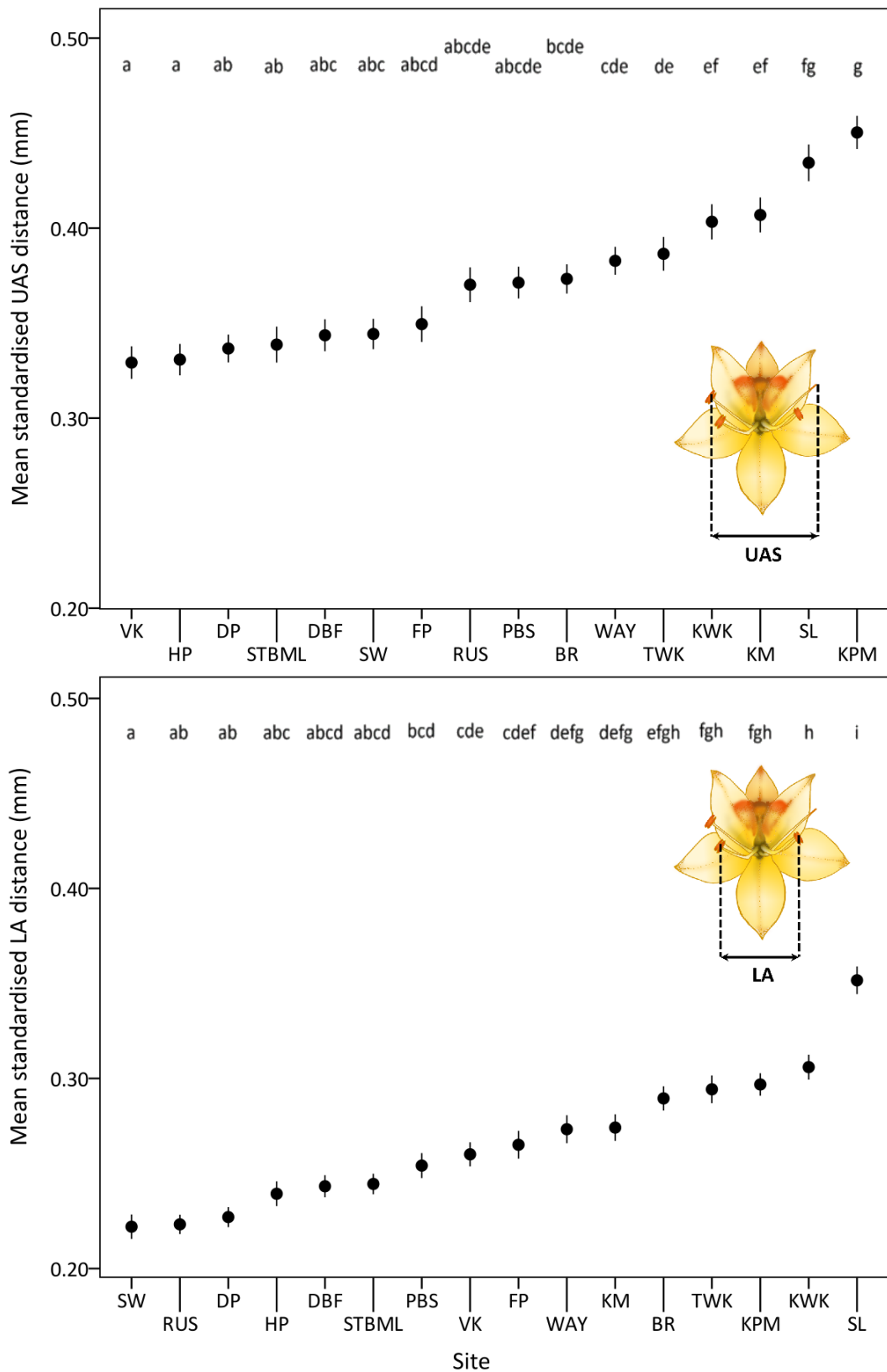


Figure 2.4: Means \pm SE of standardised floral distances for 16 *W. paniculata* populations for UAS (top) and LA (bottom) floral measurements. Sites that have letters in common are not significantly different from each other. See Table A.1 for site abbreviations.

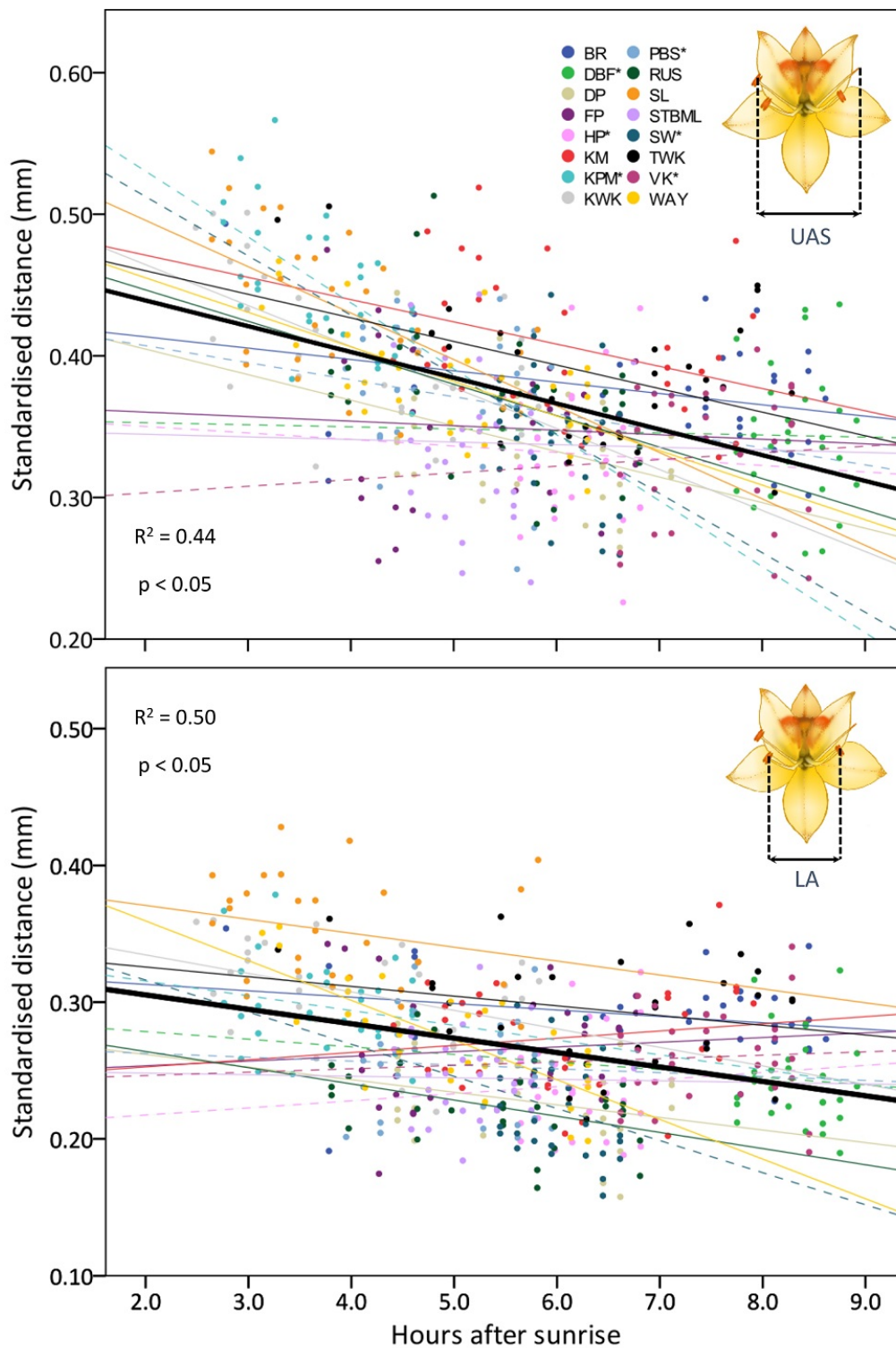


Figure 2.5: The effect of time of day (hours after sunrise) on the standardised floral distance for UAS (top) and LA (bottom) measurements of 16 *W. paniculata* populations. Sites indicated with an asterisk and dashed lines were measured over less than 2.5 hours, while those measured over a period of more than 2.5 hours have solid lines. Linear trends for the pooled data are indicated in bold black lines. R^2 and p -values reflect results for the pooled data

Pollinator community composition

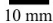















Wachendorfia paniculata was visited by a total of 25 insect species (appendix table A.2) across all geographical sites, with 12 being classified as functional pollinators (table 2.1). On average (\pm SD), a *W. paniculata* flower received 2.53 ± 2.55 functional visits per hour. The population at Driehoekpad nature reserve (DP) had the highest diversity of visitors (10 species), six of which were bees. Du Bois Farm (DBF) had the lowest species diversity (4 species), with honey bees being the only functional pollinators in the population.



Figure 2.6: Honey bees (*Apis mellifera capensis*, left) were the most common pollinators of *W. paniculata*, while carpenter bees (*Xylocopa caffra*, right) were the largest pollinators. Note the typical *W. paniculata* pollen deposition visible on the wings of the honey bee. Photographs: Bruce Anderson.

Across all populations, various bee species made up 99% of all visits to *Wachendorfia* flowers. Of all pollinator species, Cape honey bees (*Apis mellifera capensis*, fig. 2.6) were the most widespread, abundant and consistent visitors to *W. paniculata* with an overall mean (\pm SD) visitation rate of 2.63 ± 2.74 visits per flower per hour across all sites, making up 94% of all visits (appendix fig. A.1). Honey bees were present at all sites and the most abundant pollinators at 13 out of 15 populations (appendix table A.2 & A.3). Solitary digger bees from the tribe Anthophorini were the second-most abundant and widespread group of pollinators to visit *W. paniculata*, with a presence of at least one of four species at 12 out of 15 populations.

Table 2.1: A list of pollinator species that were found to visit *W. paniculata* across 15 populations. Means \pm SE and (number) of insects measured to obtain wingspans used to calculate the grand weighted wingspan in each population. The number of sites at which a species was present represents how widespread a species was. The mean number of times (\pm SD) that a species was likely to be encountered during a 15-minute random walk is shown as a measure of abundance of each species across all sites.

Species	Mean wingspan \pm SE (mm)	# Sites present	Mean # encounters/random walk \pm SD
  <i>Xylocopa caffra</i> f.	51.38 \pm 0.24 (4)	2	0.16 \pm 0.61
 <i>Xylocopa caffra</i> m.	42.5 \pm 0.50 (2)	2	-
 <i>Philoliche</i> sp. 1	39.25 \pm 0.43 (4)	1	0.05 \pm 0.19
 <i>Australoechus hirtus</i>	33.17 \pm 1.18 (6)	1	0.22 \pm 0.85
 <i>Xylocopa rufitarsis</i>	31.83 \pm 1.83 (3)	3	0.05 \pm 0.12
 <i>Anthophora</i> sp. 1	27.70 \pm 0.58 (5)	5	0.35 \pm 0.70
 <i>Rediviva parva</i> f.	25.00 (1)	1	0.04 \pm 0.14
 <i>Anthophora</i> sp. 2 (large)	25.00 (1)	4	0.01 \pm 0.03
 <i>Philoliche</i> sp. 2	23.00 (1)	1	0.14 \pm 0.56
 <i>Anthophora</i> sp. 3	23.00 (1)	2	0.03 \pm 0.10
 <i>Amegilla</i> sp. 1	23.00 (1)	4	0.03 \pm 0.05
 <i>Apis mellifera capensis</i> f.	22.60 \pm 0.29 (5)	15	9.92 \pm 9.56
 <i>Rediviva parva</i> m.	21.83 \pm 0.44 (3)	2	0.18 \pm 0.69
 <i>Anthophora</i> sp. 2 (small)	21.25 \pm 0.25 (2)	3	0.11 \pm 0.36
 <i>Bombylius</i> sp. 1	19.00 (1)	3	0.02 \pm 0.04

Contrary to expectation, large pollinators, such as carpenter bees (*Xylocopa caffra*, fig. 2.6), were infrequent, sporadic pollinators of *Wachendorfia paniculata*. Large carpenter bees (*X. caffra*) had a mean overall visitation rate of 0.01 (± 0.04 SD) visits per flower per hour and comprised only 0.1% of all flower visits and 2% of total encounters on random walks. Only three populations had *X. caffra* present (appendix table A.2), and only the Stellenbosch Mountain (STBML) population was visited consistently (comprising 20% of all pollinators that were recorded during random walks). Three populations were visited by red-legged carpenter bees (*Xylocopa rufitarsis*), comprising 1% (FP), 2% (RUS) and 0.04% (STBML) of the total number of pollinators observed during random walks. A single population, Waylands Flower Reserve (WAY), was visited almost exclusively by two large fly species from the genera *Philoliche* (Tabanidae) and *Australoechus* (Bombyliidae), which visited a flower on average 0.05 and 1.13 (± 2.58 SD) times per hour, respectively.

Effects of pollinator visitation rates on geographic floral variation

Mean LA distance decreased significantly with an increase in the overall visitation rate (AIC = -59.87, $\beta = -0.24$, $t_{15,13} = -2.45$, $p = 0.029$; fig. 2.7) as well as the honey bee visitation rate (AIC = -59.24, $\beta = -0.25$, $t_{15,13} = -2.65$, $p = 0.020$; fig. 2.7). Therefore, for every additional functional pollinator visit per flower per hour, LA would decrease by 0.24 mm and for every additional honey bee visit per flower per hour, LA would decrease by 0.25 mm per hour. Visitation rate did not have a significant effect on mean UAS for either the overall (AIC = -59.98, $\beta = -0.16$, $t_{15,13} = -1.79$, $p = 0.097$; fig. 2.7) or honey bee visitation rates (AIC = -59.60, $\beta = -0.12$, $t_{15,13} = -1.38$, $p = 0.191$; fig. 2.7).

The effects of pollinator wingspan on geographic floral variation

There was no observable association between the grand mean functional pollinator wingspan and the degree of reproductive separation (UAS: $n = 15$, $r_s = 0.22$, $p = 0.428$; LA: $n = 15$, $r_s = 0.15$, $p = 0.585$; appendix fig.A.2).

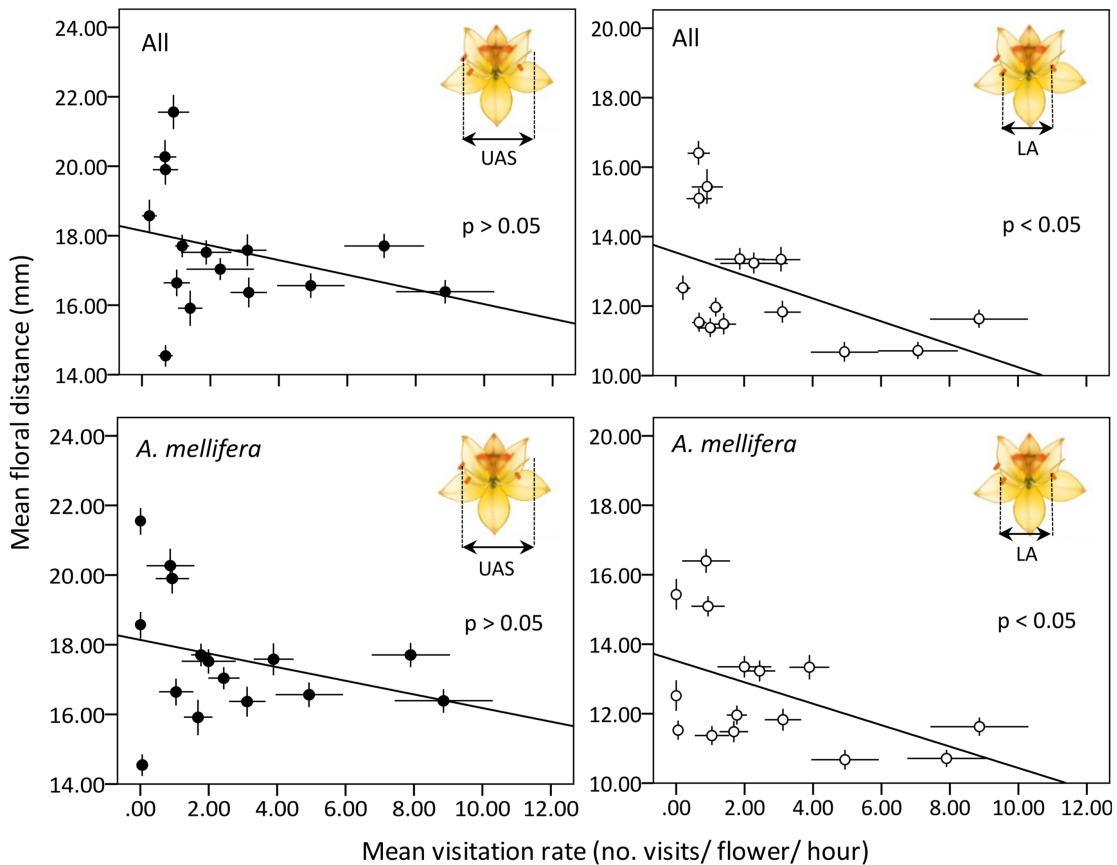


Figure 2.7: Mean absolute floral distance \pm SE (UAS – filled circles and LA – unfilled circles) for fifteen *W. paniculata* populations plotted against the mean \pm SE functional pollinator visitation rate recorded for each site. The top two figures have the overall visitation rate per site as the predictor variable, which includes all functional pollinator types, whilst the two bottom figures have honey bee visitation rate as the predictor variable, which excludes all other visitors. Linear and exponential decay curves were fitted, but since exponential decay only improved the R^2 marginally (by 1%), it was decided to use linear trends to simplify the statistical analyses.

DISCUSSION

Geographic variation in floral morphology has been known to result from divergent selective pressures generated by shifts in pollinator assemblages across a landscape (Grant, 1949; Stebbins, 1970; Anderson *et al.*, 2010; Johnson, 2010; Theron *et al.*, 2019; but see Ellis and Johnson, 2009). In this study, I documented the geographic variation in the degree of reproductive separation for *Wachendorfia paniculata*, and investigated whether this variation associated with population-level shifts in pollinator community composition.

Wachendorfia paniculata populations showed considerable variation in the distances between reproductive structures across the landscape, which can partly be explained by flower size, location, time of day and pollinator visitation rate, but not by mean pollinator wingspan. Below, I discuss these associations with particular reference to the idea that geographic variation in floral morphology is an adaptation to pollinator assemblages (*sensu* Stebbins 1970; Johnson, 2010).

Associations between floral phenotype and pollinator community

Even though *W. paniculata* was visited by a diverse array of insects, the yellow colouration and high visitation rates by various bees suggest that bee species are the primary pollinators. The spectral reflectance pattern (appendix section II fig. A.3) of a contrasting UV-absorbing nectar guide at the centre and UV-reflecting outer edges of the tepals is also consistent with many bee pollination syndromes (Papiorek *et al.*, 2016), although some tabanid fly species are also attracted to similar yellow and UV contrasting patterns (Ellis and Johnson, 2009).

Large pollinators such as *Xylocopa caffra* were mostly sporadic and infrequent pollinators in the few populations where they were present, contradicting the prediction of Jesson and Barrett (2002) that large pollinators are important for the pollination of *W. paniculata*. It seems most likely that the high fruit set (per. obs.) and high outcrossing rates (0.79 – 0.98, see Jesson and Barrett, 2002) in *W. paniculata* pop-

ulations are the consequences of frequent visits by smaller pollinators such as honey bees, which have been known to pick up large amounts of *W. paniculata* pollen on their wings (Minnaar, 2018).

A decrease in herkogamy or reproductive separation is often associated with a shift towards selfing when pollinators are limited (Ruan *et al.*, 2009a; De Waal *et al.*, 2012). My results refute this hypothesis since the narrowing of the distance between the lower anthers is driven by an increase in mean pollinator visitation rate, and the stigmas and anthers never touch. Smaller separation distances have also been proposed to allow for generalist pollination by being adapted to a subset of efficient pollinators (Herrera, 1996).

The narrowing of the two lower anthers in response to a high visitation rate suggests that frequent visits by small pollinators (i.e. honey bees) in a population could be driving the evolution of smaller distances between the lower anthers. This follows Stebbins' (1970) most effective pollinator principle which assumes that a flower would adapt to the most frequent and/or most efficient pollinator. Honey bee pollination may not generate the high proportions of inter-morph pollen movement as observed for carpenter bee pollination (see Minnaar and Anderson, 2021), but their high abundance and visit frequency might offset this (Stebbins, 1970; Madjidian *et al.*, 2008; Rader *et al.*, 2009).

Grand mean functional pollinator weighted wingspan did not predict the degree of reproductive separation in a population. Additionally, visitation rate could not explain the variation in UAS distance. There are many possible explanations for these results, and I highlight three possibilities here. Firstly, the absence of an association could suggest that the mechanical fit between the pollinator and the reproductive structures does not have to be exact to be effective (Galen, 1999; Huang and Shi, 2013). Small pollinators were often observed approaching flowers from the side, which allowed them to make contact with the reproductive structures on one side despite their wingspan being narrow. Thus, the effectiveness of enantiostyly is

still preserved, even if pollinators don't make contact with all the reproductive parts during a single visit. Minnaar and Anderson (2021) found that less than 1% of pollen was deposited on the opposing side of a pollinator, thus showing that enantiostyly in *W. paniculata* is effective at laterally separating pollen from the two morphs, despite matching not being very precise.

Secondly, it should be considered that pollinator environments might have changed in recent history and that alternative pollinator-driven patterns were more convincing in the past (Garcia *et al.*, 2020; Pauw *et al.*, 2020). For example, *Xylocopa* spp. might have been frequent pollinators of *W. paniculata* (see Scott Elliott, 1890), and might have driven associations with UAS distance. Temporal variation in pollinator assemblages may dilute selection pressures within plant communities, obscuring patterns of association between plant phenotypes and pollinator environments (Herrera 1996). Consequently, extant floral phenotypes (UAS distance in this case) might be anachronisms – adaptations to past pollinator types that have either become rare over time or vary greatly between years (Pauw *et al.*, 2020).

Modern disturbances, such as alien plant invasions (Dietzsch *et al.*, 2011), urbanisation (Ushimaru *et al.*, 2014) and the introduction of managed honey bee hives could exacerbate temporal changes in pollinator communities (Steffan-Dewenter *et al.*, 2002; Henry and Rodet, 2018). In particular, smaller *W. paniculata* populations, caused by less extensive contemporary fires, may not attract large solitary bee pollinators (Steffan-Dewenter *et al.*, 2002). Furthermore, agriculture and beekeeping may have artificially inflated honey bee numbers in the CFR (Geerts and Pauw, 2011), which has been suggested to disrupt local pollinator communities (see Cane and Tepedino, 2017; Henry and Rodet, 2018; Hung *et al.*, 2019).

If the degree of reproductive separation is not driven by variation in pollinator size, it could possibly be explained using Bateman's (1948) principle. It has been argued that male fitness relies more heavily on the frequency of pollinator visits (Webb and Lloyd, 1986; Delph, 1996; Aizen and Basilio, 1998) than female fitness, since

a higher number of successful visits is needed to fulfil the male function (depletion of anthers) than the female function (seed set). In theory, *W. paniculata* stigmas require at most three successful pollinator visits to saturate the female function, and this can be easily achieved when honey bees make stochastic contact from the side when in flight. To satisfy the male function, however, precise wing contact with the lower anthers might be necessary in populations with high numbers of honey bees, effecting a narrowing in the LA distance to make contact with their narrow wingspans.

The highly variable nature of visitation rate data may be expected to obscure potential relationships with floral morphology, resulting in type II errors, but with reasonable sample sizes is unlikely to generate the significant relationships found here (type I errors). Regardless, the effects of different pollinator parameters on reproductive separation in this study should be considered tentatively and conservatively. One would need several days over multiple years of detailed pollinator observations across a large number of populations to draw strong conclusions regarding the selective effects that pollinators might have on *W. paniculata*, and to account for seasonal fluctuations in pollinator assemblages. Many studies (such as Fishbein and Lawrence Venable, 1996) have cautioned against drawing such conclusions about the identity and selective effects of important pollinators over one or two seasons, since pollinator effectiveness can vary greatly between years because of fluctuations in pollinator abundances. In mitigation, the only population visited primarily by flies in my study was also surveyed by Goldberg (1996), 25 years prior to this study. Goldberg (1996) also found that the same species of flies were by far the most important visitors, suggesting some stability in pollinator communities across years.

Floral movement over time

A moderate amount of variation in reproductive separation distances could be explained by the time of day and the site at which flowers were measured. When

compared to measurements taken over time in chapter 3, the model could accurately predict the rate of decrease in LA and UAS distances over time when site was taken into account. Floral narrowing might serve as a reproductive assurance strategy: if visitation rates are low, narrowing of the span between stigmas and anthers throughout the day increases the likelihood of reproductive structures making contact with the wings of smaller pollinators, facilitating regular pollen deposition and receipt (Ruan *et al.*, 2009a). This might also increase the probability of pollinator-assisted selfing and intra-morph pollination, since pollen from the stigma-side anther is more likely to come into contact with the stigma later in the day as they move towards each other. Floral narrowing warrants further investigation to see if this may play a functionally significant role in pollen placement and receipt, and is examined thoroughly in chapter 3.

Conclusion

For many species, fitness trade-offs between pollination, herbivory (Ramos and Schiestl, 2019), resource availability (Lambrecht and Dawson, 2007) and climate (Weber *et al.*, 2020) all shape the evolution of floral morphology. Studies that find an interplay between biotic and abiotic variables on geographic variation have become increasingly prevalent in recent years, but require complex community-level datasets over many seasons (as reviewed in Van der Niet *et al.*, 2014). Increasingly, it is no longer a question of which specific factor (e.g. pollinator community) drives geographic variation, but which *combination* of factors plays the most important role in shaping floral morphology (Galen 1999; Herrera *et al.*, 2006; Zhao and Wang, 2015). In conclusion, it is clear that no single mechanism can completely explain differences seen in the degree of reproductive separation in *W. paniculata* across the landscape. Rather it is more likely an intricate combination of site-specific environmental effects, allometric scaling, time of day, and past and present pollinator communities. The inferences made in this study are purely correlative, and future studies need to investigate fitness trade-offs, relative pollen contributions of anthers

to stigmas by different pollinator species, as well as detailed pollinator surveys over time to account for temporal fluctuations in pollinator communities.

APPENDIX A

I. SUPPLEMENTARY FIGURES & TABLES

Table A.1: A list of 16 *Wachendorfia paniculata* populations that were sampled during this study, including site abbreviations, names, elevations and GPS coordinates.

Site Abbreviation	Site Name	Elevation (m)	Coordinates	
BR	Vanderstelpass, Bot Rivier	84	-34.1854	19.22328
DBF	Du Bois Farm	173	-34.5231	19.61882
DP	Driehoekpad Nature Reserve	182	-33.4538	18.74367
FP	Franschhoek Pass	671	-33.9176	19.15821
HP	Houwhoek Pass	307	-34.2042	19.16102
KM	Kylemore	265	-33.9102	18.96790
KPM	Klapmuts Railway	177	-33.8050	18.87323
KWK	Karwyderskraal turnoff	53	-34.2636	19.18238
PBS	Pringle Bay School	25	-34.3391	18.84474
RUS	Rustenburg	202	-33.9112	18.89195
SL	Sir Lowry's Pass	136	-34.1312	18.91680
STBML	Stellenbosch Mountain	152	-33.9419	18.87432
SW	Swellendam	172	-34.0116	20.46289
TWK	Theewaterskloof Dam	308	-34.0188	19.20816
VK	Vlooiakraal Farm	58	-34.7001	19.76259
WAY	Waylands Flower Reserve	139	-33.4077	18.41675

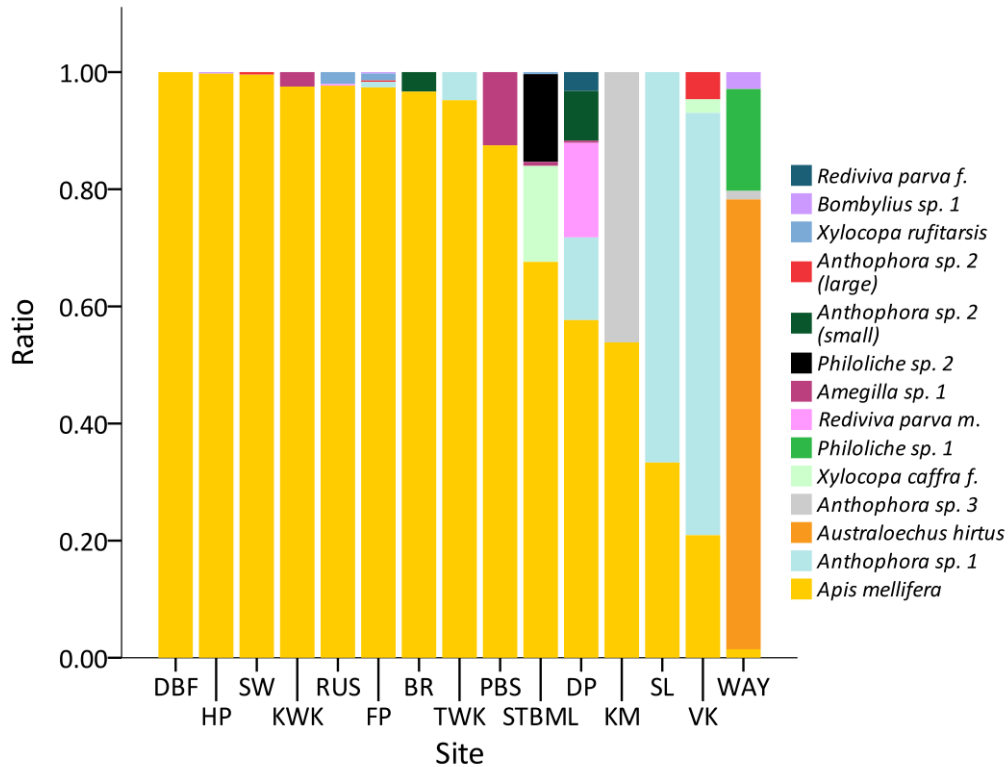


Figure A.1: The ratio of functionally significant pollinators of *W. paniculata* observed during random walks in 15 populations. Pollinator species names are arranged in ascending order of overall pollinator abundance.

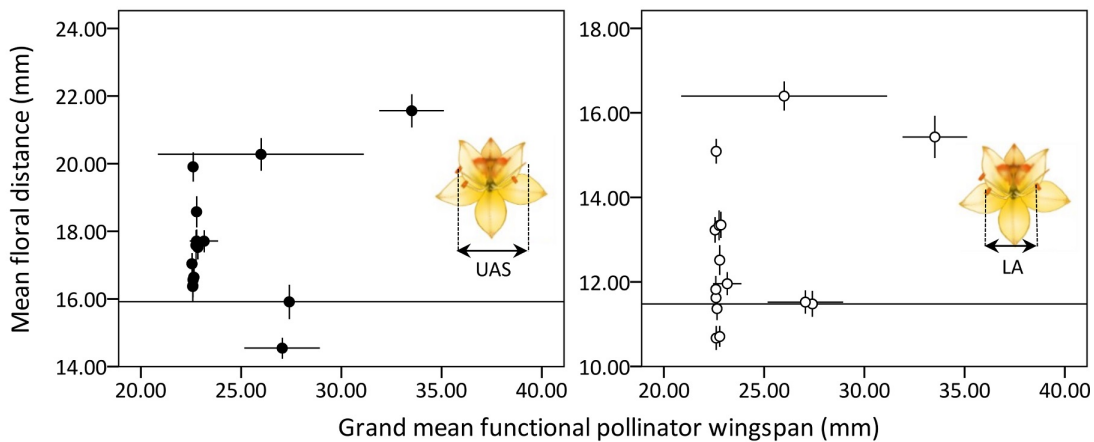


Figure A.2: Mean \pm SE absolute UAS (filled circles) and LA (unfilled circles) distances plotted against the grand mean functional pollinator wingspan \pm SE. The Stellenbosch Mountain population had a disproportionately large SE (± 33.52), which has been truncated for display purposes.

Table A.2: A complete list of insect visitors (ordered alphabetically) to *W. paniculata* flowers during plot observations. The total number of visitors recorded at a particular site during plot observations are shown for functionally significant pollinators. Black dots indicate that a visitor was present at that site, but not deemed functionally significant. Site names with asterisks only had a single day of observations.

Species	BR	DBF	DP	FP	HP	KM	KWK	PBS*	RUS	SL*	STBML	SW	TWK	VK	WAY
Order Coleoptera															
Family Scarabaeidae															
<i>Peritrichia cinerea</i>	-	-	●	-	●	-	-	-	-	-	-	-	-	-	-
Order Diptera															
Family Bombyliidae															
<i>Australoechus hirtus</i>	-	-	-	-	-	-	-	-	-	-	-	-	-	-	31
<i>Bombylius</i> sp. 1	-	-	-	1	-	-	-	-	-	-	-	-	-	-	-
Unidentified small fly	-	-	-	-	●	-	-	●	-	-	-	-	-	-	-
Family Empiidae															
<i>Empis</i> sp. 1	-	-	●	-	●	●	-	-	●	-	●	-	-	-	-
<i>Empis</i> sp. 2	-	-	-	-	-	-	-	-	-	-	-	●	-	-	-
Family Syrphidae															
<i>Allograpta fuscotibialis</i>	-	●	-	●	-	●	●	-	●	-	●	●	-	●	-
Unidentified med. fly	-	-	-	●	-	-	-	-	-	-	●	-	-	-	-
Family Tabanidae															
<i>Philoliche</i> sp. 1	-	-	-	-	-	-	-	-	-	-	-	-	-	-	1
<i>Philoliche</i> sp. 2	-	-	-	-	-	-	-	-	-	-	2	-	-	-	-
Order Hymenoptera															
Family Apidae															
<i>Allodapula</i> spp.	-	●	●	-	-	●	-	-	●	-	●	●	●	-	-
<i>Amegilla</i> sp. 1	-	-	-	-	-	1	-	-	-	-	-	-	-	-	1
<i>Anthophora</i> sp. 1	-	-	-	25	-	-	-	-	-	4	-	-	-	28	2

Species (continued)	BR	DBF	DP	FP	HP	KM	KWK	PBS*	RUS	SL*	STBML	SW	TWK	VK	WAY
Family Apidae (cont.)															
<i>Anthophora</i> sp. 2 (small)	0.09	-	-	-	-	-	-	-	-	-	-	-	-	-	-
<i>Anthophora</i> sp. 2 (large)	-	-	-	3	-	-	-	-	-	-	-	-	2	-	-
<i>Anthophora</i> sp. 3	-	-	1	-	-	-	1	2	-	-	-	-	-	2	-
<i>Apis mellifera</i>	55	313	72	124	175	-	20	17	319	2	94	124	18	2	-
<i>Ceratina</i> sp. 1	•	•	-	•	•	•	•	-	•	-	•	-	•	-	-
<i>Xylocopa caffra</i>	-	-	-	1	-	-	-	-	-	-	1	-	-	-	-
<i>Xylocopa rufitarsis</i>	-	-	-	-	-	-	-	-	1	-	-	-	-	-	-
Family Halictidae															
<i>Halictus</i> sp. 1	-	-	-	-	-	-	-	-	•	-	-	-	-	•	-
Family Megachilidae															
<i>Megachile</i> sp. 1	-	-	•	-	•	-	-	-	•	-	-	•	-	-	•
Family Melittidae															
<i>Rediviva parva</i> f.	-	-	9	-	-	-	-	-	-	-	-	-	-	-	-
<i>Rediviva parva</i> m.	-	-	10	-	-	-	-	-	1	-	-	-	-	-	-
Order Lepidoptera															
Family Hesperidae															
<i>Afrogegenes letterstedti</i>	-	-	-	-	•	-	-	-	-	-	-	-	-	-	-
Family Nymphalidae															
<i>Melampias huebneri</i>	-	-	-	-	-	-	-	-	-	-	-	•	-	-	-
<i>Vanessa cardui</i>	-	-	-	-	-	-	•	-	-	-	-	-	•	-	-
Family Pieridae															
<i>Mylothris agathina</i>	•	-	-	-	-	-	-	-	-	-	-	-	-	-	-
<i>Pieris brassicae</i>	-	-	-	-	-	-	-	-	-	-	•	-	-	-	-
Total plot observations	14	20	15	18	17	9	14	9	17	4	20	17	9	19	16
Total functional species	2	1	5	4	1	1	2	2	3	2	3	1	2	3	4
Mean visitation /h	2.29	8.86	1.18	3.08	3.12	0.22	0.69	1.02	7.08	0.67	1.41	4.93	1.88	0.69	0.92

Table A.3: A complete list of insect visitors (ordered alphabetically) to *W. paniculata* flowers during random walks. The total number of visitors recorded at a particular site during random walks are shown for functionally significant pollinators. Black dots indicate that a visitor was present at that site, but not deemed functionally significant. Site names with asterisks only had a single day of observations.

Species	BR	DBF	DP	FP	HP	KM	KWK	PBS*	RUS	SL*	STBML	SW	TWK	VK	WAY
Order Coleoptera															
Family Scarabaeidae															
<i>Peritrichia cinerea</i>	-	-	●	-	●	-	-	-	-	-	-	-	-	-	-
Order Diptera															
Family Bombyliidae															
<i>Australoechus hirtus</i>	-	-	-	-	-	-	-	-	-	-	-	-	-	-	53
<i>Bombylius</i> sp. 1	-	-	-	1	1	-	-	-	-	-	-	-	-	-	2
Unidentified small fly	-	-	-	-	●	-	-	●	-	-	-	-	-	-	-
Family Empididae															
<i>Empis</i> sp. 1	-	-	●	-	●	●	-	-	●	-	●	-	-	-	-
<i>Empis</i> sp. 2	-	-	-	-	-	-	-	-	-	-	-	●	-	-	-
Family Syrphidae															
<i>Allograpta fuscotibialis</i>	-	●	-	●	-	●	●	-	●	-	●	●	-	●	-
Unidentified med. fly	-	-	-	●	-	-	-	-	-	-	●	-	-	-	-
Family Tabanidae															
<i>Philoliche</i> sp. 1	-	-	-	-	-	-	-	-	-	-	-	-	-	-	12
<i>Philoliche</i> sp. 2	-	-	-	-	-	-	-	-	-	-	43	-	-	-	-
Order Hymenoptera															
Family Apidae															
<i>Allodapula</i> spp.	-	●	●	-	-	●	-	-	●	-	●	●	●	-	-
<i>Amegilla</i> sp. 1	-	-	-	-	-	6	-	-	-	-	-	-	-	-	-
<i>Anthophora</i> sp. 1	-	-	35	4	-	-	-	-	-	2	-	-	5	31	-

Species (continued)	BR	DBF	DP	FP	HP	KM	KWK	PBS*	RUS	SL*	STBML	SW	TWK	VK	WAY
Family Apidae (cont.)															
<i>Anthophora</i> sp. 2 (small)	2	-	21	-	-	-	-	-	-	-	-	-	-	-	1
<i>Anthophora</i> sp. 2 (large)	-	-	-	1	-	-	-	-	-	-	-	1	-	2	-
<i>Anthophora</i> sp. 3	-	-	1	-	-	-	2	1	-	-	2	-	-	-	-
<i>Apis mellifera</i>	58	558	143	409	396	7	79	7	337	1	194	222	99	9	1
<i>Ceratina</i> sp. 1	●	●	-	●	●	●	●	-	●	-	●	-	●	-	-
<i>Xylocopa caffra</i>	-	-	-	-	-	-	-	-	-	-	47	-	-	1	-
<i>Xylocopa rufitarsis</i>	-	-	-	5	-	-	-	-	7	-	1	-	-	-	-
Family Halictidae															
<i>Halictus</i> sp. 1	-	-	-	-	-	-	-	-	●	-	-	-	-	●	-
Family Megachilidae															
<i>Megachile</i> sp. 1	-	-	●	-	●	-	-	-	●	-	-	●	-	-	●
Family Melittidae															
<i>Rediviva parva</i> f.	-	-	8	-	-	-	-	-	-	-	-	-	-	-	-
<i>Rediviva parva</i> m.	-	-	40	-	-	-	-	-	1	-	-	-	-	-	-
Order Lepidoptera															
Family Hesperiiidae															
<i>Afrogegenes letterstedti</i>	-	-	-	-	●	-	-	-	-	-	-	-	-	-	-
Family Nymphalidae															
<i>Melampias huebneri</i>	-	-	-	-	-	-	-	-	-	-	-	●	-	-	-
<i>Vanessa cardui</i>	-	-	-	-	-	-	●	-	-	-	-	-	●	-	-
Family Pieridae															
<i>Mylothris agathina</i>	●	-	-	-	-	-	-	-	-	-	-	-	-	-	-
<i>Pieris brassicae</i>	-	-	-	-	-	-	-	-	-	-	●	-	-	-	-
Total random walks	14	20	15	18	17	15	14	9	17	4	20	17	9	19	16
Total functional species	2	1	6	5	2	2	2	2	3	2	5	1	2	4	5

II. SPECTRAL REFLECTANCE

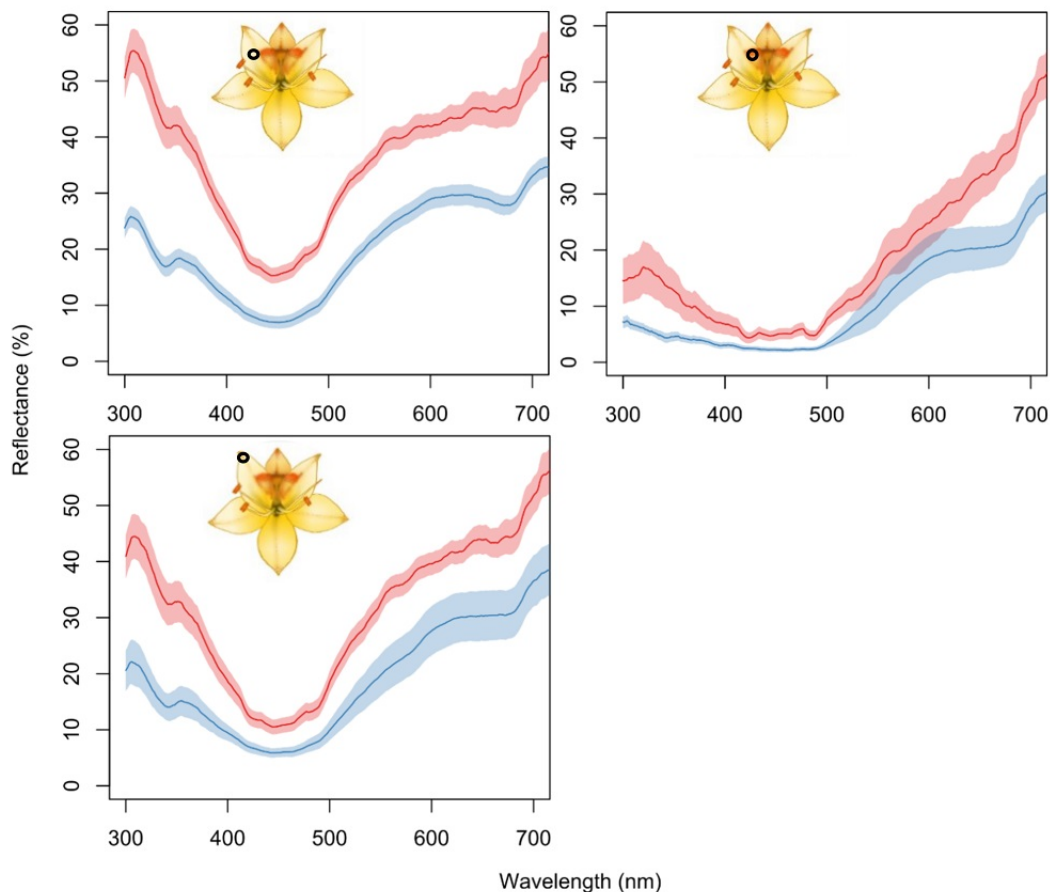


Figure A.3: Aggregate plots of mean \pm SE spectral reflectance measurements done for flowers from WAY (red; $n = 9$) and DBF (blue; $n = 8$). Points of interest (black circles) included the nectar guide (top right), the distal tip (bottom left) and the middle (top left) of the tepal.

The spectral reflectance of the top side tepal of flowers from the predominantly fly-pollinated Waylands (WAY, $n = 9$) and honey bee-pollinated Du Bois Farm (DBF, $n = 8$) populations were measured using an Ocean Optics USB4000 spectrometer. Three points of interest were measured, namely the nectar guide, the distal tip and the centre of the tepal. Aggregate plots were compiled in R using the pavo package (Maia et al., 2019). A UV signal was present on flowers at both WAY and DBF. Aggregate plots of the combined data from both sites are displayed in appendix fig. A.3.

CHAPTER 3

STAYING ON TARGET? THE FUNCTIONAL SIGNIFICANCE OF FLORAL MOVEMENT IN A HANDED FLOWER

ABSTRACT

Various functions pertaining to reproductivity have been proposed for floral movement. *Wachendorfia paniculata*, a handed flower species (where the style points left or right), displays floral movement by decreasing the separation distances between the reproductive structures over time. I examined whether floral movement holds any functional significance for *W. paniculata*. I aimed to ascertain the degree of floral movement, and to determine whether floral narrowing could act as a reproductive assurance mechanism by making more regular contact with pollinators over time. In a single population, I measured floral separation distances over time, which decreased substantially in the early part of the day. Pollinator visits to virgin donor and recipient plants revealed that the likelihood of stigmatic pollen receipt remained constant over time and movement, and was dependent on the density of pollen on bee wings. I suggest that while floral movement does not result in selfing, it might still act as a reproductive assurance mechanism. Anthers labelled with fluorescent markers (quantum dots) showed that lower anthers are more likely to deposit pollen at smaller separation distances, affecting pollinator pollen loads late in the day. Anther movement lacks a clear biological explanation, but possibly tracks stigmatic movement. I suggest that stigmatic position prioritises pollen quality in the morning but shifts towards maximizing the chances of pollen receipt later in the day, which requires further study. I conclude that floral movement possibly improves pollination accuracy and ensures pollination by making more regular and targeted contact with pollinator wings over time.

INTRODUCTION

Plants are commonly perceived to be sedentary and immobile organisms when compared to animals. As a result, the notion that plants can perform relatively rapid movements has long been a source of interest in the scientific community. Plants have been known to react quickly to capture prey (e.g. Venus flytraps, *Dionaea muscipula*), avoid herbivory (e.g. *Mimosa pudica*; Amador-Vargas *et al.*, 2014) and track the sun (e.g. *Helianthus annuus*; Kutschera and Briggs, 2016), among other functions (Bynum and Smith, 2001; Armbruster and Muchhala, 2020). The movement of floral structures, however, is thought to be mostly related to reproductive function (see Ruan and da Silva, 2011). For example, Darwin (1862) noted how active changes in the position of orchid pollinia appear to reduce the risk of autogamy (selfing within the same flower), simultaneously promoting outcrossing (see also Peter and Johnson, 2006). Many examples of floral reconfiguration have since been described, ranging from relatively simple (e.g. Ruan *et al.*, 2010) to highly complex (Ren and Tang, 2012).

Ruan and da Silva (2011) outlined four general hypotheses that explain the adaptive significance of movement in floral structures, namely the maximising of outcrossing and/ or prevention of selfing (Darwin, 1862; Ruan *et al.*, 2010), reproductive assurance through delayed selfing (Kalisz *et al.*, 1999; Nagy *et al.*, 1999; Ruan *et al.*, 2010; Ren and Tang, 2012), reduction in male-female sexual interference (Webb and Lloyd, 1986) and tolerance of environmental stress (see Bynum and Smith, 2001). For example, stylar curvature in *Eremurus altaicus* prevents selfing and promotes outcrossing by bending the stigma away from the anthers until it is perpendicular to the stamens during dehiscence (Gu *et al.*, 2018). Only after the anthers finished dispersing their pollen does the style move back to its original position. Floral movement where anthers and stigmas move toward each other to eventually touch has commonly been interpreted to act as a reproductive assurance mechanism via delayed autonomous selfing (Kalisz *et al.*, 1999; Ruan *et al.*, 2009a, 2009b; Liu *et al.*,

2020). For example, *Kosteletzkya virginica* employs ‘movement herkogamy,’ where the stigma-anther separation distance changes over time (Ruan *et al.*, 2004, 2009a, 2009b). Unpollinated stigmas bend down towards the anthers until they eventually touch, thereby ensuring pollination towards the conclusion of anthesis (Ruan *et al.*, 2009a). In this way, selfing is delayed until the period for outcrossing has passed, which maximises the pollen export effort, while ensuring pollination when pollinators are scarce (Kalisz *et al.*, 1999; Ruan and da Silva, 2011; Liu *et al.*, 2020). Mechanisms where male and female structures move further apart, or exchange positions, might reduce inter-sexual interference within a flower by preventing male and female structures from obstructing each other during a pollinator’s visit (Fetscher *et al.*, 2002; Yang *et al.*, 2004; Sun *et al.*, 2007). In *Mimulus aurantiacus*, pollen export was 2.8 times higher when the touch-sensitive stigmas were closed compared to when they were open (Fetscher *et al.*, 2002), thereby preventing the stigma from obstructing the function of the anthers.

Floral movement can play more than one adaptively significant role in a flower. In *Ruta graveolens*, for example, each of the stamens move towards the centre of the flower in succession, taking turns to elevate and retreat to their original positions (Ren and Tang, 2012). At the end of anthesis, all stamens move towards the centre to envelop the style. This complex sequence of movements serves multiple functions, namely to dispense pollen in doses to pollinators, to prevent interference between dehiscent and dehiscent anthers as well as to ensure self-pollination at the end of a flower’s life. In *Alpinia* flowers (Zingiberaceae) that display flexistyly, there exists two morphs that differ in the timing and position of male and female function by allowing stigmas to move up or down to receive pollen from the opposite morph, while avoiding pollen from the same morph (Li *et al.*, 2001). Therefore, the combination of dimorphism, floral movement and dichogamy allows the flowers to promote outcrossing, avoid selfing and reduce sexual interference (Sun *et al.*, 2007).

Armbruster *et al.* (2009) emphasised the importance of pollination accuracy in

herkogamous flowers: imprecise matching of stigmas and anther positions generally reduces pollen transfer efficiency by lowering both the chances of pollen receipt by the stigma and siring success (Armbruster *et al.*, 2014). Anther position is a key factor that determines the precision and regularity with which contact is made with pollinators (Ren and Tang, 2010; Armbruster and Muchhala, 2020). Similarly, stigmatic accuracy is important for successful pollination, as a mismatch in pollen pickup and deposition sites on a pollinator's body can reduce the efficacy of pollen transfer (Armbruster *et al.*, 2014; Armbruster and Muchhala, 2020). Herkogamy (the spatial separation of anthers and stigmas), in its simplest form, functions to prevent autogamy or to reduce sexual interference (Webb and Lloyd, 1986). However, it also increases the risk of a mismatch between pollen deposition and pickup sites if the degree of herkogamy is too extreme (Barrett, 2002; Armbruster *et al.*, 2014; Ye *et al.*, 2019). Additionally, extreme reproductive separation reduces the likelihood that a visiting pollinator (especially a small one) would make contact with both male and female parts simultaneously (Ruan and da Silva, 2011). This reduces the overall efficiency of pollination, which could be especially detrimental to short-lived flowers that have a short time window for pollen export and receipt. The reduction of reproductive separation distances over time could potentially mitigate this problem, in a way acting as a reproductive assurance mechanism (Liu *et al.*, 2020).

Wachendorfia paniculata is a common geophyte in the Cape Floristic Region, South Africa, with a form of reciprocally herkogamous flowers known as dimorphic enantiostyly. Here, plants can be classified as left- or right- handed, depending on which way their styles are deflected. *Wachendorfia paniculata* inflorescences bear on average between three and five flowers per day, each of which only lasts for ten to twelve hours. Common floral visitors include small bee species, such as honey bees (*Apis mellifera capensis*), solitary bees (tribe Anthophorini), and occasionally larger insects such as carpenter bees (*Xylocopa* spp.) and flies (see chapter 2). Each *Wachendorfia paniculata* flower has three stamens that are widely spaced apart: one deflected to the same side as the style and two deflected to the opposite

side (fig. 3.1). Small visitors, such as honey bees, were often discounted as effective pollinators of *W. paniculata* in the past (Goldberg, 1996; Ornduff and Dulberger, 1978; Helme and Linder, 1992), because it was envisaged that only large-bodied pollinators would make contact with the widely-spaced anthers. However, Minnaar (2018) found that pollen is placed predominantly on the beating wings of pollinators and that anthers from different sides of the flower place pollen on different sides of the pollinator. While honey bees rarely made contact with the reproductive parts of *W. paniculata* flowers, they nevertheless carried large pollen loads on their wings (see Minnaar, 2018 and chapter 3).

The pollen segregation caused by enantiostyly is thought to improve outcrossing efficiency by promoting pollen transfer between rather than within morphs (Minnaar, 2018; Ornduff and Dulberger, 1978; Barrett *et al.*, 2000). In *W. paniculata*, most of the pollen received by stigmas originates from the opposite morph, but a small intra-morph and self-component is also contributed by the stigma-side anther (Minnaar and Anderson, 2021). At first, the presence of the stigma-side anther may seem detrimental, as it increases the risk of selfing, thereby reducing the veracity of outcrossed pollen movement. However, it carries an advantage when mates of the opposite morph are limited, such as when morph ratios are skewed during a founder event. In these instances, the stigma-side anther may promote pollen movement within morphs (Minnaar and Anderson, 2021). While it has been established that selfing in *W. paniculata* results in reduced reproductive output (Ornduff and Dulberger, 1978; Jesson and Barrett, 2002), the effect of intra-morph crossing remains unclear. Ornduff and Dulberger (1978) indicated that intra-morph crossings set less seed, whereas Jesson and Barrett (2002) found inconsistent evidence for this.

Minnaar and Anderson (2021) found that the 2:1 anther arrangement of *W. paniculata* resulted in two-dimensional mosaics of pollen quality on the wings of carpenter bees (*Xylocopa caffra*), with mostly between-morph pollen nearer the wing tips and a mixture of within- and between-morph pollen nearer to the body. They also indi-

cated that the stigma is positioned considerably wider and higher than the anthers, which allows it to target areas on carpenter bee wings where the quality of the pollen is highest (Minnaar and Anderson, 2021). Interestingly, Minnaar and Anderson (2021) did not find strong evidence for pollen quality mosaics on honey bees – the widely-spaced upper anthers responsible for most intermorph pollen movement rarely made contact with honey bees; only occasionally placing pollen onto the wing tips. In populations where large pollinators are absent, or when overall visitation rates are low, the wide separation of the stigma and anthers could potentially be detrimental. The fact that large pollinators are generally rare pollinators of *W. paniculata* (see chapter 2 and appendix B section IV), and that reproductive separation distances varied temporally (see chapter 2), made me ponder whether rapid shifts towards smaller reproductive separation distances could be advantageous in populations that are dominated by small pollinators.

Wachendorfia species are known to narrow the separation distances between the anthers and stigma over time, but the functional significance of this has not been investigated. Jesson and Barrett (2002) examined floral movement in the anther closest to the stigma for three *Wachendorfia* species and found that it resulted in delayed autonomous selfing for the highly self-compatible *W. brachyandra*, but not for *W. paniculata* or *W. thyrsiflora*. *Wachendorfia brachyandra* flowers have poorly developed herkogamy, which allows stigmas and anthers to touch at the end of the day, whilst *W. thyrsiflora* and *W. paniculata* flowers have widely-spaced reproductive structures that rarely touch directly. It was suggested that the larger display sizes of the two latter species might rather facilitate geitonogamy (selfing within the same plant) instead of delayed autonomous selfing (Jesson and Barrett, 2002). In this way, pollen from the stigma-side anther might reach stigmas of flowers within the same inflorescence. *Wachendorfia paniculata* is considered to be self-compatible, but self-pollinations have been known to lead to a reduced seed set (Ornduff and Dulberger, 1978; Jesson and Barrett, 2002). Pollinator-facilitated autogamy (*sensu* Lloyd, 1992) might also be possible if a pollinator picks up stigma-side pollen upon

landing and deposits it as it departs. Since the flowers of *W. paniculata* only last for a single day, floral movement might be an important mechanism to promote reproductive assurance in the absence of large or frequent pollinators.

In this chapter I aim to ascertain the extent of floral movement in *W. paniculata* and whether it holds any functional significance for pollination in a honey bee-dominated population. I hypothesise that the decrease in the distances between reproductive parts increases the likelihood of pollinator wings making contact with the stigma and/or anthers later in the day; ensuring pollination when larger pollinators are absent or when visitation rates are low. I predict that the narrowing of the distance between reproductive structures will increase the likelihood of successful pollen deposition onto honey bee wings throughout the day. Moreover, if stylar movement increases the regularity of stigmatic contact with pollinators, this might maintain high rates of stigmatic pollen receipt as pollen loads on pollinators decrease through the day. Studies that investigate the relationship between pollinator pollen loads and pollen receipt over time are exceedingly rare (see Delmas *et al.*, 2016). To my knowledge, this is the first study that attempts to document a major proportion of the pollination pathway of a flower over the course of its entire lifespan in both experimental and naturally-occurring contexts.

MATERIALS AND METHODS

Study site

A single population of *W. paniculata* was studied near Franschoek Pass, Western Cape, South Africa (-33.917561; 19.156434) for a period of eight weeks between October and December 2019. Seven months prior to the commencement of experiments, a veld fire cleared most of the vegetation on the western side of the pass, resulting in mass flowering of *W. paniculata* plants along the Western mountain slopes. A study site of approximately 15 000 – 20 000 m² was selected close to the road. Flowering times followed an altitudinal gradient, where plants occurring higher up on the slope flowered later in the season.

Narrowing of reproductive separation distances

To ascertain the degree and variation of floral movement within the population, five flowers were randomly selected per day and were photographed *in situ* with a Sony RX 100 VI camera (Sony, Tokyo, Japan) at hourly intervals. This was done from when the flowers opened (between 3 and 4.5 hours after sunrise) until the flowers started to close (between 11 and 12.5 hours after sunrise). This was done over six days spread throughout the season (n = 30 flowers). Accurate measurements of the distances between floral parts were obtained by mounting a ruler at a fixed distance from the camera, and aligning it parallel to the floral parts to be measured. The distance between the opposite upper anther and the stigma (UAS), the distance between the lower stigma-side anther and the stigma (LAS) and the distance between the two lower anthers (LA) were determined (fig. 3.1A) using ImageJ (version 1.52n; Abramoff et al., 2004).

The average rate of narrowing was in some instances positively associated with the distance of the initial measurement between floral structures LA and UAS (LA: Pearson $r = 0.71$, $p < 0.001$; UAS: Pearson $r = 0.57$, $p = 0.002$; LAS: Pearson $r =$

0.295, $p = 0.10$). That is to say, the further two structures were apart when a flower opened, the faster the distance between them narrowed to cover a larger distance between structures. In light of this, all floral measurements were standardised for the first measurement taken per flower; subsequently, measurements were expressed as a proportion of the total distance initially measured. Standardised distance measurements (i.e. proportion narrowing) were used to determine how UAS, LA and LAS distances change over time, while absolute (unstandardised measurements) distances were used in the remainder of the analyses regarding pollen movement and placement (see section below). This is because the placement of pollen onto bee wings and stigmas is expected to depend on the fit between honey bees and the absolute stigma-anther distances.

I fitted generalised linear mixed models with a gaussian error distribution (identity link) using the package `glmmTMB` (Brooks *et al.*, 2017) in R (version 3.6.0) to analyse the extent and rate of floral movement throughout the day. The three standardised distance measurements (UAS, LA and LAS) were response variables, hours after sunrise was a fixed effect, and day and flower identification (ID) were random effects. The relationship between time and floral narrowing was fitted with an orthogonal polynomial term to the second degree for LAS and UAS measurements. The `glmmTMB` package (Brooks *et al.*, 2017) allows for uncomplicated and flexible model specification using the frequentist approach – it covers multiple distribution families, has the option to build hurdle models to deal with zero-inflated count data and accommodates functions for model selection using Akaike Information Criterion (AIC) values, making it the ideal package to deal with complex data from multiple distribution families. All analyses were performed in R version 3.6.0 (R core team, 2020).

Pollen movement and placement

To determine whether pollen contributions and deposition patterns change as the degree of reproductive separation narrows over time, donor (donating pollen) and recipient (receiving pollen) inflorescences were presented to foraging honey bees (*Apis mellifera capensis*) in the field. These inflorescences were presented at different times of day and they displayed varying degrees of reproductive separation. The day before experiments commenced, I covered plants with fine mesh bags to prevent unaccounted-for visits.

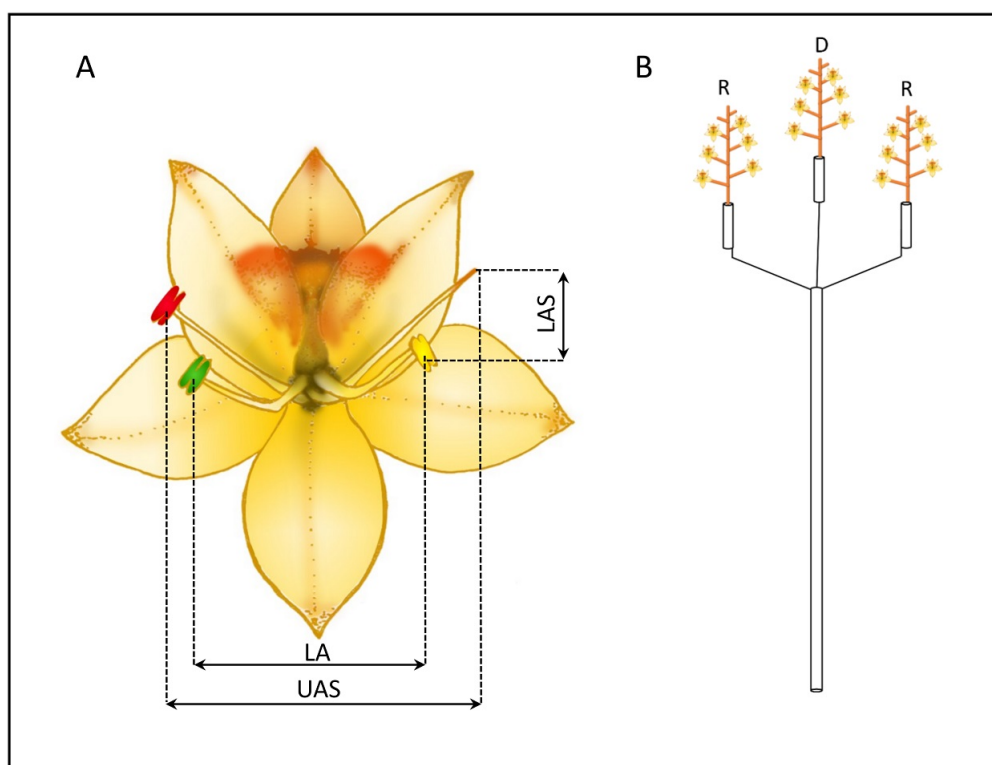


Figure 3.1: A) Floral measurements performed on flowers to determine whether movement over time is significant (UAS, LA and LAS). Anther colours correspond to the colours of quantum-dot solutions used to label lower opposite anther (green), stigma-side anther (yellow) and upper anther (red) pollen grains of left-handed donors. B) Schematic of how the inflorescence presentation pole was designed, and how left-handed donor (D) and right-handed recipient (R) inflorescences were arranged during the quantum dot tracking experiment.

I presented inflorescences to individual foraging honey bees using a custom ‘presentation pole’. Three inflorescences were mounted side by side at the end of a 1.5m PVC pipe, with the middle inflorescence situated slightly more toward the front, to

create an inverted V-shape (fig. 3.1B). Each of these were placed in 15ml water-filled centrifuge tubes and secured with florist wire to prevent them from rotating or falling out.

The middle inflorescence, which bees tended to visit first, was a single left-handed donor inflorescence, while the recipient inflorescences on each side were right-handed (fig. 3.1B). To determine whether pollen contributions from the individual anthers onto bee wings and stigmas change with floral narrowing, quantum dots were used to label pollen grains of the donor inflorescence (see section I below).

The donor inflorescence was presented to a foraging bee by placing the presentation pole in line with a bee's flight path. The bee was allowed to visit multiple donor flowers and the adjacent recipient flowers before being killed in an effort to limit the circulation of quantum dots in the population. Care was taken to keep the flowers in an upright position when placed in the path of a foraging honey bee. Capturing the bee also allowed me to quantify quantum dot-labelled pollen loads as well as pre-existing pollen loads on its wings (see section III below). Each bee was killed by letting it fly into a plastic killing jar (Bioquip Products Inc., Rancho Dominguez, California, USA) that was held over the flower as it finished feeding. Potassium cyanide was used to swiftly euthanize the bees, thus limiting pollen loss. Each bee was pinned immediately after capture without handling its wings.

After each round of visits by a bee, the stigmas of visited recipient flowers were removed and placed in a single vial per recipient inflorescence. The time of day and total number of visited donor and recipient flowers were also noted. Donor inflorescences were replaced after five rounds of bee visits or when flowers became unattractive to pollinators (e.g. through considerable wilting).

Captured bees and collected recipient stigmas were viewed inside a UV-excitation box (manufactured according to the specifications outlined in Minnaar and Anderson, 2019) to count the labelled pollen grains that were deposited during visitation (see sections II & III below).

After checking for quantum dot-labelled grains on the harvested stigmas, the styles were set in fuchsin gel on microscope slides to count the total number of labelled and unlabelled pollen grains (see section II below) on each stigma using a light microscope. Total pollinator pollen loads were counted separately using a dissection microscope (see section III below).

I. Quantum dot labelling

Quantum dots are nanoparticles that fluoresce under UV light, and can be used to efficiently track individual pollen grains as they move between flowers and pollen vectors (Minnaar and Anderson, 2019). For each donor inflorescence, individual anthers were designated specific colour labels (fig. 3.1A). Corresponding quantum dot solutions of red (31.25 mg/ml; 650 nm), green (31.25 mg/ml; 550 nm) and yellow (7.5 mg/ml; 590 nm) were prepared according to the methods described by Minnaar and Anderson (2019). I drew up 100 μ l of quantum dot solution using a micropipette and filtered tips. The pipette tip was touched to the distal end of the anther and observed for visible saturation of the pollen grains, slightly pressing down on the plunger if necessary. This was repeated for each colour (one pipette tip per colour) until all anthers on a donor inflorescence were labelled. Later it was found that green labels were hard to visualize and so analyses were only done with contributions from the stigma-side (yellow) and upper (red) anthers (fig. 3.1).

II. Stigmatic pollen loads

Only 2 out of 383 recipient stigmas received yellow-labelled pollen and none received red-labelled pollen. Because of this, the total number of pollen grains received by a stigma (both labelled and unlabelled) were used to determine whether the number and incidence of pollen grains received by a stigma changed with floral movement.

Various GLMM models were fitted: negative binomial, zero-inflated Poisson and truncated Poisson models with combinations of the variables mean UAS, overall wing pollen density, day identification (ID), bee ID and recipient ID. The most appropriate models were selected using Akaike's information criterion (AIC), where

the model with the lowest AIC value is considered the best (Burnham and Anderson 2002). The top two models fell within $2 \Delta\text{AIC}$ of each other – with the second-best model including day as a random factor. The best and most intuitive model was a hurdle model (family: truncated Poisson with zero-inflation), where the number of grains per stigma was the response variable, mean absolute UAS distance (averaged per hour and obtained from *Narrowing of reproductive separation distances*, above) and the total pollen load density of bee wings were fixed factors and bee ID and recipient inflorescence ID were random factors.

III. Pollen loads on bee wings

Only 23 out of 128 bees had quantum dot-labelled pollen placed on their wings, causing the data to be zero-inflated. To determine whether floral movement increases the likelihood of lower anther and upper anther pollen deposition onto a bee's wing, hurdle models were fitted using glmmTMB (family: truncated Poisson with zero-inflation). The best model was selected according to the lowest AIC value. The sequence of bee visits to a donor inflorescence was excluded early on in the selection process as a random factor. For both upper and stigma-side anthers, the top two models were very similar ($<2 \Delta\text{AIC}$). Of the two top models, I selected the one that was ecologically more appropriate, which included the number of red or yellow labelled grains on a wing as a response variable, mean absolute UAS or LA distance (averaged per hour and obtained from *Narrowing of reproductive separation distances*, above), the overall wing pollen density and the total numbers of donor and recipient visits as fixed factors, and bee and donor IDs as random factors. For this experiment, the contributions from the stigma-side anther were assumed to be similar to those of the opposite lower anther, as both mirror each other's position (Minnaar and Anderson, 2021) and have the same number of pollen grains (Ornduff and Dulberger, 1978).

'Heat maps' of the approximate distribution of labelled pollen grains on bee wings were generated according to the time at which each grain was deposited (i.e. grains

deposited later in the day were assigned a darker colour shade). This was done by assigning a colour shade to the hour after sunrise at which each pollen grain was deposited using the conditional formatting tab in Excel, which was then converted into the mean floral distance measured at each hour. The mean UAS distance was used for upper (red) anthers, while the mean LA distance was used for lower (yellow) anthers. Each wing cell was coloured according to the mean floral distance at which grains were deposited in that cell (appendix fig. B.4). This was used to draw ‘heat maps’ by approximating where the highest concentration of pollen received late in the day (or at smaller floral distances) was located on the wing (fig. 3.5 and appendix fig. B.4).

Total pollen loads on bee wings (including both pre-existing and labelled pollen) were manually counted under a dissecting microscope. Only the wings corresponding to the side where the stigma made contact were used, as wing loads were assumed to be roughly equal on both sides. Wing pollen loads were divided into three sections, namely the wing tips, the central forewing and the hindwing (fig. 3.4 and 3.6), which were counted separately. A photograph was taken of a single bee wing, and the area of each of the respective sections was determined with ImageJ (version 1.52n; Abramoff et al., 2004). This was used to determine the density of pollen grains for each section, as well as an averaged density over the total wing area.

To determine how the density of pollen on a bee wing changes over time, and whether it differs between different parts of the wing, a 2-way ANOVA (with a Tukey HSD posthoc test) was performed with time interval (hour after sunrise) and wing section type as independent variables and log-transformed pollen density on wings as the dependent variable.

RESULTS

Narrowing of reproductive separation distances

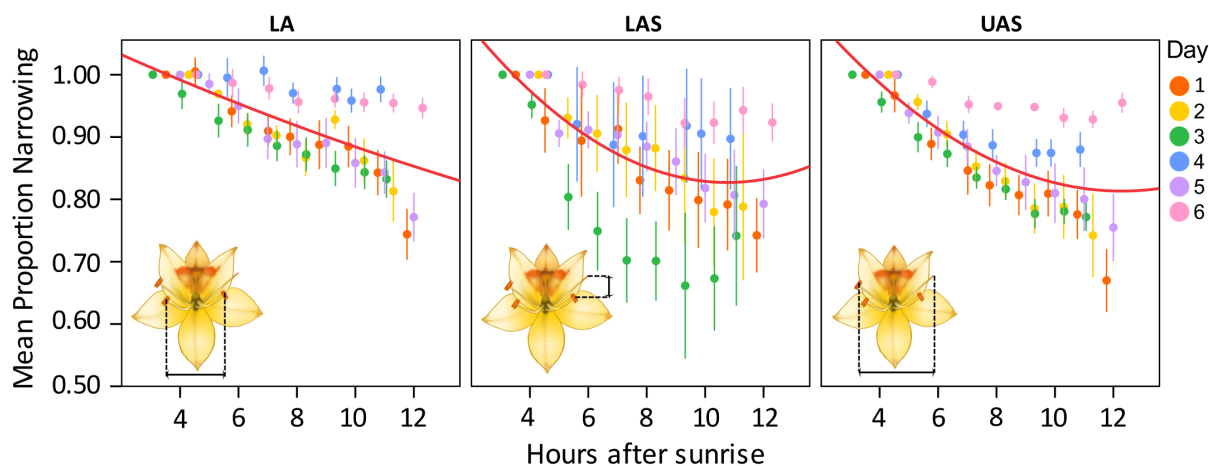


Figure 3.2: Means \pm SE of the standardised floral measurements (as a proportion of the initial measurement of each flower) over time. Days on which measurements were taken are displayed in different colours. Flower insets illustrate the respective measurements that were taken.

The distance between floral structures narrowed significantly over time (table 3.1; fig. 3.2 and appendix fig. B.1), and movement was highly variable (e.g. the maximum UAS percentage narrowing at the time of final measurement was 46.11%, while the minimum was only 0.43%). On average (\pm SD), LA distance narrowed by an absolute total distance of 2.33 ± 1.82 mm or $10.73\% \pm 7.55\%$ (mean \pm SD final LA at 10 – 13 hours after sunrise: 12.25 ± 1.87 mm), UAS narrowed by 4.60 ± 3.16 mm or $16.01\% \pm 11.12\%$ (mean \pm SD final UAS distance at 10 – 13 hours after sunrise: 17.26 ± 2.06 mm) and LAS narrowed by 1.47 ± 1.33 mm or $14.96\% \pm 14.12\%$ (mean \pm SD final LAS distance at 10 – 13 hours after sunrise: 5.73 ± 1.18 mm). The grand mean difference between UAS and LA ((mean UAS am - mean LA am) - (mean UAS pm - mean LA pm)) decreased from 8.49 mm to 4.65 mm; i.e. the stigma was horizontally closer to the lower anthers in the late afternoon than early in the day.

Table 3.1: Model output of floral narrowing over time describing the fixed effects, their coefficient estimates, standard errors, z - and p -values, as well as the pseudo- R^2 values for each model. Significant p -values are printed in bold text.

Response variable	Fixed effect	Estimate	SE	z	p	R^2_m	R^2_c
UAS narrowing	Hours after sunrise	-1.01	0.04	-23.31	< 0.001	-	-
	(Hours after sunrise) ²	0.25	0.04	5.96	< 0.001	0.43	0.83
LA narrowing	Hours after sunrise	-0.77	0.04	-17.53	< 0.001	0.17	0.77
LAS narrowing	Hours after sunrise	-0.95	0.08	-12.20	< 0.001	-	-
	(Hours after sunrise) ²	0.35	0.08	4.55	< 0.001	0.33	0.76

Stigmatic pollen loads

93 out of 383 stigmas picked up pollen from a pollinator – the likelihood of the stigma picking up pollen remained constant as the mean absolute UAS distance decreased, as did the number of grains when pollen was received (table 3.2, fig. 3.3). A similar pattern was observed when time was included as a fixed factor, instead of UAS distance (zero-inflated model: hours after sunrise coefficient estimate = -0.07, SE = 0.06, $z = -1.10$, $p = 0.270$). The likelihood that a stigma would receive pollen increased with increasing overall wing pollen density (table 3.2, fig. 3.4). Central forewing and wing tip pollen density drove the significant trend (fig. 3.4), as hindwing pollen density was not significant (appendix table B.1). The likelihood of stigmatic pollen receipt appeared to increase after approximately 20 grains per mm² had been exceeded on the overall wing (fig. 3.4). The central forewing section remained consistently above this threshold, while both the hindwing and wing tip sections fell short most of the time (fig. 3.6).

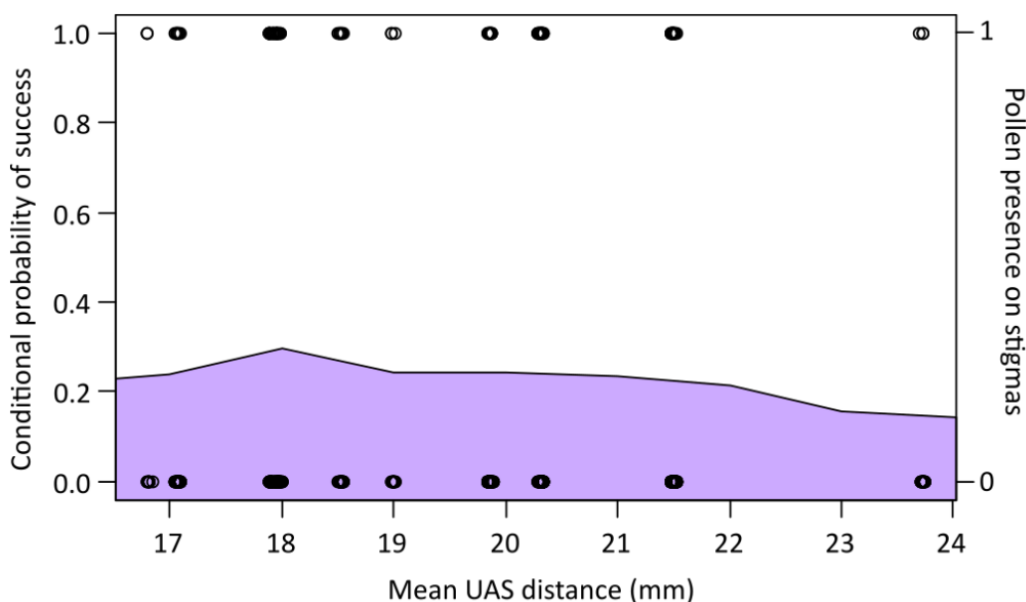


Figure 3.3: Conditional density plot (filled areas) showing how the mean absolute UAS distance (mm) is associated with the conditional probability of pollen receipt by the stigma (conditional probability of success). Open circles show the raw distribution of data points when pollen grains were received (1) or not (0).

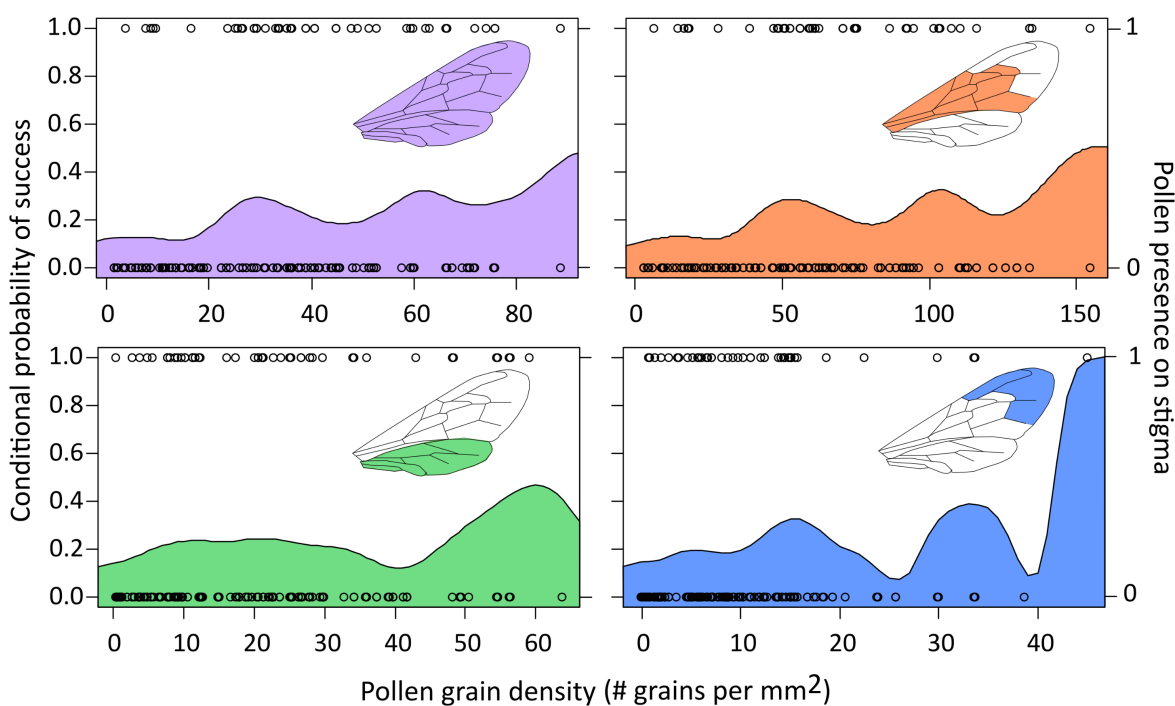


Figure 3.4: Conditional density plots (filled areas) showing how the density of pollen grains on different parts of bee wings (indicated by colour-fills on wing diagram insets) is associated with the conditional probability of pollen receipt by the stigma (conditional probability of success). Open circles show the raw distribution of data points when pollen grains were received (1) or not (0).

Table 3.2: Output for the hurdle model performed to determine whether stigma pollen receipt changed with floral narrowing (absolute UAS distance measured in mm) and if it is influenced by overall wing pollen density (number of grains per mm²). Fixed effects, coefficient estimates, standard errors and z - and p -values are displayed for the conditional truncated Poisson model, as well as the zero-inflated model. For the zero-inflated model, the results describe the probability of having an extra zero in the dataset. Significant effects are printed in bold text.

Response variable	Fixed effect	Estimate	SE	z	p
Conditional model					
Pollen count on stigma	Mean UAS distance	0.14	0.10	1.39	0.165
	Overall wing density	0.01	0.01	0.86	0.390
Zero-inflated model					
Pollen presence on stigma	Mean UAS distance	0.14	0.10	1.38	0.166
	Overall wing density	-0.02	0.01	2.34	0.019

Pollen loads on bee wings

23 bees out of 128 received labelled pollen (17 yellow; 9 red; 3 both). The likelihood of lower anther pollen being deposited onto a visiting bee's wing increased significantly as the mean distance between the lower anthers decreased, while the likelihood of upper anther pollen being deposited remained consistently low regardless of mean absolute UAS distance (table 3.3 zero-inflated models; fig. 3.5). A similar pattern was seen when hours after sunrise was included as a fixed factor instead of LA distance, which showed that lower anther pollen deposition incidence increased significantly between 9 and 13 hours after sunrise (zero-inflated model: hours after sunrise coefficient estimate = -0.36, SE = 0.13, $z = -2.90$, $p = 0.004$).

When lower anther labelled pollen was picked up by a bee wing, the number of labelled grains deposited per visit increased significantly as the distance between the lower anthers narrowed (table 3.3 conditional models). However, this significant increase is driven by a single observation where 13 yellow grains were deposited on a bee wing later in the day. An increase in the number of recipient visits increased the likelihood of yellow grains being picked up (table 3.3 zero-inflated model). However, this marginally significant result (estimate = -0.42, SE = 0.21, $z = -1.98$, $p = 0.048$)

has no biologically meaningful explanation. The number of red-labelled grains did not change significantly with mean UAS distance (table 3.3 conditional models). Placement of labelled pollen on bee wings generally appeared to concentrate in the central part of the wings later in the day, apparently moving inward from the edges (fig. 3.5 and appendix fig. B.4).

Table 3.3: Output for the hurdle models performed to determine whether the contribution and deposition of pollen from quantum dot-labelled anthers onto bee wings changed with floral narrowing (mean floral distance in mm). Anther types and their associated fixed effects, coefficient estimates, standard errors and z - and p -values are displayed for the conditional truncated Poisson models, as well as the zero-inflated models. Fixed effects include the mean floral distance (averaged over hour and measured in mm), the overall wing pollen density (# grains per mm²) and the total number of recipient and donor flowers visited by each bee. For the zero-inflated model, the results describe the probability of having an extra zero in the dataset. Significant effects are printed in bold text.

Response variable	Fixed effect	Estimate	SE	z	p
Conditional models					
Lower anther (yellow) pollen count	Mean LA distance	-0.52	0.18	-2.82	0.005
	Overall wing density	0.005	0.008	0.61	0.539
	Recipient visits	0.15	0.14	1.10	0.270
	Donor visits	-0.17	0.16	-1.05	0.292
Upper anther (red) pollen count	Mean UAS distance	-0.06	0.10	-0.56	0.573
	Overall wing density	-0.01	0.02	-0.53	0.595
	Recipient visits	-0.13	0.20	-0.63	0.526
	Donor visits	0.29	0.23	1.26	0.207
Zero-inflated models					
Lower anther (yellow) pollen presence	Mean LA distance	0.84	0.36	2.32	0.021
	Overall wing density	-0.02	0.01	-1.40	0.161
	Recipient visits	-0.42	0.21	-1.98	0.048
	Donor visits	0.29	0.26	1.12	0.256
Upper anther (red) pollen presence	Mean UAS distance	0.39	0.24	1.63	0.103
	Overall wing density	-0.04	0.02	1.88	0.061
	Recipient visits	-0.03	0.27	-0.17	0.906
	Donor visits	-0.33	0.27	-1.20	0.231

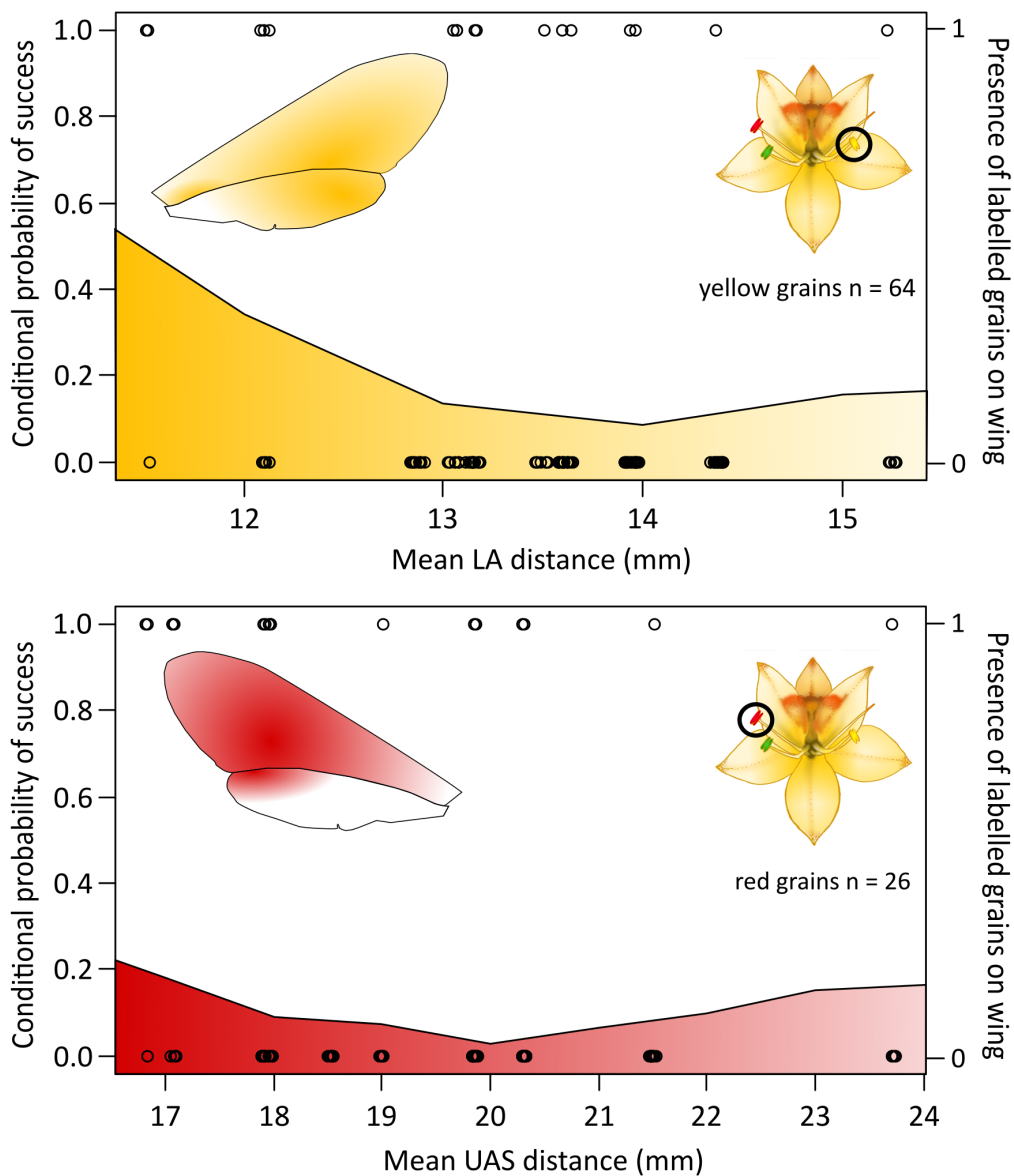


Figure 3.5: Conditional density plots (filled areas) showing how the mean floral distance (UAS or LA) is associated with the conditional probability that bee wings received yellow- or red-labelled pollen (conditional probability of success). Open circles show the raw distribution of data points when labelled pollen grains were present on a bee (1) or not (0). Wing heat map insets display a rough distribution of all the labelled grains received, with darker colours representing grains received when floral distances were narrower (i.e. later in the day). For further reference see appendix fig. B.4.

Mean pollen density on bee wings differed significantly over time ($F_{(9, 371)} = 22.32$, $p < 0.001$; fig. 3.6) and between all three wing sections ($F_{(2, 371)} = 205.61$, $p < 0.001$). The density on the hind wing was significantly higher than on the wing tip ($p < 0.001$), but significantly lower than on the central forewing ($p < 0.001$). Overall

wing pollen density was at its highest between 3 – 4 hours after sunrise ($\sim 9\text{h}00 - 10\text{h}00$; overall mean \pm SE: 59.71 ± 5.38 grains per mm^2), after which it decreased and plateaued after 4 hours after sunrise (overall mean \pm SE at 4 – 5 hours after sunrise: 37.12 ± 4.50 grains per mm^2). Wing pollen density then decreased sharply between 8 – 10 hours after sunrise (overall mean \pm SE at 9 – 10 hours after sunrise: 8.98 ± 1.26 grains per mm^2) and gradually increased slightly again in the following hours (fig. 3.6).

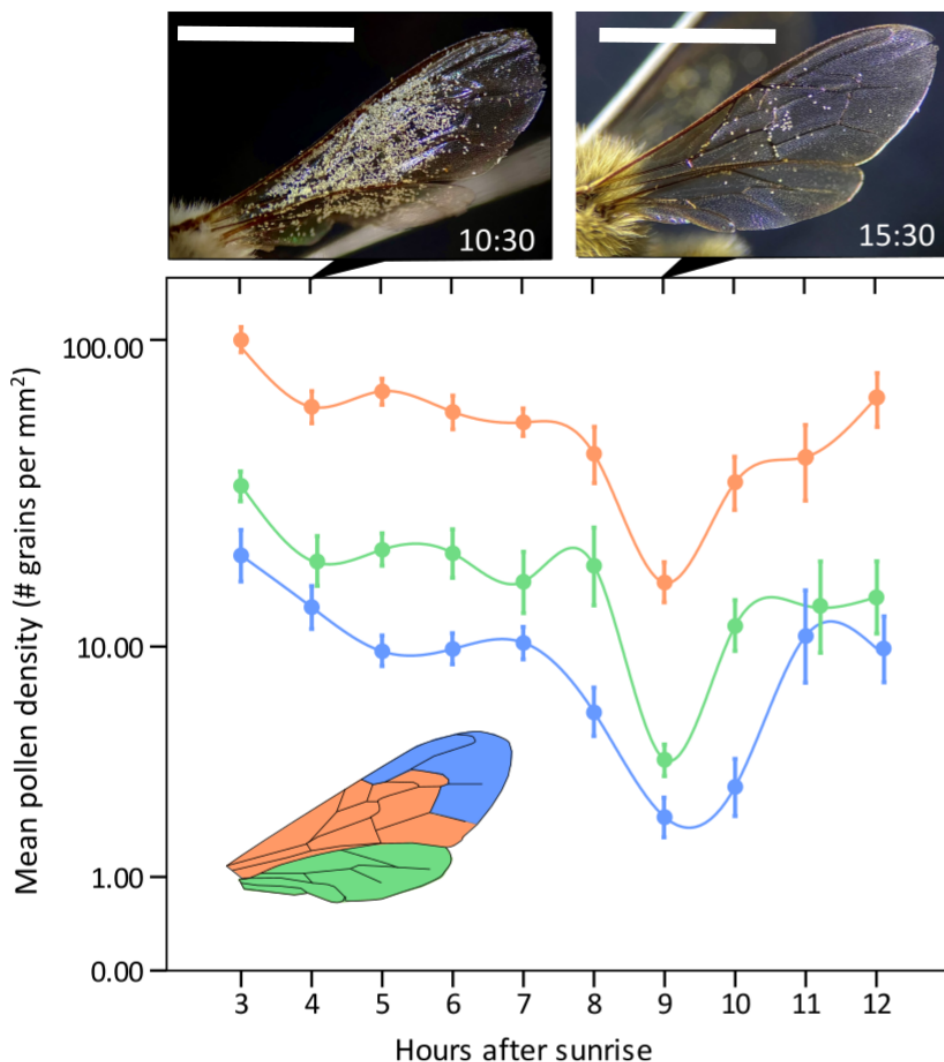


Figure 3.6: Mean (\pm SE) density of pollen grains (number of grains per mm^2) on the central forewing (orange), the hind wing (green) and the wing tip (blue) over time. The y-axis is displayed on a logarithmic scale. The photographic insets show the density of pollen grains on bee wings at 10:30 (4 – 5 hours after sunrise) and 15:30 (9 – 10 hours after sunrise). Scale bars represent 5 mm.

DISCUSSION

Wachendorfia paniculata displays significant floral narrowing, where the lateral and vertical separation distances between reproductive structures decrease over time. My findings suggest that this movement could play a functionally significant role in pollination. For short-lived flowers, the short time window for pollination magnifies the trade-off between pollen quality and pollen receipt: while high-quality outcross pollen transfer is most beneficial, floral structures must still be positioned in a way that promotes successful pollination within a short period of time (e.g. Liu *et al.*, 2020; Ruan *et al.*, 2004). Below I provide evidence suggesting that floral movement in *W. paniculata* might serve to balance these two variables.

Stylar movement as a reproductive assurance mechanism

Honey bees deposited pollen onto stigmas very infrequently – only 24% of recipient flowers that were visited by bees received pollen, less than 3% of which received pollen from quantum dot-labelled anthers. Infrequent incidences of effective pollen transfer are not unusual and have been recorded in species such as *Lapeirousia anceps* (see Minnaar *et al.*, 2019). The low rate of labelled pollen pickup and deposition by honey bees can have several causes. Firstly, stochastic pollen pickups might be commonplace, but few studies have been able to confirm this since fresh pollen couldn't be easily distinguished from pre-existing pollen until now (Minnaar *et al.*, 2019). The fact that *W. paniculata* pollen is placed on the vigorously beating wings of pollinators could also explain why so little labelled pollen remains on the wings. The generally poor fit between honey bees and *W. paniculata* parts might also lead to stochastic pickup rates. Lastly, the presence of pre-existing pollen might preclude the pickup of new pollen if the wing is saturated and if the presence of pollen prevents new pollen from attaching securely to the wing.

I found that the wing pollen loads on honey bees decreased over time until 10 hours after sunrise, after which they increased gradually again. The central forewings

and wing tips consistently carried the highest and lowest concentrations of pollen, respectively. Furthermore, the chances of stigmatic pollen receipt decreased with decreasing wing pollen densities, particularly on the central forewings and the wing tips. Despite the temporal variation in pollen loads, the incidence and magnitude of stigmatic pollen receipt remained unchanged over both time and UAS distance. I suggest that this discrepancy arises because the movement of the stigmas during the day facilitates increasingly regular contact with the wings later in the day, when wing-pollen is generally scarcer. Thus, while stigma contact is rare in the morning, the likelihood of the stigma picking up pollen when it eventually makes contact is high because of higher overall wing pollen densities. As the stigma moves over time, it makes more regular contact with the wings, but the stigma has a lower chance of picking up pollen per contact because of smaller pollinator pollen loads.

By increasing the frequency of contact between reproductive structures and pollinators, the narrowing of reproductive separation might improve pollination accuracy over time and maximise pollen movement, which is vital when pollinators are scarce. Given that the flowers of *W. paniculata* are short-lived, they might be particularly vulnerable to pollen limitation in the springtime (the peak flowering period) when bouts of adverse weather conditions may limit pollinator activity (Jesson and Barrett, 2002). Besides this, pollinator diversity and visitation rates have been known to be spatially variable for *W. paniculata* (see chapter 2).

However, if smaller reproductive separation distances improve pollination accuracy through increasingly regular pollinator contact, the question remains why floral structures are widely spaced to begin with. Below, I consider non-mutually exclusive explanations, which involve a trade-off between prioritising outcrossing and maximising pollen receipt later in the day.

In the past, reproductive assurance in plants has been strictly characterised by obligate or facultative selfing strategies (see Lloyd, 1992) such as autonomous selfing (pollination within the same flower), delayed selfing and facilitated selfing (selfing

aided by pollinators). Lloyd (1992) argued that facilitated selfing rarely benefits flowering plants, as its effect is negligible when pollinators are plentiful and is completely impractical when pollinators are absent (but see Anderson *et al.* 2003). In the context of floral movement, reproductive assurance through delayed autonomous selfing is a commonly cited function of rapid anther-stigma distance narrowing (Kalisz *et al.*, 1999; Nagy *et al.*, 1999; Ruan *et al.*, 2010; Ren and Tang, 2012). According to Lloyd (1992), delayed selfing is the most advantageous reproductive assurance strategy, as it gives precedence to fertilization via outcrossing but later ensures pollen receipt by selfing.

Even though Jesson and Barrett (2002) established that stigma-anther narrowing in *W. paniculata* does not result in delayed autonomous selfing, it might still confer reproductive assurance. The stigma's position possibly changes in response to pollen quality mosaics observed on pollinators by Minnaar and Anderson (2021). I propose that the extremely wide stigma position early in the day corresponds with 'hotspots' of wing pollen that contain a high outcross: self-pollen component. In the morning when overall pollen availability is high, the stigma can afford to target high-quality patches found on the wing tips (in the case of honey bees) or on large pollinators (if they are present). However, as these areas become depleted of pollen, the stigma moves inwards towards areas which have higher pollen densities but lower quality pollen (see Minnaar, 2018). Despite the fact that large pollinators were found to be sporadic pollinators of *W. paniculata* (see chapter 2 and appendix B section IV), floral narrowing might still act as a bet-hedging strategy by allowing larger pollinators to be prioritised during the peak pollination period if they are present.

This strategy doesn't entirely comply with the classic reproductive assurance strategies of delayed or facilitated selfing (Lloyd, 1992), since self-pollen receipt is not its intended purpose. Rather, the stigma's original position prioritises outcrossing and avoids selfing, while subsequent positions prioritise pollen receipt by targeting pollen-rich areas, which incidentally have a self-pollen component. Evidently,

the drawbacks of possibly selfing are outweighed by the benefits of receiving any kind of pollen, regardless of its quality. This could be of value in populations with highly skewed morph ratios, low pollinator visitation rates or an absence of large pollinators. In these situations, the mixture of self-, inter- and intra-morph pollen maximises the available mating pool, especially when compared to theoretical flowers that only have anthers situated opposite the stigma (Minnaar and Anderson, 2021).

Targeting high-quality pollen early in the day is important because pollen arriving early on a stigma usually has a greater chance of fertilizing ovules than pollen which is deposited later (*sensu* Harder and Wilson, 1994). This is likely a major consideration for short-lived flowers (Harder and Wilson, 1994) and since *W. paniculata* flowers only have three ovules, the early receipt of any self-pollen is likely to discount any outcrossed pollen that lands later in the day.

When *W. paniculata* flowers open, the stigmas are often positioned substantially higher and further back than the anthers (appendix fig. B.1; appendix fig. B.2; Minnaar, 2018). This is also perhaps a strategy that prevents high rates of facilitated selfing and/ or intersexual interference between the stigma and the stigma-side anther (Barrett, 2002; Armbruster *et al.*, 2014). If not for this extreme initial ‘vertical herkogamy’, seed discounting could occur, where high amounts of self-pollen clog the stigma, reducing seed set (Barrett, 2002). This way, pollen export and outcrossing are unhindered early in the day (Kalisz *et al.*, 1999; Ruan and da Silva, 2011; Liu *et al.*, 2020), while stylar movement ensures regular contact rates later in the day, after most pollen from the stigma-side anther has been dispersed.

Lloyd (1992) proposed that selection against facilitated selfing might have led to the evolution of extreme forms of herkogamy. Likewise, Armbruster *et al.* (2009; 2014) suggested that greater stigma/ anther accuracy should select for narrower separation distances, while reduced sexual interference should select for greater separation or herkogamy. Interestingly, this opposing selection conundrum was mitigated by

movement herkogamy in *Parnassia epunctulata*, which reduces sexual interference and preserves adaptive accuracy (Armbruster *et al.*, 2014). A combination of dichogamy, successive anther presentation and style elongation allowed anthers and stigmas to be accurately positioned without interfering with each other and reduced the distance between areas of pollen deposition and receipt. In light of this, rapid floral narrowing in *W. paniculata* might moderate the conflict between selection against sexual interference and selection for adequate pollination accuracy.

In *W. paniculata*, more extreme herkogamy at the start of the day appears to be a mechanism to select for higher-quality pollen early on, while narrowing increases accuracy and facilitates reproductive assurance later in the day. Similarly, Ruan *et al.* (2009a) found that stylar movement in *Kosteletzkya virginica* had dual functions. Initially, stylar bending positioned the stigma in the direct path of a visitor, maximising the likelihood of contact. Then, further bending of unpollinated stigmas resulted in reproductive assurance via delayed selfing when pollinators were limited by inclement weather (Ruan *et al.*, 2004, 2009a).

Rate of stylar movement

It is unlikely that floral movement is solely caused by the wilting or closure of the flower, as most of the stylar movement occurred well before floral wilting or corolla closure was observed in the field. Stylar curvature was considerably faster early in the day and slowed down in the afternoon (fig. 3.2). This could suggest that rapid movement is more important in the morning, when most stigmas are still highly receptive and not yet fully saturated (appendix fig. B.5 & B.6). I found that the reproductive viability of flowers decreased substantially later in the day, as fruit set decreased from 71% success in the morning to between 35% and 41% success in the afternoon (appendix section II; fig. B.5). Furthermore, in this population, the stigmas of most flowers saturated (≥ 3 grains on stigma) between 5 and 7 hours after sunrise, perhaps negating the need for movement later in the day (appendix section III; fig. B.6).

For the short-lived *Ipomoea purpurea*, Liu *et al.* (2020) also found that pollen germination was diminished later in the day because of increasing ambient temperatures. However, the flower still managed to self-pollinate at the end of anthesis via movement herkogamy, having prioritised high-quality pollen receipt and germination in the early morning.

Anther movement

When compared to the total UAS narrowing, lower anthers did not appear to narrow as noticeably, only moving ~ 1 mm either way (appendix fig. B.2). Nevertheless, lower anthers deposited pollen onto bee wings with greater regularity at narrower separation distances. This finding could account for the unexpected increase of wing pollen loads that was observed between 10 and 13 hours after sunrise (fig. 3.6), since the timing of increased pollen deposition likelihood also coincides with that of higher wing pollen loads late in the day. This increase may not however impact pollination success, since flower viability is reduced and most stigmas would likely be saturated by this time.

Given that narrow anthers result in less sporadic pollen placement on pollinators, it is unclear what advantage widely-spaced anthers may confer early in the day. It is possible that the advantage of wide anthers is not related to the frequency of contact with pollinators but about the location of contact. If the stigma is widely spaced at the start of the day, it may make sense for anthers to approximately mirror the stigma's position, thus improving the accuracy of anther-stigma positioning. From the heat maps (fig. 3.5 and appendix fig. B.4) it appears that anther placement becomes more targeted toward the central part of the wing later in the day. Consequently, changes in the position of the stigma over time are bound to change the 'adaptive optimum', possibly forcing anther positions to shift accordingly (Armbruster *et al.*, 2009).

Alternatively, the reason for anther movement might be purely physical by nature.

It is possible that stigma and anther movements are inextricably linked – meaning that the stigma cannot move without the anthers moving as well. This could be the case if the stigma and anthers share the same ontogenetic origin, or the same mechanistic avenue for movement.

Conclusion

Evidently, floral movement in *W. paniculata* is a complex mechanism that can have multiple functions that interlink and fortify each other. My results suggest that the stigma and anthers move to improve pollination accuracy over time by making more regular and targeted contact with pollinator wings, thereby increasing pollination efficiency and acting as a reproductive assurance mechanism. Tentatively, it appears that stigmas prioritise areas with a high proportion of outcross vs. self-pollen early in the day and later shift toward areas with high pollen quantities but lower pollen quality. In this way, *W. paniculata* navigates a trade-off regarding pollen receipt – by being selective towards high quality pollen in the early morning, but allowing for successful pollination later in the day, even if reproductive viability is diminished.

APPENDIX B

I. SUPPLEMENTARY FIGURES & TABLES

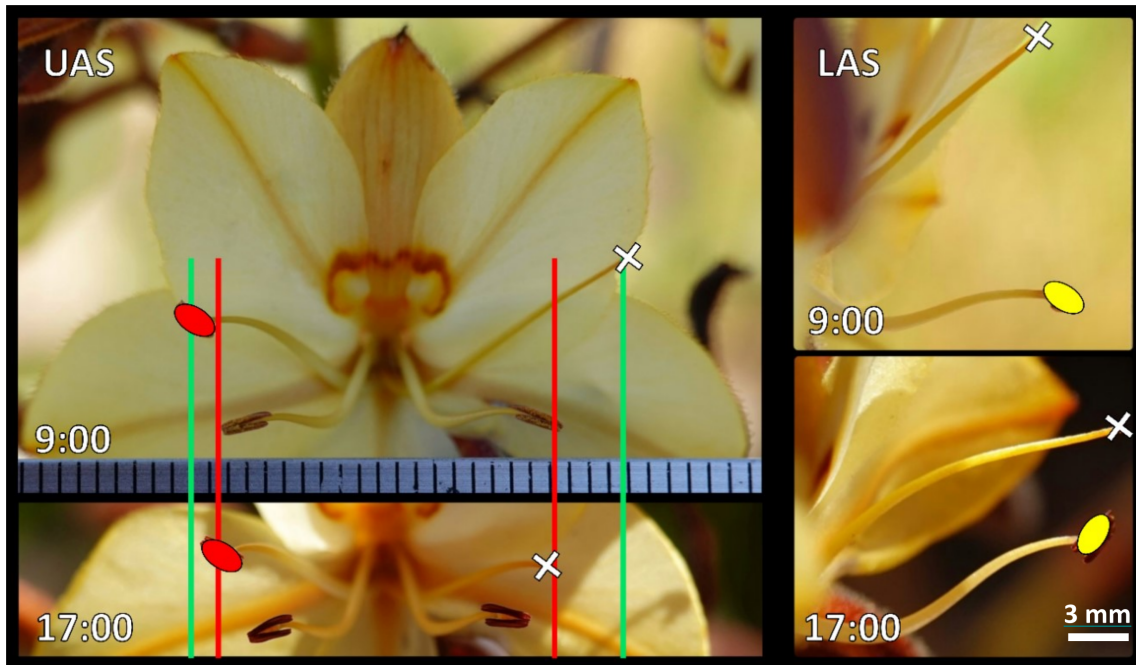


Figure B.1: An example of how floral structures narrow over the course of the day for a single *W. paniculata* flower in the field. The green lines show the starting positions of the upper anther (red oval) and the stigma (white cross), whereas red lines show the end positions. For LAS, the yellow oval represents the position of the lower stigma-side anther, while the white cross represents the position of the stigma, which visibly move toward each other between 9:00 and 17:00. The scale bar for UAS is denoted in mm.

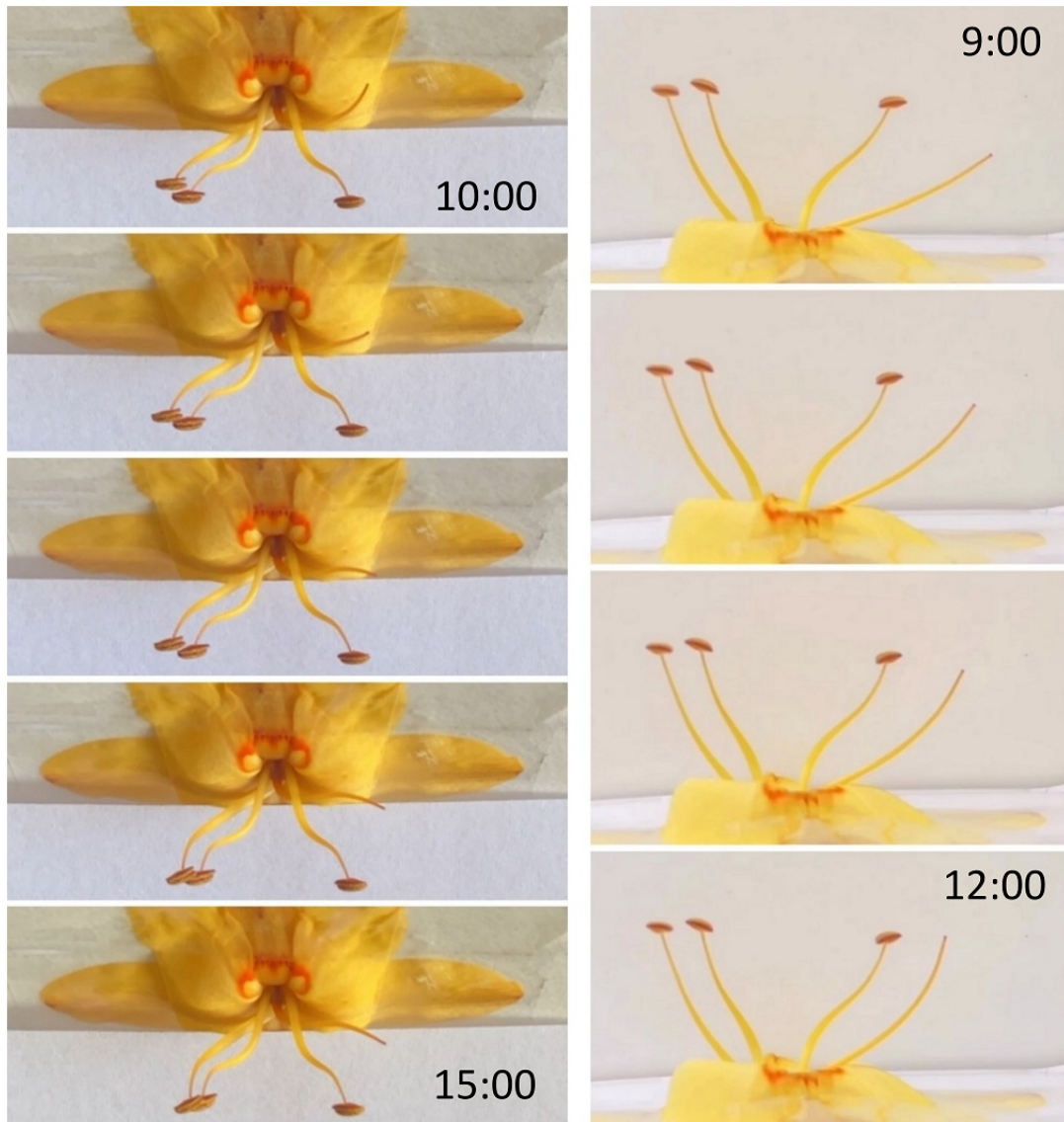


Figure B.2: Time-lapse footage of two cut flowers (left: front view; right: distal view) that were picked the previous day and allowed to open naturally. The tepals were taped to a piece of cardboard to prevent the corolla from moving. Note the wide-angled position of the stigma upon opening.

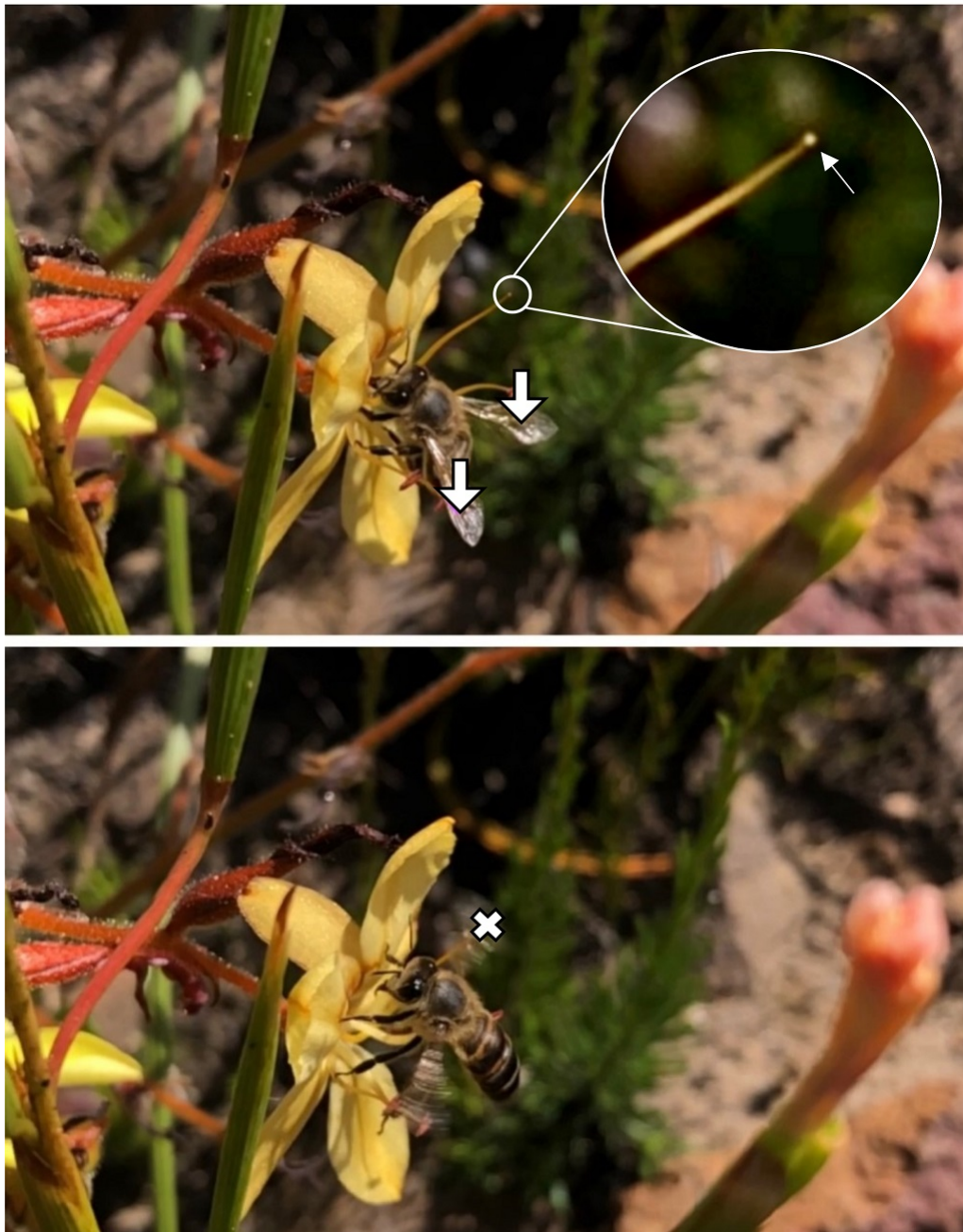


Figure B.3: A honey bee visiting a *W. paniculata* flower. A white cross shows the point of stigma contact upon departure (bottom), while arrows show where lower anthers made contact during landing (top). Bright yellow pollen is clearly visible on the stigma in the top frame (inset). Photos: Kayleigh Murray

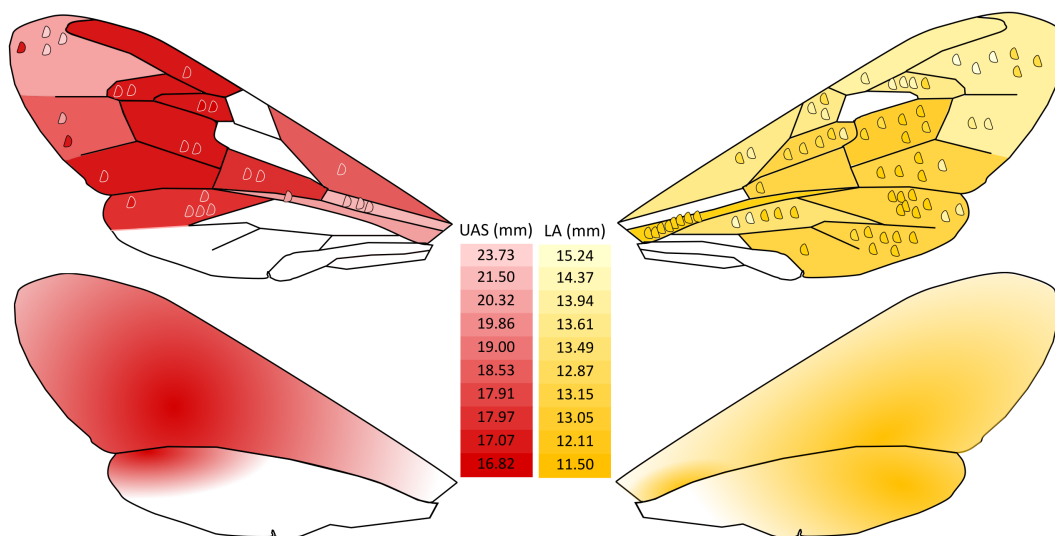


Figure B.4: Diagrams depicting the approximate distribution and numbers of quantum dot-labelled grains deposited by lower (yellow) and upper (red) anthers onto bee wings. Darker shades correspond with smaller mean floral distances and later times of the day. The top diagram displays the raw distribution of all pollen grains, coloured according to the time of day at which they were received. Wing cell colour reflects the average floral distance or hour after sunrise at which a grain was deposited. This was used to generate the heat maps in the bottom diagram by approximating the concentration of colour in the top figure.

Table B.1: Output for the hurdle models performed to determine whether stigma pollen receipt changes with floral narrowing and if it is influenced by wing pollen density (number of grains per mm²) from different wing sections. Fixed effects, coefficient estimates, standard errors and z - and p -values are displayed for the conditional truncated Poisson models, as well as the zero-inflated models. For the zero-inflated model, the results describe the probability of having an extra zero in the dataset. Significant effects are printed in bold text.

Response variable	Fixed effect	Estimate	SE	z	p
Conditional model					
Pollen count on stigma	Mean UAS distance	0.01	0.01	1.11	0.266
	Central forewing density	0.13	0.10	1.24	0.215
Zero-inflated model					
Pollen presence on stigma	Mean UAS distance	0.15	0.10	1.45	0.147
	Central forewing density	-0.01	0.01	-2.46	0.014
Conditional model					
Pollen count on stigma	Mean UAS distance	0.19	0.10	1.95	0.052
	Hindwing density	-0.001	0.01	-0.06	-0.949
Zero-inflated model					
Pollen presence on stigma	Mean UAS distance	0.08	0.10	0.86	0.391
	Hindwing density	-0.01	0.01	-1.32	0.188
Conditional model					
Pollen count on stigma	Mean UAS distance	0.17	0.10	1.77	0.078
	Wing tip density	0.01	0.02	0.47	0.637
Zero-inflated model					
Pollen presence on stigma	Mean UAS distance	0.10	0.09	1.03	0.303
	Wing tip density	-0.04	0.02	-2.10	0.036

II. REPRODUCTIVE VIABILITY

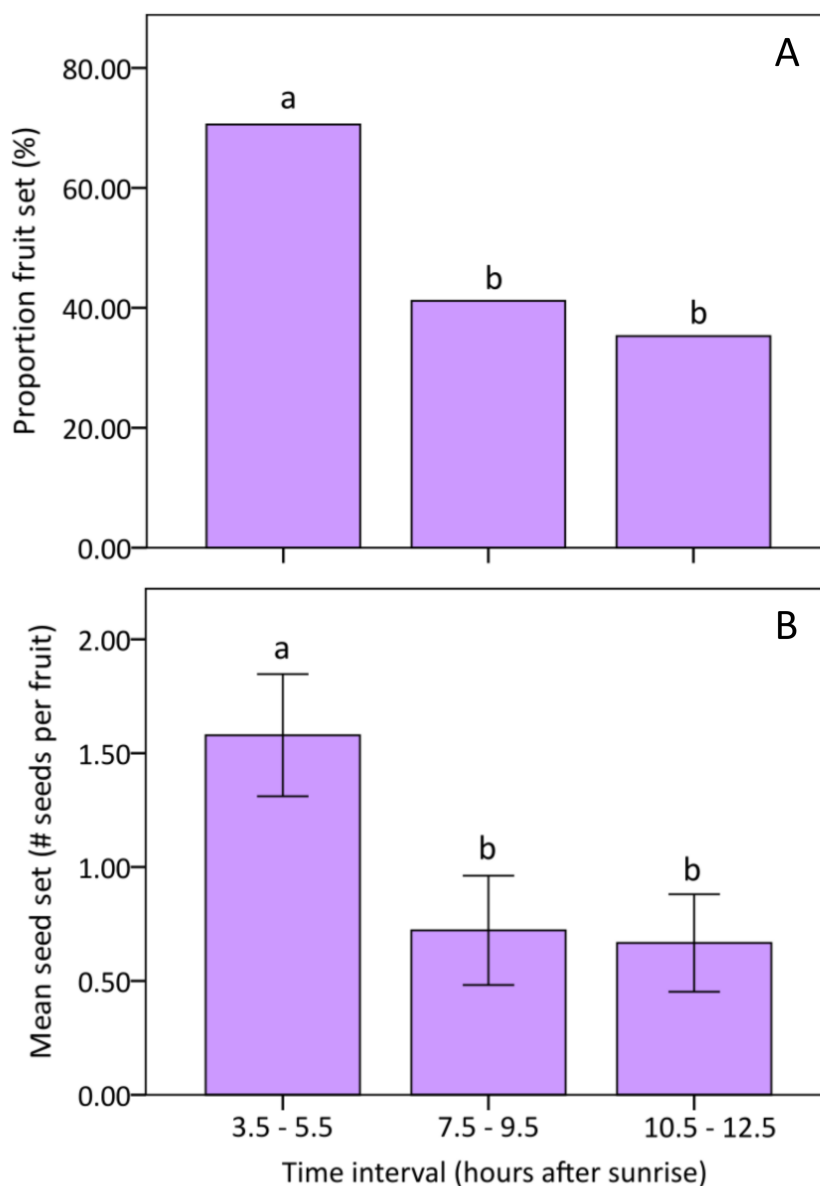


Figure B.5: The proportion of total fruit that developed after being hand-pollinated at different times of the day (A) and the mean seed set per fruit that developed after being hand-pollinated at different times (B). 3.5 – 5.5 hours after sunrise was during the morning, whilst the other two intervals occurred in the afternoon. Intervals that share the same letter are not significantly different from each other ($p > 0.05$).

Stigmas are known to become unreceptive towards the end of their lifespan, while pollen is also known to become unviable over time, resulting in a reduced seed set (e.g. Liu et al., 2020). To determine whether the flowers are still reproductively viable in the afternoon, flowers were hand-pollinated at three different time intervals

throughout the day. Right-handed plants ($n = 17$) were covered with a mesh bag the day before the experiment. On the morning of the experiment, approximately 15 upper anthers from left-handed plants were haphazardly collected just after dehiscence, placed in a vial and shaken vigorously to release their pollen. Between 3.5 and 5.5 hours after sunrise ($\sim 9\text{h}00 - 11\text{h}00$) this pollen was generously applied to the stigma of a single right-handed flower per plant using a clean insect pin, and the plant was carefully covered again. After pollination, the vial was kept cool in a cooler box to preserve pollen viability. This procedure was repeated again in the afternoon at 7.5 – 9.5 hours after sunrise ($\sim 13\text{h}00 - 15\text{h}00$) and 10.5 – 12.5 hours after sunrise ($\sim 16\text{h}00 - 18\text{h}00$). All covered flowers were emasculated at 3.5 hours after sunrise to prevent accidental selfing. Plants were left covered until the following day, and then opened to let the fruits develop for two weeks. Even though the fruits were not fully mature by this time, it was still possible to determine whether a seed had formed.

Fruit set was defined as the number of fruits bearing at least one viable seed. Fruits that contained aborted seed embryos were not included in the analyses. To evaluate whether fruit set was more successful in the morning or early and/or late afternoon, a 3×3 Cochran's Q test was performed. Similar to the Chi-square test, the Cochran's Q test evaluates whether the proportions of three or more binary and dependent variables are equal to each other in a population. Pairwise McNemar tests with holm adjustments provided pairwise comparisons between treatments. To determine if seed set differed between the morning and early or late afternoon, a Friedman test was done, followed by a sign test (with holm-adjusted p -values) to display pairwise comparisons.

70.59% of fruits that were pollinated in the morning developed, while only 41.18% and 35.29% developed in the early and late afternoon, respectively (Cochran's $Q_{(2)} = 7.75$, $n = 17$, $p = 0.021$; appendix fig. B.5). Pairwise McNemar comparisons with holm adjustments showed that inflorescences produced significantly fewer fruits

when pollinated in the early or late afternoon than in the morning (early pm – am: $Z = 2.24$, $p = 0.038$; late pm – am: $Z = 2.45$, $p = 0.038$). The two afternoon treatments did not differ significantly from each other ($Z = 0.45$, $p = 0.655$). 50.98% of seeds developed in the morning, whilst only 25.49% and 21.57% of seeds developed in the early and late afternoon, respectively. Mean seed set differed significantly between pollination treatments (Friedman $\chi^2_{(2)} = 11.56$, $p = 0.003$; appendix fig. B.5). Mean seed set per fruit was significantly higher in the morning than in either of the afternoon treatments (am – early pm: $S_{(7)} = 7.00$, $p = 0.023$; am – late pm: $S_{(11)} = 10.00$, $p = 0.023$), and seed set did not differ between afternoon treatments (early pm – late pm: $S_{(7)} = 5.00$, $p = 0.450$).

It should be kept in mind that the observed decrease in reproductive viability could be a symptom of temperature sensitivity – this experiment was conducted at the end of the flowering season (mid-December), when ground-level temperatures often exceed 30 degrees Celsius. High ambient temperatures have been known to disable at least one pathway to pollination (e.g. Liu et al., 2020). Therefore, reproductive viability might last for longer in cooler temperatures such as during the spring, when *W. paniculata* is at its flowering peak.

III. STIGMA SATURATION RATE

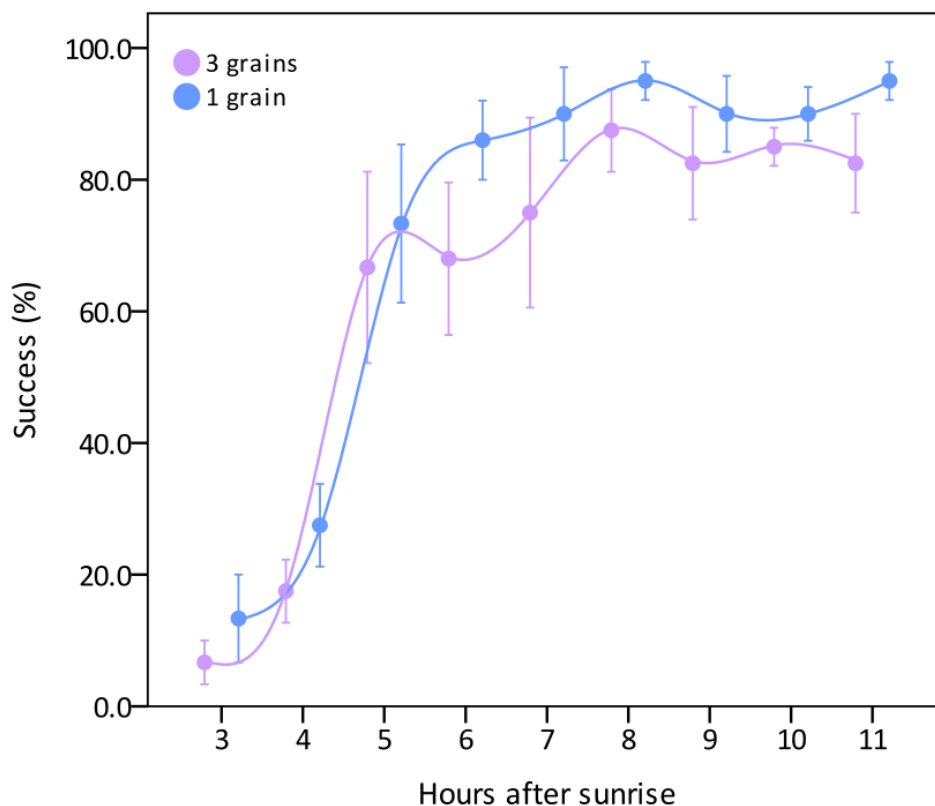


Figure B.6: Stigma saturation over time. The mean percentage of harvested stigmas that had at least one pollen grain (blue) and three pollen grains (purple) over time.

To generate a timeline of pollen deposition and subsequent stigma saturation, stigmas from naturally pollinated plants were collected throughout the day within the peak flowering period. Care was taken to sample on days when the weather allowed for good pollinator visitation rates. From the onset of anthesis, ten stigmas were collected at random every hour over four days. The style was carefully removed with fine-tipped forceps, placed in individual Eppendorf tubes and kept cool until it could be frozen. The number of pollen grains on stigmas were manually counted using light microscopy after the styles had been set in fuchsin gel on microscope slides.

The proportion of stigmas that received at least one pollen grain (minimum number needed for one seed) and three pollen grains (minimum number to saturate all

ovules) were plotted on appendix fig. B.6, which shows that pollen receipt reached its maximum at 8 hours after sunrise ($\sim 14\text{h}00$), where more than 90% of stigmas received at least one grain. The most pollen was received between 4 and 5 hours after sunrise, where the proportion of stigmas that received pollen increased by more than 40%, after which the rate of pollen receipt started to slow down. Proportion tests showed that proportions of stigmas that received pollen changed significantly throughout the day (1 grain – $\chi^2_{(8)} = 145.36$, $p < 0.001$; 3 grains – $\chi^2_{(8)} = 113.45$, $p < 0.001$). Pairwise proportion tests (holm-adjusted) showed that only the first two hours (3 and 4 hours after sunrise) differed significantly from the rest of the day ($p < 0.01$), suggesting that stigmas saturated very quickly in the morning by 5 hours after sunrise ($\sim 11\text{h}00$).

IV. POLLINATOR VISITATION RATES & ABUNDANCES

Pollinator visitation rates were observed over three days in 2019 – one at the height of the flowering peak and two at the end of the season. Pollinator observations were done for 15 minutes every hour after anthesis in the Franschhoek Pass population. Two different plots of flowers (mean plot size 6 m²) were alternated every hour, and the number of flowers visited by each pollinator within 15 minutes was noted. Honey bees comprised 93.68% of all visits, with a total of 267 honeybee visits, while nine visits were by *Xylocopa rufitarsis*, four visits by a large *Thyreus* sp., two visits by both *Thyreus delumbatus* and an *Amegilla* sp., and one visit by a *Megachile* sp.

The mean \pm SD overall visitation rate declined gradually over time from the highest mean visitation rate of 4.07 ± 2.97 bees per flower per hour at 4 hours after sunrise to the lowest mean visitation rate of 2.07 ± 3.08 bees per flower per hour at 11 hours after sunrise. Visitation rates were highly variable between days. Thus, to compare visitation rates between days, raw visitation rate values were z-transformed (Fijen and Kleijn, 2017), grouped by hours after sunrise, and analysed using a one-way

ANOVA. Visitation rates were not found to differ significantly over time ($F_{(8, 17)} = 0.80$, $p = 0.610$; appendix fig. B.7).

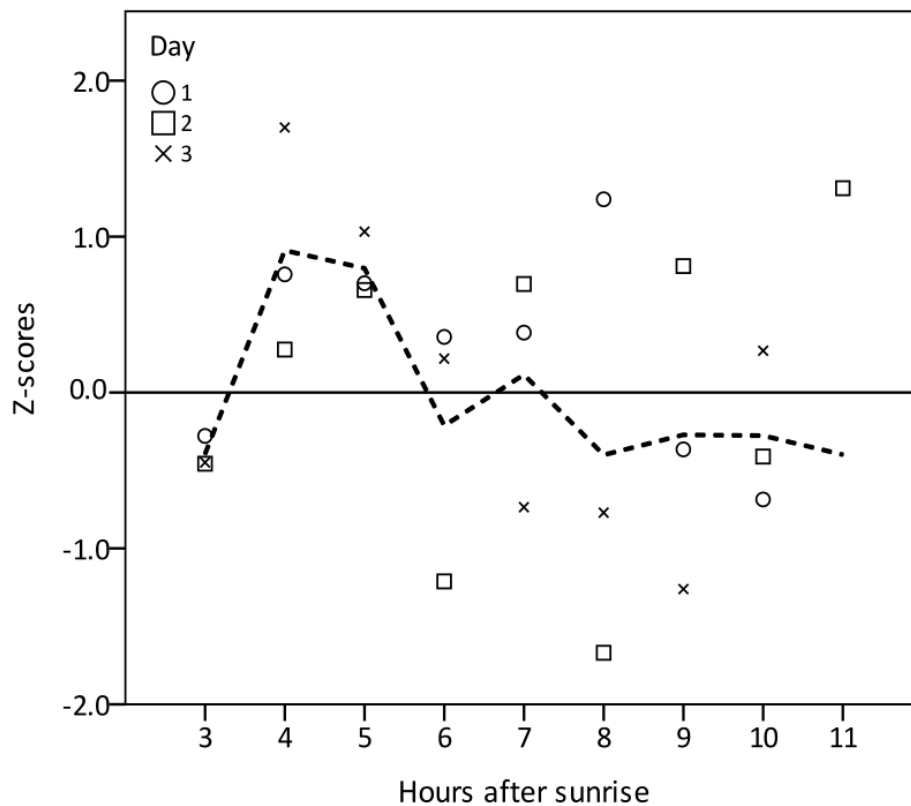


Figure B.7: Z-standardised honeybee visitation rates over time, which corrects data so that the mean for each day equals zero, which controls for variation in data between days. Different symbols show the variation of visitation rates between different days, while the dashed line represents the visitation rate averaged over all days.

CHAPTER 4

GENERAL CONCLUSIONS

This study provided insights into the pollination biology of a single enantiostylous flower species at both large (inter-population) and small (intra-population) scales within natural and experimental contexts. It presents valuable information about the natural history of *W. paniculata*, as well as the function of its floral configuration; firmly situating it within the broader literature regarding enantiostyly, phenotypic variation and floral movement.

The study of phenotypic variation in floral morphology is challenging, as various past and present selective pressures commonly shape extant patterns of variation. These selective pressures often involve a complex interplay between genetic, ecological and environmental variables within which pollinator selection plays a minor role (Galen 1999; Herrera *et al.*, 2006; Van der Niet *et al.*, 2014; Zhao and Wang, 2015). It appears that this is also true in the present study, as the observed spatial and temporal variation in the degree of reproductive separation cannot be entirely explained by contemporary patterns of pollinator-driven selection alone.

Geographic variation in the distances between reproductive parts could partly be explained through allometric scaling with flower size, honey bee visitation rates and floral movement over time, but not average pollinator wingspan. However, the absence of a trend regarding pollinator fit does not necessarily mean that flowers were never adapted to specific pollinators – the proliferation of beekeeping may have changed pollinator assemblages in recent history, so that past pollinator-driven patterns may now be obscured (Steffan-Dewenter *et al.*, 2002; Henry and Rodet, 2018; García *et al.*, 2020; Pauw *et al.*, 2020).

Contrary to past predictions (see Goldberg, 1996; Ornduff and Dulberger 1978; Helme and Linder 1992), large-bodied insects did not feature as prominent pollinators of *W. paniculata* (see chapter 2 and appendix B section IV), and their presence or absence seemingly did not affect average separation distances between stigmas

and anthers. Even though it wasn't a principal focus of the study, it became apparent that honey bees are effective pollinators of *W. paniculata*, and I propose that they, and other small bee species (such as Anthophorid bees), are now the most important pollinators in most populations (but see Willmer *et al.* 2017). My results indicate that honey bees are the most widespread and frequent (see chapter 2 and appendix B section IV) visitors of *W. paniculata*, and that they are capable of effecting good seed set (appendix C section I; fig. C.1). High visitation rates and high abundances appear to offset any pollination inefficiency that might arise from inconsistent contact rates with stigmas. Furthermore, in my first data chapter I demonstrated that high visitation rates by honey bees might select for smaller separation distances between lower anthers, signalling their importance for *W. paniculata*. It is believed that the male function in flowers is more difficult to satisfy than female function, as more effort is required to export all pollen grains than to fertilise all ovules (Bateman, 1948; Webb and Lloyd, 1986; Delph, 1996). This is especially true for flowers with a high pollen to ovule ratio, such as *W. paniculata*, which only has three ovules. Therefore, it makes sense that the average distance between lower anthers would narrow in response to more frequent honey bee visits (see chapter 2). However, this same pressure wouldn't necessarily affect the generally wide position of the stigma, since female function can easily become saturated through occasional contact with pollinators (but see chapter 3). Quick saturation is especially likely when pollinators are abundant. However, when pollinators are scarce, the extremely wide and high position of the stigma might be detrimental to female fitness, which may necessitate stylar movement over the course of anthesis to improve chances of pollen receipt (see chapter 3).

Since I found that large pollinators are uncommon pollinators of *W. paniculata*, and that distances between reproductive structures vary over time (see chapter 2), I questioned whether floral narrowing could be of benefit in populations that are dominated by small pollinators.

The likelihood of overall stigmatic pollen receipt remained unchanged over time and floral narrowing, even though pollen availability (pollinator pollen loads) fluctuated. I suggested that stigmatic movement might be a functional consequence of having to balance receipt of pollen with receipt of high-quality pollen. Here, high-quality pollen is targeted early in the day. Stigma movement later in the day increases the frequency of contact with pollinators, and aligns with areas on bee wings with higher pollen loads. It also increases the likelihood of receiving intra-morph pollen (which can have a self-pollen component), therefore acting similar to reproductive assurance. In addition, I proposed that the wide-angled starting position of the style might limit interference between the stigma and the stigma-side anther until the anther has dispersed most of its pollen. Both these mechanisms could prioritise the receipt of high-quality outcross pollen early in the day, while increasing the chances of pollination via intra-morph pollen later in the day, acting as reproductive assurance when pollinators are scarce (see Ruan *et al.* 2009a; Liu *et al.* 2020). The reason for lower anther movement was less clear, but could perhaps allow the anthers to match the stigma position over time to improve pollination accuracy (in the context of Armbruster *et al.* 2009). However, it is also possible that stigma and anther movements are inextricably connected via the same mechanism; meaning that the stigma cannot move without the anthers moving as well.

In chapter 2 an increase in pollinator visitation rate leads to a reduction in the distance between the lower anthers, which contrasts with chapter 3 where pollinator limitation appears to drive smaller LA distances. While these results may seem contradictory, they are not. Chapter 2 investigated floral narrowing at the inter-population scale whereas chapter 3 investigated it at the intra-population scale. Furthermore, in chapter 2 I suggest that the narrowing of the distance between the lower anthers is an evolutionary response to increased visitation rates by smaller pollinators over many generations. I propose that over time, flowers try to match the most common and/or efficient pollinators that are present in a population. Chapter 3 illustrates the flexibility of the flower's response to unpredictable pollinator envi-

ronments on any given day. Within a single population, individual flowers have the ability to react to low visitation rates by accommodating smaller pollinators when large pollinators are absent and by possibly selecting for high quality pollen in the mornings, but allowing for reproductive assurance in the afternoon. Moreover, in chapter 3 I found that the larger the initial distance between the structures, the further the structures moved over time. In other words, a population with a narrower mean reproductive separation distance will require less floral movement to accommodate smaller pollinators than a population with a large mean reproductive separation distance.

It is important to consider that this study was purely correlative and that extensive research is needed to shed more light on the findings at hand. Intensive study is still required to collect reliable pollinator community estimates over multiple flowering seasons and to test fitness trade-offs between environmental and ecological variables. Regarding floral movement, further studies should test how floral narrowing performs under different pollination scenarios (e.g. large vs. small pollinators; low vs. high visitation rates). Experiments that track stigma placement are needed to confirm whether the stigma makes more frequent contact with bee wings and if it shifts from targeting wing tips to central wings over time. To determine whether vertical stylar movement might mitigate selection for increasing pollination accuracy and selection against intersexual interference, one would need to determine whether the timing of stigma-side anther depletion coincides with minimum LAS distance, and whether pollination accuracy improves through stigmatic movement.

In summary, it appears that at least some of the observed geographic variation in reproductive separation can be explained by pollinator selection that is imposed by small pollinators. Additionally, temporal variation via floral movement might improve pollination accuracy and achieve reproductive assurance in populations where large pollinators are absent or when visitation rates are low. I conclude that while geographic and temporal variation in the degree of reproductive separation is likely

to be influenced by multiple biotic and abiotic factors, it appears that pollinator availability in general has a role in shaping the floral configuration of *W. paniculata*.

APPENDIX C

I. HONEY BEE EFFICIENCY

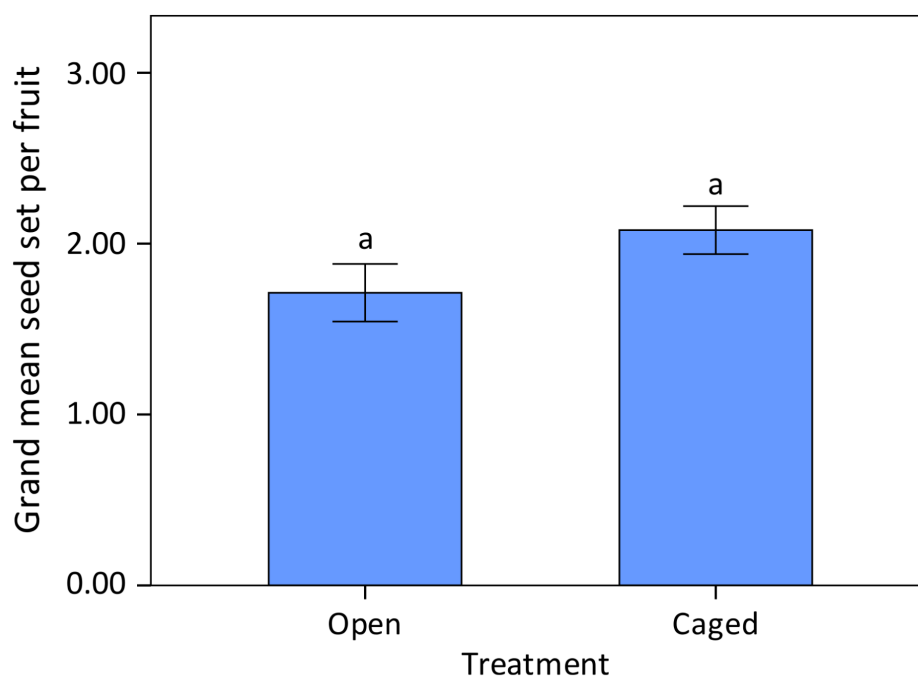


Figure C.1: Grand mean (\pm SE) seed set of inflorescences that were left open or caged to exclude large pollinators. Bars that share letters are not significantly different from each other.

After observing the low contact rate of honey bee wings with *W. paniculata* stigmas, it became apparent that it was necessary to confirm whether honey bees alone are capable of successful pollination of *W. paniculata*. To do this, 20 plants in the Franschhoek Pass population were covered by plastic mesh cages (mesh size of 15 mm \times 15 mm) which excluded large pollinators such as carpenter bees (*Xylocopa* spp.), but included honey bees and smaller solitary bees. For each plant, four buds that were due to open in the following two days were tagged and all open flowers were removed. Seeds of the four tagged fruits were harvested after three weeks, before the inflorescences could dry out and disperse seeds.

These fruits were compared to the fruit of 20 uncovered plants that flowered dur-

ing the same time period. Unfortunately, these inflorescences were harvested for a different experiment and were not labelled. Consequently, four fruits closest to the central stem were randomly selected, and the seeds were counted to provide a baseline value for the natural pollination scenario where all pollinator types are included.

Mean seed set per plant was analysed using an independent t-test to determine whether naturally pollinated plants (open) and exclusively honey bee-pollinated plants (caged) differ in their reproductive output. 69.91% and 56.96% of ovules developed into seeds for caged and open plants, respectively. The mean seed set per plant did not differ significantly between caged and open plants (independent $t_{(36.14)} = 1.67$, $p = 0.103$; appendix fig. C.1).

REFERENCES

- Abramoff MD, Magalhaes PJ, Ram SJ. 2004. Image Processing with ImageJ. *Biophotonics International* 11: 36–42.
- Aizen MA, Basilio A. 1998. Sex differential nectar secretion in protandrous *Alstroemeria aurea* (Alstroemeriaceae): Is production altered by pollen removal and receipt? *American Journal of Botany* 85: 245–252.
- Amador-Vargas S, Dominguez M, León G, Maldonado B, Murillo J, Vides GL. 2014. Leaf-folding response of a sensitive plant shows context-dependent behavioral plasticity. *Plant Ecology* 215: 1445–1454.
- Anderson B, Alexandersson R, Johnson SD. 2010. Evolution and coexistence of pollination ecotypes in an African *Gladiolus* (Iridaceae). *Evolution* 64: 960–972.
- Anderson B, Midgley JJ, Stewart BA. 2003. Facilitated selfing offers reproductive assurance: A mutualism between a hemipteran and carnivorous plant. *American Journal of Botany* 90: 1009–1015.
- Anderson B, Ros P, Wiese TJ, Ellis AG. 2014. Intraspecific divergence and convergence of floral tube length in specialized pollination interactions. *Proceedings of the Royal Society B: Biological Sciences* 281: 20141420.
- Armbruster WS, Corbet SA, Vey AJM, Liu SJ, Huang SQ. 2014. In the right place at the right time: *Parnassia* resolves the herkogamy dilemma by accurate repositioning of stamens and stigmas. *Annals of Botany* 113: 97–103.
- Armbruster WS, Hansen TF, Pélabon C, Pérez-Barrales R, Maad J. 2009. The adaptive accuracy of flowers: Measurement and microevolutionary patterns. *Annals of Botany* 103: 1529–1545.
- Armbruster WS, Muchhala N. 2020. Floral reorientation: the restoration of pollination accuracy after accidents. *New Phytologist* 227: 232–243.
- Barrett SCH. 2002. Sexual interference of the floral kind. *Heredity* 88: 154–159.

- Barrett SCH, Jesson LK, Baker AM. 2000. The Evolution and Function of Styelar Polymorphisms in Flowering Plants. *Annals of Botany* 85: 253–265.
- Bateman AJ. 1948. Intra-sexual selection in *Drosophila*. *Heredity* 2: 349–368.
- Bates D, Mächler M, Bolker B, Walker S. 2015. Fitting Linear Mixed-Effects Models Using lme4. *Journal of Statistical Software* 67: 1–48.
- Boberg E, Alexandersson R, Jonsson M, Maad J, Ågren J, Nilsson LA. 2014. Pollinator shifts and the evolution of spur length in the moth-pollinated orchid *Platanthera bifolia*. *Annals of Botany* 113: 267–275.
- Brooks ME, Kristensen K, van Benthem KJ, Magnusson A, Berg CW, Nielsen A, Skaug HJ, Mächler M, Bolker BM. 2017. glmmTMB balances speed and flexibility among packages for zero-inflated generalized linear mixed modeling. *R Journal* 9: 378–400.
- Brys R, Jacquemyn H, Hermy M, Beeckman T. 2008. Pollen deposition rates and the functioning of distyly in the perennial *Pulmonaria officinalis* (Boraginaceae). *Plant Systematics and Evolution* 273: 1–12.
- Burnham KP, Anderson DR. 2002. *Model selection and multimodel inference: a practice information-theoretic approach*. Springer, New York
- Bynum MR, Smith WK. 2001. Floral movements in response to thunderstorms improve reproductive effort in the alpine species *Gentiana algida* (Gentianaceae). *American Journal of Botany* 88: 1088–1095.
- Cane JH, Tepedino VJ. 2017. Gauging the Effect of Honey Bee Pollen Collection on Native Bee Communities. *Conservation Letters* 10: 205–210.
- Cochran WG. 1977. *Sampling Techniques* (3rd edition). Wiley, New York.
- Cruden ARW, Hermann-Parker SM. 2016. Butterfly Pollination of *Caesalpinia pulcherrima*, with Observations on a Psychophilous Syndrome. *Journal of Ecology* 67: 155–168.

- Daniels RJ, Johnson SD, Peter CI. 2020. Flower orientation in *Gloriosa superba* (Colchicaceae) promotes cross-pollination via butterfly wings. *Annals of Botany* 125: 1137–1149.
- Darwin, C. 1862. *On various contrivances by which British and foreign orchids are fertilised by insects*. John Murray, London.
- Darwin CR. 1877. *The different forms of flowers on plants of the same species*. John Murray, London.
- Delmas CEL, Fort TLC, Escaravage N, Pornon A. 2016. Pollen transfer in fragmented plant populations: insight from the pollen loads of pollinators and stigmas in a mass-flowering species. *Ecology and Evolution* 6: 5663–5673.
- Delph LF. 1996. Flower Size Dimorphism in Plants with Unisexual Flowers. In: Lloyd DG, Barrett SCH, eds. *Floral biology: studies on floral evolution in animal-pollinated plants*. Springer Science and Business Media.
- De Waal C, Anderson B, Barrett SCH. 2012. The natural history of pollination and mating in bird-pollinated *Babiana* (Iridaceae). *Annals of Botany* 109: 667–679.
- Dietzsch AC, Stanley DA, Stout JC. 2011. Relative abundance of an invasive alien plant affects native pollination processes. *Oecologia* 167: 469–479.
- Ellis AG, Johnson SD. 2009. The evolution of floral variation without pollinator shifts in *Gorteria diffusa* (Asteraceae). *American Journal of Botany* 96: 793–801.
- Fetscher AE, Rupert SM, Kohn JR. 2002. Hummingbird foraging position is altered by the touch-sensitive stigma of bush monkeyflower. *Oecologia* 133: 551–558.
- Fijen TPM, Kleijn D. 2017. How to efficiently obtain accurate estimates of flower visitation rates by pollinators. *Basic and Applied Ecology* 19: 11–18.
- Fishbein M, Lawrence Venable D. 1996. Diversity and temporal change in the effective pollinators of *Asclepias tuberosa*. *Ecology* 77: 1061–1073.

- Galen C. 1999. Why Do Flowers Vary? *BioScience* 49: 631–640.
- García M, Benítez-Vieyra S, Sérsic AN, Pauw A, Cocucci AA, Traveset A, Sazatornil F, Paiaro V. 2020. Is variation in flower shape and length among native and non-native populations of *Nicotiana glauca* a product of pollinator-mediated selection? *Evolutionary Ecology* 34: 893–913.
- Geerts S, Pauw A. 2011. Farming with native bees (*Apis mellifera* subsp. *capensis* Esch.) has varied effects on nectar-feeding bird communities in South African fynbos vegetation. *Population Ecology* 53: 333–339.
- Goldberg K. 1996. Neglected pollinator syndromes in seasonally inundated Renosterveld. BSc (hons) project, University of Cape Town, South Africa.
- Gómez JM, Bosch J, Perfectti F, Fernández JD, Abdelaziz M, Camacho JPM. 2008. Spatial variation in selection on corolla shape in a generalist plant is promoted by the preference patterns of its local pollinators. *Proceedings of the Royal Society B: Biological Sciences* 275: 2241–2249.
- Grant V. 1949. Pollination systems as isolating mechanisms in angiosperms. *Evolution* 3: 82–97.
- Gu W, Miao M, Fan J-F. 2018. Dichogamy and style curvature avoid self-pollination in *Eremurus altaicus*. *Current Science* 114: 384–387.
- Harder LD, Wilson WG. 1994. Floral evolution and male reproductive success: Optimal dispensing schedules for pollen dispersal by animal-pollinated plants. *Evolutionary Ecology* 8: 542–559.
- Helme NA, Linder HP. 1992. Morphology, evolution and taxonomy of *Wachendorfia* (Haemodoraceae). *Bothalia* 22: 59–75.
- Henry M, Rodet G. 2018. Controlling the impact of the managed honeybee on wild bees in protected areas. *Scientific Reports* 8: 1–10.
- Herrera C. 1996. Floral traits and plant adaptation to insect pollinators. In: Lloyd DG, Barrett, eds. *Floral Biology: Studies on Floral Evolution in Animal-*

- Pollinated Plants*. New York: Chapman and Hall.
- Herrera CM, Castellanos MC, Medrano M. 2006. Geographical context of floral evolution: towards an improved research programme in floral diversification. In: Harder LD, Barrett SCH, eds. *Ecology and Evolution of Flowers*. Oxford University Press, 278–294.
- Holmqvist JP, Manktelow M, Daniel TF. 2005. Wing Pollination By Bees in *Mexacanthus* (Acanthaceae)? *Acta Botánica Mexicana* 71: 11–17.
- Huang SQ, Shi XQ. 2013. Floral isolation in *Pedicularis*: How do congeners with shared pollinators minimize reproductive interference? *New Phytologist* 199: 858–865.
- Hung KLJ, Kingston JM, Lee A, Holway DA, Kohn JR. 2019. Non-native honey bees disproportionately dominate the most abundant floral resources in a biodiversity hotspot. *Proceedings of the Royal Society B: Biological Sciences* 286.
- Jesson LK, Barrett SCH. 2002. Enantiostyly in *Wachendorfia* (Haemodoraceae): The influence of reproductive systems on the maintenance of the polymorphism. *American Journal of Botany* 89: 253–262.
- Jesson LK, Barrett SCH. 2003. The Comparative Biology of Mirror-Image Flowers. *International Journal of Plant Sciences* 164: S237–S249.
- Jesson LK, Barrett SCH. 2005. Experimental tests of the function of mirror-image flowers. *Biological Journal of the Linnean Society* 85: 167–179.
- Jesson LK, Barrett SCH, Day T. 2003a. A theoretical investigation of the evolution and maintenance of mirror-image flowers. *The American Naturalist* 161: 916–930.
- Jesson LK, Kang J, Wagner SL, Barrett SCH, Dengler NG. 2003b. The development of enantiostyly. *American Journal of Botany* 90: 183–195.
- Johnson SD. 2006. Pollinator-driven speciation in plants. In: Harder LD, Bar-

- rett SCH, eds. *Ecology and Evolution of Flowers*. Oxford University Press, 295–310.
- Johnson SD. 2010. The pollination niche and its role in the diversification and maintenance of the southern African flora. *Philosophical Transactions of the Royal Society B: Biological Sciences* 365: 499–516.
- Kalisz S, Vogler D, Fails B, Finer M, Shepard E, Herman T, Gonzales R. 1999. The mechanism of delayed selfing in *Collinsia verna* (Scrophulariaceae). *American Journal of Botany* 86: 1239–1247.
- Kálmán K, Medvegy A, Péntzes Z, Mihalik E. 2007. Morph-specific variation of floral traits associated with reciprocal herkogamy in natural populations of *Primula vulgaris* and *Primula veris*. *Plant Systematics and Evolution* 268: 15–27.
- Kutschera U, Briggs WR. 2016. Phototropic solar tracking in sunflower plants: an integrative perspective. *Annals of botany*, 117: 1-8.
- Lambrecht SC, Dawson TE. 2007. Correlated variation of floral and leaf traits along a moisture availability gradient. *Oecologia* 151: 574–583.
- Lázaro A, Seguí J, Santamaría L. 2020. Continuous variation in herkogamy enhances the reproductive response of *Lonicera implexa* to spatial variation in pollinator assemblages. *AoB PLANTS* 12: 1–10.
- Li QJ, Xu ZF, Kress WJ, Xia YM, Zhang L, Deng XB, Gao JY, Bai ZL. 2001. Flexible style that encourages outcrossing. *Nature* 410: 432-432.
- Liu CC, Gui MY, Sun YC, Wang XF, He H, Wang TX, Li JY. 2020. Doubly guaranteed mechanism for pollination and fertilization in *Ipomoea purpurea*. *Plant Biology* 22: 910–916.
- Lloyd DG. 1992. Self- and Cross-Fertilization in Plants. II. The Selection of Self-Fertilization. *International Journal of Plant Sciences* 153: 358–369.
- Madjidian JA, Morales CL, Smith HG. 2008. Displacement of a native by an alien

- bumblebee: Lower pollinator efficiency overcome by overwhelmingly higher visitation frequency. *Oecologia* 156: 835–845.
- Maia R, Gruson H, Endler JA, White TE. 2019. pavo 2: new tools for the spectral and spatial analysis of colour in R. *Methods in Ecology and Evolution*, 10: 1097-1107.
- Minnaar C. 2018. Novel insights into pollen movement and floral evolution revealed by quantum dots. PhD dissertation, Stellenbosch University, South Africa.
- Minnaar C, Anderson B. 2021. A combination of pollen mosaics on pollinators and floral handedness facilitates the increase of outcross pollen movement. *Current Biology* 31: 1-5.
- Minnaar C, Anderson B. 2019. Using quantum dots as pollen labels to track the fates of individual pollen grains. *Methods in Ecology and Evolution* 10: 604–614.
- Minnaar C, de Jager ML, Anderson B. 2019. Intraspecific divergence in floral-tube length promotes asymmetric pollen movement and reproductive isolation. *New Phytologist* 224: 1160–1170.
- Morais JM, Consolaro HN, Bergamini LL, Ferrero V. 2020. Patterns of pollen flow in monomorphic enantiostylous species: the importance of floral morphology and pollinators' size. *Plant Systematics and Evolution* 306.
- Muchhala N, Brown Z, Armbruster WS, Potts MD. 2010. Competition Drives Specialization in Pollination Systems through Costs to Male Fitness. *The American Naturalist* 176: 732–743.
- Nagy ES, Strong L, Galloway LF. 1999. Contribution of delayed autonomous selfing to reproductive success in Mountain Laurel, *Kalmia latifolia* (Ericaceae). *American Midland Naturalist* 142: 39–46.
- Newman E, Manning J, Anderson B. 2015. Local adaptation: Mechanical fit between floral ecotypes of *Nerine humilis* (Amaryllidaceae) and pollinator communities. *Evolution* 69: 2262–2275.

- Opedal ØH. 2019. The evolvability of animal-pollinated flowers: towards predicting adaptation to novel pollinator communities. *New Phytologist* 221: 1128–1135.
- Opedal ØH, Bolstad GH, Hansen TF, Armbruster WS, Christophe P. 2017. The evolvability of herkogamy: Quantifying the evolutionary potential of a composite trait. *Evolution*, 71(6), pp.1572-1586.
- Ornduff R, Dulberger R. 1978. Floral Enantiomorphy and the Reproductive System of *Wachendorfia paniculata* (Haemodoraceae). *New Phytologist* 80: 427–434.
- Papiorek S, Junker RR, Alves-dos-Santos I, Melo GAR, Amaral-Neto LP, Sazima M, Wolowski M, Freitas L, Lunau K. 2016. Bees, birds and yellow flowers: Pollinator-dependent convergent evolution of UV patterns. *Plant Biology* 18: 46–55.
- Pauw A. 2005. Inversostyly: a new styelar polymorphism in an oil-secreting plant, *Hemimeris racemosa* (Scrophulariaceae). *American Journal of Botany* 92: 1878-1886.
- Pauw A, Cocucci AA, Sérsic AN. 2020. The least effective pollinator principle: specialized morphology despite generalized ecology. *Plant Biology* 22: 924–931.
- Pérez-Barrales R, Pino R, Albaladejo RG, Arroyo J. 2009. Geographic variation of flower traits in *Narcissus papyraceus* (Amaryllidaceae): Do pollinators matter? *Journal of Biogeography* 36: 1411–1422.
- Peter CI, Johnson SD. 2006. Doing the twist: A test of Darwin’s cross-pollination hypothesis for pollinarium reconfiguration. *Biology Letters* 2: 65–68.
- Peter CI, Johnson SD. 2014. A pollinator shift explains floral divergence in an orchid species complex in South Africa. *Annals of Botany* 113: 277–288.
- Pinheiro J, Bates D, DebRoy S, Sarkar D, R Core Team (2021). nlme: Linear and Nonlinear Mixed Effects Models. *R package version* 3.1-152.
- Rader R, Howlett BG, Cunningham SA, Westcott DA, Newstrom-Lloyd LE, Walker MK, Teulon DAJ, Edwards W. 2009. Alternative pollinator taxa are equally

- efficient but not as effective as the honeybee in a mass flowering crop. *Journal of Applied Ecology* 46: 1080–1087.
- Rafiński JN. 1979. Geographic variability of flower colour in *Crocus scepusiensis* (Iridaceae). *Plant Systematics and Evolution* 131: 107–125.
- Ramos SE, Schiestl FP. 2019. Rapid plant evolution driven by the interaction of pollination and herbivory. *Science* 364: 193–196.
- R Core Team. 2020. R: A language and environment for statistical computing. R Foundation for Statistical Computing, Vienna, Austria.
- Ren MX, Tang JY. 2010. Anther fusion enhances pollen removal in *Campsis grandiflora*, a hermaphroditic flower with didynamous stamens. *International Journal of Plant Sciences* 171: 275–282.
- Ren MX, Tang JY. 2012. Up and down: Stamen movements in *Ruta graveolens* (Rutaceae) enhance both outcrossing and delayed selfing. *Annals of Botany* 110: 1017–1025.
- Ruan CJ, Mopper S, Da Silva JAT, Qin P, Zhang QX, Shan Y. 2009a. Context-dependent style curvature in *Kosteletzkya virginica* (Malvaceae) offers reproductive assurance under unpredictable pollinator environments. *Plant Systematics and Evolution* 277: 207–215.
- Ruan CJ, Qin P, He ZX. 2004. Delayed autonomous selfing in *Kosteletzkya virginica* (Malvaceae). *South African Journal of Botany* 70: 640–645.
- Ruan CJ, Qin P, Teixeira Da Silva Jaime A, Zhang QX. 2009b. Movement herkogamy in *Kosteletzkya virginica*: Effect on reproductive success and contribution to pollen receipt and reproductive assurance. *Shengtai Xuebao/ Acta Ecologica Sinica* 29: 98–103.
- Ruan CJ, da Silva JAT. 2011. Adaptive significance of floral movement. *Critical Reviews in Plant Sciences* 30: 293–328.
- Ruan CJ, da Silva JAT, Qin P. 2010. Style curvature and its adaptive significance

- in the Malvaceae. *Plant Systematics and Evolution* 288: 13–23.
- Scott Elliot GF. 1891. Notes on the fertilisation of South African and Madagascar flowering plants. *Annals of Botany* 5: 333–405.
- Solís-Montero L, Vallejo-Marín M. 2017. Does the morphological fit between flowers and pollinators affect pollen deposition? An experimental test in a buzz-pollinated species with anther dimorphism. *Ecology and Evolution* 7: 2706–2715.
- Stebbins GL. 1970. Adaptive Radiation of Reproductive Characteristics in Angiosperms, I: Pollination Mechanisms. *Annual Review of Ecology and Systematics* 1: 307–326.
- Steffan-Dewenter I, Münzenberg U, Bürger C, Thies C, Tschardt T. 2002. Scale-dependent effects of landscape context on three pollinator guilds. *Ecology* 83: 1421–1432.
- Sun S, Gao JY, Liao WJ, Li QJ, Zhang DY. 2007. Adaptive significance of flexibility in *Alpinia blepharocalyx* (Zingiberaceae): A hand-pollination experiment. *Annals of Botany* 99: 661–666.
- Takebayashi N, Wolf DE, Delph LF. 2006. Effect of variation in herkogamy on outcrossing within a population of *Gilia achilleifolia*. *Heredity* 96: 159–165.
- Theron GL, de Waal C, Barrett SCH, Anderson B. 2019. Geographic variation of reproductive traits and competition for pollinators in a bird-pollinated plant. *Ecology and Evolution* 9: 10122–10134.
- Thioulouse J, Dray S, Dufour A, Siberchicot A, Jombart T, Pavoine S. 2018. *Multivariate Analysis of Ecological Data with ade4*. Springer, New York.
- Ushimaru A, Kobayashi A, Dohzono I. 2014. Does urbanization promote floral diversification? Implications from changes in herkogamy with pollinator availability in an urban-rural area. *American Naturalist* 184: 258–267.
- Vallejo-Marín M, Da Silva EM, Sargent RD, Barrett SCH. 2010. Trait correlates and functional significance of heteranthery in flowering plants. *New Phytologist*

188: 418–425.

- Van Der Niet T, Peakall R, Johnson SD. 2014. Pollinator-driven ecological speciation in plants: New evidence and future perspectives. *Annals of Botany* 113: 199–211.
- Webb CJ, Lloyd DG. 1986. The avoidance of interference between the presentation of pollen and stigmas in angiosperms II. Herkogamy. *New Zealand Journal of Botany* 24: 163–178.
- Weber UK, Nuismer SL, Espíndola A. 2020. Patterns of floral morphology in relation to climate and floral visitors. *Annals of Botany* 125: 433–445.
- Willmer PG, Cunnold H, Ballantyne G. 2017. Insights from measuring pollen deposition: quantifying the pre-eminence of bees as flower visitors and effective pollinators. *Arthropod-Plant Interactions* 11: 411–425.
- Yang SX, Yang CF, Zhang T, Wang QF. 2004. A mechanism facilitates of pollination due to stigma behavior in *Campsis radicans* (Bignoniaceae). *Acta Botanica Sinica* 46: 1071–1074.
- Ye ZM, Jin XF, Yang J, Wang QF, Yang CF. 2019. Accurate position exchange of stamen and stigma by movement in opposite direction resolves the herkogamy dilemma in a protandrous plant, *Ajuga decumbens* (Labiatae). *AoB PLANTS* 11: 1–6.
- Zhao ZG, Wang YK. 2015. Selection by pollinators on floral traits in generalized *Trollius ranunculoides* (Ranunculaceae) along altitudinal gradients. *PLoS ONE* 10: 1–16.